PACIFIC EARTHQUAKE ENGINEERING RESEARCH CENTER

Development of Time Histories for IEEE693 Testing and Analysis (Including Seismically Isolated Equipment)

Shakhzod M. Takhirov
Department of Civil and Environmental Engineering
University of California, Berkeley

Eric Fujisaki
Consultant and Chair of IEEE693 Working Group
Martinez, California

Leon Kempner
Bonneville Power Administration
Vancouver, Washington

Michael Riley
Bonneville Power Administration
Vancouver, Washington

Brian Low
Pacific Gas & Electric Company
San Ramon, California

PEER Report No. 2017/10
Pacific Earthquake Engineering Research Center
Headquarters at the University of California, Berkeley

December 2017

PEER 2017/10
December 2017

Development of Time Histories for IEEE693 Testing and Analysis (Including Seismically Isolated Equipment)

Shakhzod M. Takhirov
Department of Civil and Environmental Engineering
University of California, Berkeley

Eric Fujisaki
Consulting Civil Engineer
Martinez, California

Leon Kempner
Bonneville Power Administration
Vancouver, Washington

Michael Riley
Bonneville Power Administration
Vancouver, Washington

Brian Low
Pacific Gas & Electric Company
San Ramon, California

PEER Report No. 2017/10
Pacific Earthquake Engineering Research Center
Headquarters at the University of California, Berkeley

December 2017

ABSTRACT

This study was undertaken to address new developments in IEEE P693/D16 [IEEE693 WG 2017], account for the new strong-motion records from the recent major earthquakes, and assess their effects on the spectral demand. A large set of both crustal and subduction type records was investigated based on a number of parameters and intensity measures. The best candidates were selected as seed motions. The motions were matched to the IEEE693 spectrum in a time domain at 5% damping, which follows the guidance of IEEE P693/D16 [IEEE693 WG 2017]. In addition, three three-component synthetic time histories were generated. All modified and generated time histories were arranged into a suite of time histories proposed for use in IEEE693 seismic qualification analysis and testing. The suite consisted of four IEEE693-spectrum-compatible time histories modified from crustal records, one IEEE693-spectrum-compatible time history modified from a subduction record, and three IEEE693-spectrum-compatible synthetic time histories. The spectral matching was conducted with a tight tolerance to remain within a 15% strip above the IEEE693 spectra in a wide-frequency range. It was shown that the conservatism of the IEEE693 spectrum is different for crustal and subduction type records. Based on the results of the investigation, the study summarizes the basis for changes to the requirements for development of input time histories given in IEEE P693/D16, and considerations for input motion specifications for a future edition of the standard.

ACKNOWLEDGMENTS

The authors greatly appreciate the project's sponsor, the Electric Power Research Institute (EPRI). Any opinions, findings, and conclusions or recommendations expressed in this material are those of the author(s) and do not necessarily reflect those of the National Science Foundation or the Pacific Earthquake Engineering Research Center at the University of California, Berkeley.

CONTENTS

LIST OF TABLES

LIST OF FIGURES

1 Overview of Previous and Ongoing Related Research

1.1 INTRODUCTION

A study conducted earlier on a number of strong motions [Takhirov et al. 2004] resulted in the development of a three-component strong motion called TestQke4IEEE. Based on a detailed analysis, the best candidate (seed motion) was selected from a large set of strong motions. TestQke4IEEE was developed from a historic record obtained during the 1992 Landers earthquake by matching its spectra to the current IEEE Std 693-2005 [IEEE 2005] spectra at 2% critical damping. The spectral matching was performed in a time domain. As a result, the TestQke4IEEE spectra closely matched the IEEE Std 693-2005 [IEEE 2005] spectra starting at about 0.3 Hz. For more than a decade, this strong motion has been successfully used for seismic qualification testing and analysis. This study was undertaken to address new developments in the IEEE P693/D16 [IEEE693 WG 2017], account for the new strong-motion records from recent major earthquakes, and assess their effects on the spectral demand. IEEE P693/D16 [IEEE693 WG 2017] is the most recent draft of the next version of the recommended practice. The requirements for development of input time histories for use in shake-table testing and analysis given in IEEE P693/D16 [IEEE693 WG 2017] are similar to those given in IEEE Std 693-2005 [IEEE 2005] except that spectral matching is to be performed at 5% instead of 2% damping, and the requirements for high cycle count and intermediate tolerance band checks have been eliminated. IEEE P693/D16 [IEEE693 WG 2017] also describes the requirements for the design, analysis, and testing of seismic protective devices and equipment/device systems. Such protected systems are required in IEEE P693/D16 [IEEE693 WG 2017] to be subjected to multiple spectrum-compatible histories when those systems are qualified by analysis. The histories developed in this project include coverage of low-frequency demand issues so that the new time histories can be used with the new Annex W in IEEE P693/D16 [IEEE693 WG 2017]. Although subduction earthquakes are specifically excluded from consideration in IEEE P693/D16, a spectrum-compatible history that satisfies the requirements of the draft standard has been developed in this project.

1.2 REVIEW OF MAJOR RECENT DEVELOPMENTS

This section summarizes recent major developments related to the research topic of this study.

1.2.1 Dataset used in Boore-Atkinson NGA Ground Motion Relations

A paper published in 2008 by Boore and Atkinson [2008] summarizes the results of an extensive study and contains ground-motion prediction equations (GMPEs) for average horizontal-component ground motions as a function of earthquake moment magnitude, distance from source to site, local average shear-wave velocity, and fault type. A detailed report was published by the Pacific Earthquake Engineering Research Center (PEER) [Boore and Atkinson 2007]. The prediction equations were obtained for peak ground acceleration (PGA), peak ground velocity (PGV), and 5%-damped pseudo-absolute-acceleration spectra (PSA) at frequencies between 0.1 Hz and 100 Hz. They were derived by empirical regression of an extensive strong-motion database compiled by PEER's Next Generation Attenuation (NGA) project [Power et al. 2008]. A number of records were frequency dependent (for PSA analysis), and in case of frequencies greater than 1 Hz, the study utilized 1574 records from 58 mainshocks in the distance range from 0 km to 400 km.

This research used an orientation-independent measure called RotI50 [Boore et al. 2006], which represents the geometric mean determined from the 50th percentile values of the geometric means computed for all non-redundant rotation angles and all periods less than the maximum useable period. It was noted that in most cases, the differences between the geometric mean and RotI50 are not large, so this parameter can be thought of simply as an average horizontal component.

Based on earlier studies [Boore and Atkinson 1989; Atkinson 1993], the study excluded aftershock records from consideration. The studies raised concerns that the spectral scaling of aftershocks can be different from that of the mainshocks. Equations for peak ground displacement (PGD) were also excluded from consideration [Boore and Atkinson 2008] based on an earlier study [Boore and Atkinson 2007] that showed that PGD is too sensitive to the low-cut filters used in the data processing and thus cannot represent a stable measure of ground shaking. Instead of PGD, it was recommended to use response spectra at low frequencies as a parameter related to peak displacement.

1.2.2 Dataset used in NGA-West2 Campbell–Bozorgnia Ground Motion Model

The research effort by Campbell and Bozorgnia [2013] used an expanded PEER NGA-West2 ground-motion database of records from shallow crustal earthquakes in active tectonic domains. It developed a GMPE for the RotD50 horizontal components of PGA, PGV, and PSA at 21 periods ranging from 0.01 to 10 sec. The GMPE developed in this study is considered valid for estimating ground motions from shallow continental earthquakes occurring worldwide in active tectonic domains for magnitudes ranging from 3.3 to as large as 8.5, depending on the style of faulting, and distances within 300 km from the source.

The ground-motion database used in this study is a subset of the PEER ground-motion database that was recently updated as part of the PEER NGA-West2 Project [Ancheta et al. 2012;

2013]. This database includes over 21,000 three-component recordings from worldwide earthquakes with moment magnitudes ranging from 3.0 to 7.9. The subset was based on many criteria important for the seismic hazard attenuation project. In relation to the objectives of this study, the same criteria were adopted and used in the record selection for this study.

Records that were not considered included: (1) recordings having only one horizontal component or only a vertical component; (2) the Lamont Doherty Geologic Observatory recordings from the 1999 Düzce, Turkey, earthquake, which are considered to be unreliable because of their odd spectral shapes; (3) recordings from instruments designated as quality D from the 1999 Chi-Chi, Taiwan, earthquake according to the quality designation of by Lee et al. [2001], which are considered to be unreliable because of their poor quality; and (4) "aftershocks" located in the immediate vicinity of the inferred mainshock rupture plane.

1.2.3 M9 Project: Cascadia Megathrust Earthquake

The M9 project is a National Science Foundation (NSF) funded research effort at the University of Washington (UW) to understand the Pacific Northwest's (PNW) seismic risk to possible magnitude 9 (M9) Cascadia Subduction Zone (CSZ) earthquakes and subsequent tsunamis and landslides. This four-year project started in 2015, and it is built around a large-scale computational model of the PNW. The model is used to simulate and predict ground-motion time histories for a broad range of large magnitude scenarios in the CSZ.

One of the main results of the UW study [2016] is that a single rupture in the CSZ can generate several subsequent earthquakes within the CSZ. The latter will result in two major features of the seismic motions: (1) The duration of the strong motion away from the epicenter will elongate and the low-frequency energy of the earthquake motion will increase with a potential of imposing a large number of cycles with long periods; and (2) The seismic impact can be amplified in the Seattle, Everett, Tacoma, and Portland basins due to the basins' geological structure and soil conditions. The computational simulation showed that amplification in the Puget Sound Region can be four times higher with respect to seismic excitation outside of the basins. Built-environment response to the unique long-period and long-duration ground motions will be evaluated probabilistically using advanced numerical simulation.

The study is focused on many strong motions with characteristics closely matching those for the CSZ. The 2011 M9 Tohoku earthquake in Japan resulted in similar strong-motion time histories generated by subsequent smaller earthquakes following the major rupture. Based on the records of the 2011 Tohoku earthquake, it was concluded that a number of smaller (M8) earthquakes at a depth of 30–40 km was triggered by the main event. Another major earthquake with similar characteristics is the M8.8 2010 Chile earthquake that triggered many subevents with a rising time of about 2 sec. Similar features were observed in the records of the Sumatra 2004 earthquake, which was a seismic event with parameters close to that of the CSZ earthquakes. The 2001 M6.8 Nisqually and the 2011 M6.4 Vancouver Island earthquakes are also included in the study for the same reason. Based on a strong-motion analysis and subsequent numerical analysis on the computational model of the CSZ, a number of synthetic strong motions were generated for use in the structural analysis in the CSZ.

1.2.4 Recent Developments in Ground-Motion Selection and Scaling for Structural Applications (ATC-82 Project and ASCE7 Chapter 16)

The objective of this project [NIST 2011; ASCE 2017] was to improve guidance for selecting, generating, and scaling earthquake ground motions for performing a response-history analysis of low-rise and medium-rise buildings. Both code-based design and seismic performance assessment were addressed. Based on the findings identified, and considering the potential for impacting design practice in the near-term, the following topics were chosen for study: (1) selection of ground motions based on the conditional spectrum; (2) response-spectrum matching; and (3) near-fault ground motions and fault-rupture directivity.

As one of the major findings, it was concluded that at least eleven time histories are required for design analysis based on the conditional spectrum. The time histories are required to be scaled to the target spectrum in the vicinity of the resonant frequency of the building. The conditional spectrum is building-specific and site-specific, and, as such, this approach is not well-suited for the seismic qualification of substation equipment that can be installed at various sites.

2 Strong-Motion Selection

2.1 INTRODUCTION

This section discusses the results of a detailed analysis of two large sets of strong motions including the most recent ones. The first set was based on strong-motion records from shallow crustal earthquakes and the second set was based on strong-motion records from subduction type events.

2.2 STRONG-MOTION RECORDS FOR SHALLOW CRUSTAL EARTHQUAKES

This section summarizes the results of a detailed analysis of strong-motion records from shallow crustal earthquakes.

2.2.1 Crustal Dataset Selection

The majority of strong-motion records for this set were obtained from the NGA-West2 database available online [PEER 2016]. To follow the recommendations developed by others (summarized in the previous sections), the following criteria were used in the selection:

1. The horizontal distance of the station to rupture, Joyner-Boore distance or R_{JB}, is less than 50 km. When R_{JB} was not known, it was substituted by epicentral distance;
2. A strong-motion record has all three components;
3. Magnitude of the seismic event is between 5 and 9;
4. Records with very small PGA have been excluded (i.e., only records with PGA of 0.1*g* in all three directions or greater were included);
5. The aftershocks were excluded;
6. Up to 15 records from each event are included (when the event has more than 15 records); and
7. Only those records from seismic stations that are representative of free-field site conditions were considered (based on Campbell and Bozorgnia [2013] definition).

The same criteria were utilized in selecting strong-motion records from other sources. These records were mainly obtained from the Center for Engineering Strong Motion Data [CESMD 2016] and one record was obtained from a private source. A final list of the strong-motion records obtained from the NGA-West2 database and other sources is presented in Table 2.1; this set consists of 410 records from 85 events.

Table 2.1 Subset of strong motions from crustal earthquakes.

Earthquake Name	Year	Magnitude	Mechanism	No of records	Source
Imperial Valley-02	1940	6.95	Strike Slip	1	PEER NGA-West2
Northern Calif-01	1941	6.4	Strike Slip	1	PEER NGA-West2
Kern County	1952	7.36	Reverse	1	PEER NGA-West2
Northern Calif-03	1954	6.5	Strike Slip	1	PEER NGA-West2
Parkfield	1966	6.19	Strike Slip	3	PEER NGA-West2
Northern Calif-05	1967	5.6	Strike Slip	1	PEER NGA-West2
Lytle Creek	1970	5.33	Reverse Oblique	2	PEER NGA-West2
San Fernando	1971	6.61	Reverse	13	PEER NGA-West2
Managua Nicaragua-01	1972	6.24	Strike Slip	1	PEER NGA-West2
Hollister-03	1974	5.14	Strike Slip	1	PEER NGA-West2
Northern Calif-07	1975	5.2	Strike Slip	2	PEER NGA-West2
Friuli Italy-01	1976	6.5	Reverse	1	PEER NGA-West2
Gazli USSR	1976	6.8	Reverse	1	PEER NGA-West2
Izmir Turkey	1977	5.3	Normal	1	PEER NGA-West2
Basso Tirreno Italy	1978	6	Strike Slip	2	PEER NGA-West2
Santa Barbara	1978	5.92	Reverse Oblique	1	PEER NGA-West2
Tabas Iran	1978	7.35	Reverse	3	PEER NGA-West2
Coyote Lake	1979	5.74	Strike Slip	8	PEER NGA-West2
Dursunbey Turkey	1979	5.34	Normal	1	PEER NGA-West2
Imperial Valley-06	1979	6.53	Strike Slip	15	PEER NGA-West2
Montenegro Yugoslavia	1979	7.1	Reverse	5	PEER NGA-West2
Norcia Italy	1979	5.9	Normal	1	PEER NGA-West2
St Elias Alaska	1979	7.54	Reverse	1	PEER NGA-West2
Anza (Horse Canyon)-01	1980	5.19	Strike Slip	1	PEER NGA-West2
Irpinia Italy-01	1980	6.9	Normal	5	PEER NGA-West2
Livermore-01	1980	5.8	Strike Slip	2	PEER NGA-West2
Mammoth Lakes-01	1980	6.06	Normal Oblique	3	PEER NGA-West2
Victoria Mexico	1980	6.33	Strike Slip	2	PEER NGA-West2
Corinth Greece	1981	6.6	Normal Oblique	1	PEER NGA-West2
Westmorland	1981	5.9	Strike Slip	5	PEER NGA-West2
Coalinga-01	1983	6.36	Reverse	15	PEER NGA-West2
Mammoth Lakes-10	1983	5.34	Strike Slip	1	PEER NGA-West2
Bishop (Rnd Val)	1984	5.82	Strike Slip	1	PEER NGA-West2
Lazio-Abruzzo Italy	1984	5.8	Normal	1	PEER NGA-West2
Morgan Hill	1984	6.19	Strike Slip	10	PEER NGA-West2
New Zealand-01	1984	5.5	Normal	1	PEER NGA-West2
Umbria-03 Italy	1984	5.6	Normal	2	PEER NGA-West2

Table 2.1 Subset of strong motions from crustal earthquakes (continued).

Earthquake Name	Year	Magnitude	Mechanism	No of records	Source
Nahanni Canada	1985	6.76	Reverse	2	PEER NGA-West2
Chalfant Valley-02	1986	6.19	Strike Slip	5	PEER NGA-West2
Kalamata Greece-01	1986	6.2	Normal	1	PEER NGA-West2
Mt. Lewis	1986	5.6	Strike Slip	1	PEER NGA-West2
N. Palm Springs	1986	6.06	Reverse Oblique	14	PEER NGA-West2
San Salvador	1986	5.8	Strike Slip	2	PEER NGA-West2
Baja California	1987	5.5	Strike Slip	1	PEER NGA-West2
New Zealand-02	1987	6.6	Normal	1	PEER NGA-West2
Superstition Hills-01	1987	6.22	Strike Slip	1	PEER NGA-West2
Superstition Hills-02	1987	6.54	Strike Slip	3	PEER NGA-West2
Whittier Narrows-01	1987	5.99	Reverse Oblique	15	PEER NGA-West2
Spitak Armenia	1988	6.77	Reverse Oblique	1	PEER NGA-West2
Loma Prieta	1989	6.93	Reverse Oblique	15	PEER NGA-West2
Manjil Iran	1990	7.37	Strike Slip	2	PEER NGA-West2
Sicilia-Orientale Italy	1990	5.6	Strike Slip	1	PEER NGA-West2
Upland	1990	5.63	Strike Slip	2	PEER NGA-West2
Georgia USSR	1991	6.2	Reverse	1	PEER NGA-West2
Sierra Madre	1991	5.61	Reverse	7	PEER NGA-West2
Big Bear-01	1992	6.46	Strike Slip	8	PEER NGA-West2
Cape Mendocino	1992	7.01	Reverse	13	PEER NGA-West2
Erzican Turkey	1992	6.69	Strike Slip	1	PEER NGA-West2
Joshua Tree CA	1992	6.1	Strike Slip	4	PEER NGA-West2
Landers	1992	7.28	Strike Slip	15	PEER NGA-West2
Little Skull MtnNV	1992	5.65	Normal	1	PEER NGA-West2
Northridge-01	1994	6.69	Reverse	15	PEER NGA-West2
Dinar Turkey	1995	6.4	Normal	1	PEER NGA-West2
Kozani Greece-01	1995	6.4	Normal	1	PEER NGA-West2
Northwest China-01	1997	5.9	Strike Slip	1	PEER NGA-West2
Umbria Marche Italy	1997	6	Normal	5	PEER NGA-West2
San Juan Bautista	1998	5.17	Strike Slip	1	PEER NGA-West2
Chi-Chi Taiwan	1999	7.62	Reverse Oblique	15	PEER NGA-West2
Duzce Turkey	1999	7.14	Strike Slip	10	PEER NGA-West2
Hector Mine	1999	7.13	Strike Slip	3	PEER NGA-West2
Kocaeli Turkey	1999	7.51	Strike Slip	7	PEER NGA-West2
Yountville	2000	5	Strike Slip	3	PEER NGA-West2
Denali Alaska	2002	7.9	Strike Slip	1	PEER NGA-West2
Bam Iran	2003	6.6	Strike Slip	2	PEER NGA-West2

Table 2.1 Subset of strong motions from crustal earthquakes (continued).

Earthquake Name	Year	Magnitude	Mechanism	No of records	Source
San Simeon CA	2003	6.52	Reverse	5	PEER NGA-West2
Parkfield-02 CA	2004	6	Strike Slip	15	PEER NGA-West2
L'Aquila Italy	2009	6.3	Normal	5	PEER NGA-West2
Darfield New Zealand	2010	7	Strike Slip	15	PEER NGA-West2
El Mayor-Cucapah Mexico	2010	7.2	Strike Slip	15	PEER NGA-West2
Christchurch New Zealand	2011	6.2	Reverse Oblique	15	PEER NGA-West2
Hawaii 15Oct2006	2006	6.7	TBD	4	CESMD
La Habra 28mar2014	2014	5.1	TBD	15	CESMD
Petrolia 25Apr1992	1992	7.1	Strike Slip	6	CESMD
South Napa 24Aug2014	2014	6	Strike Slip	15	CESMD
Cephallonia Greece 03Feb2014	2014	6.1	Strike Slip	1	Private source

2.2.2 Major Intensity Measures of Crustal Dataset (PGA, PGV, and M_W)

The major intensity measures (IM) for all strong motions are computed. Peak ground acceleration and PGV versus R_{JB} are presented in Figure 2.1(a) and Figure 2.1(b). Because PGD, as a parameter, is too sensitive to the low-cut filters (used in the data processing) it cannot be used as a stable IM of ground shaking [Boore and Atkinson 2007]. However, PGD are presented in Figure 2.2(a) to show the upper limit that is important for seismically isolated equipment. Distribution of station proximity to the rupture versus M_W of the seismic event is presented in Figure 2.2(b).

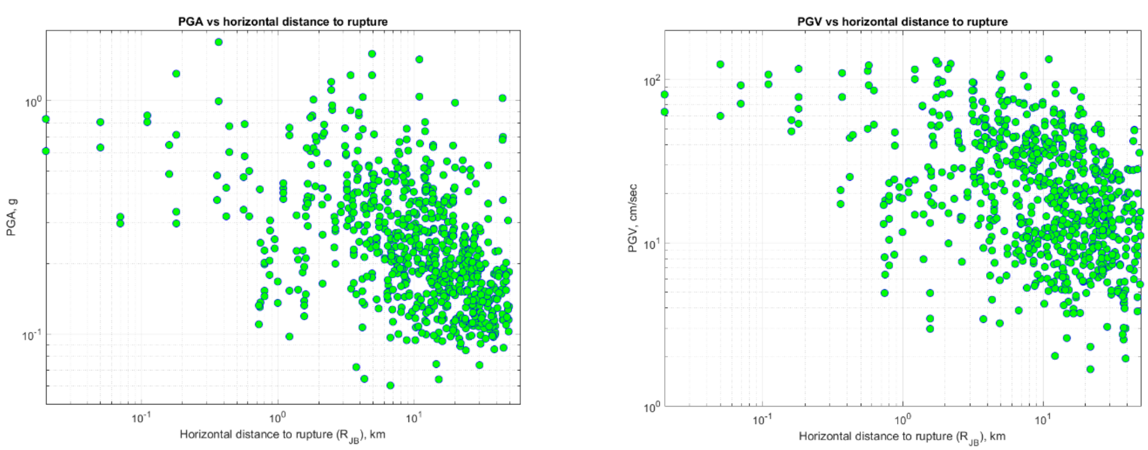

(a) (b)

Figure 2.1 PGA and PGV versus horizontal distance to rupture (R_{JB}).

Distribution of the PGA versus M_W of the seismic event is presented in Figure 2.3(a). While the PGA has a tendency to increase with increasing M_W, the plot shows that some moderate events (M_W = 5.5 in the plot) were able to generate accelerations with PGA close to 0.9g and higher. Spectral accelerations of all horizontal components of the records are presented in Figure 2.23(b). As shown in the spectral plot, some individual spectra can exceed the IEEE693 spectrum anchored at 1.0g [IEEE 2005]. In some cases, the peak spectral acceleration of an individual component can be about two times higher than that on the IEEE693 spectral plateau.

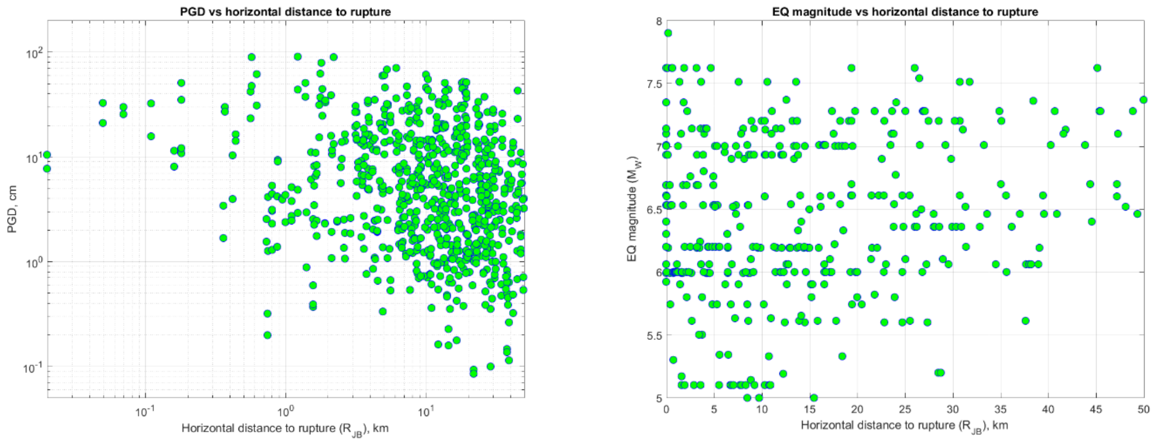

(a) **(b)**

Figure 2.2 **(a) PGD and (b) M_W versus horizontal distance to rupture (R_{JB}).**

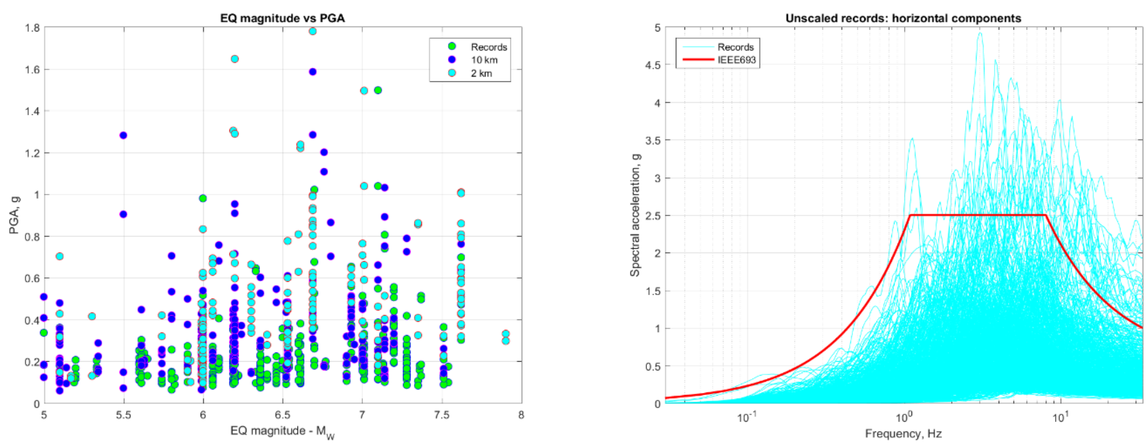

(a) **(b)**

Figure 2.3 **(a) PGA vs M_W and (b) horizontal spectral accelerations at 5% damping vs. IEEE693 High PL horizontal spectral accelerations.**

2.2.3 Root Mean Square Acceleration and Cumulative Energy

Root mean square (RMS) acceleration and cumulative energy (CE) calculations are discussed in detail in Appendix A. The RMS acceleration and the total CE for the set are presented in Figure 2.4. The plots show that there is a strong linear correlation between PGA and RMS acceleration, and PGA and total CE in a log–log scale.

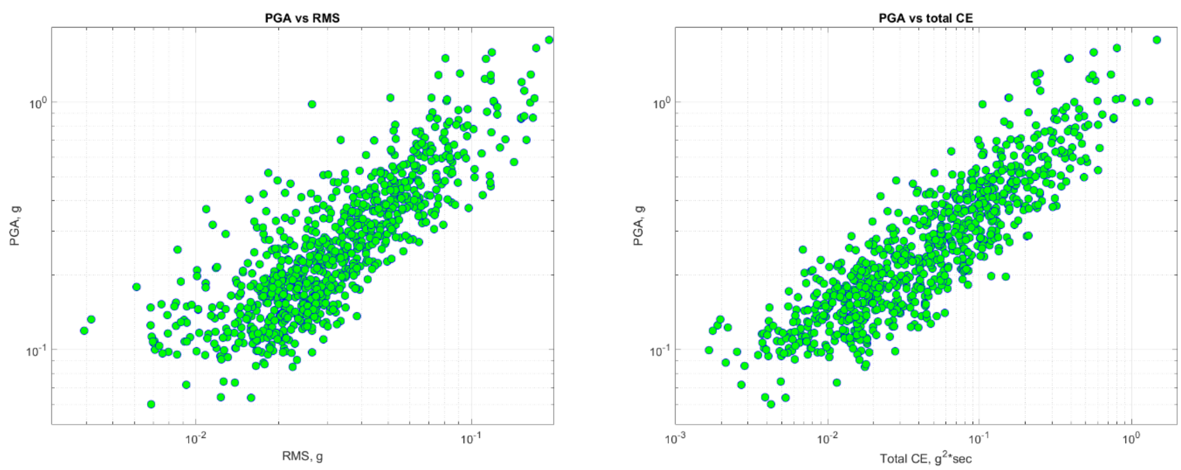

(a) **(b)**

Figure 2.4 (a) PGA vs. RMS acceleration and (b) PGA vs. total cumulative energy.

2.2.4 Duration Parameters

All duration-related parameters are discussed in detail in Appendix A. The duration of a strong-motion record in the IEEE Std 693-2005 [IEEE 2005] is defined as the time interval between when the plot of the acceleration time history reaches 25% of the maximum amplitude to the time when it falls for the last time to 25% of the maximum amplitude. For the purpose of this report, it is called a "bracketed duration." Several other definitions of duration are based on the CE; see Appendix A. These approaches define the duration as the time interval required to accumulate between α and β of the accelerogram's maximum CE. These durations are noted as $D_{\alpha\text{-}\beta}$ in this study. The common values for (α, β) pairs are (25%, 75%), (5%, 95%), and, recently introduced, (5%, 75%) [Chandramohan et al. 2016]. All these duration parameters are presented in Figures 2.5(a), 2.5(b), and 2.5(c), respectively. Another duration-related parameter, which was used in the earlier study [Takhirov et al. 2004] to account for the duration of the accelerogram's strong part is presented in Figure 2.5(d); see Appendix A. It is called the strong-part duration ratio, R_{SP}, and was defined as the ratio of time interval needed to accumulate between 25% and 75% of the maximum CE to that between 5% and 95%, or $D_{25\text{–}75}/D_{5\text{–}95}$. Please refer to Appendix A for more detail.

The IEEE Std 693-2005 [IEEE 2005] and its current draft version IEEE P693/D16 [IEEE693 WG 2017] require that the bracketed duration of the strong-motion time history used for qualification testing and analysis meets or exceeds 20 sec; see Figure 2.6(a). In addition, the IEEE Std 693-2005 [IEEE 2005] and its current draft version IEEE P693/D16 [IEEE693 WG 2017] require that the strong-part ratio of the time history be at 30% and greater. Both of these thresholds are presented in Figure 2.6(b). In both plots, the magenta region indicates a zone where the IEEE693 requirements are satisfied. Note that the correlation between the bracketed duration and the strong-part ratio shown in Figure 2.6(b) is significantly less noticeable than the correlation between $D_{25–75}$, $D_{5–95}$, and $D_{5–75}$ and the bracketed duration presented in Figures 2.7(a), 2.7(b), and 2.7(c), respectively. This serves as a justification for using the strong-part ratio as an independent duration parameter. As shown in Figure 2.7(d), a total CE divided by PGA^2 versus $D_{5–95}$ plot is close to a linear correlation. A summary of duration-related parameters for the set of shallow crustal events is presented in Table 2.2 where mean values and coefficients of variations for each parameter are listed.

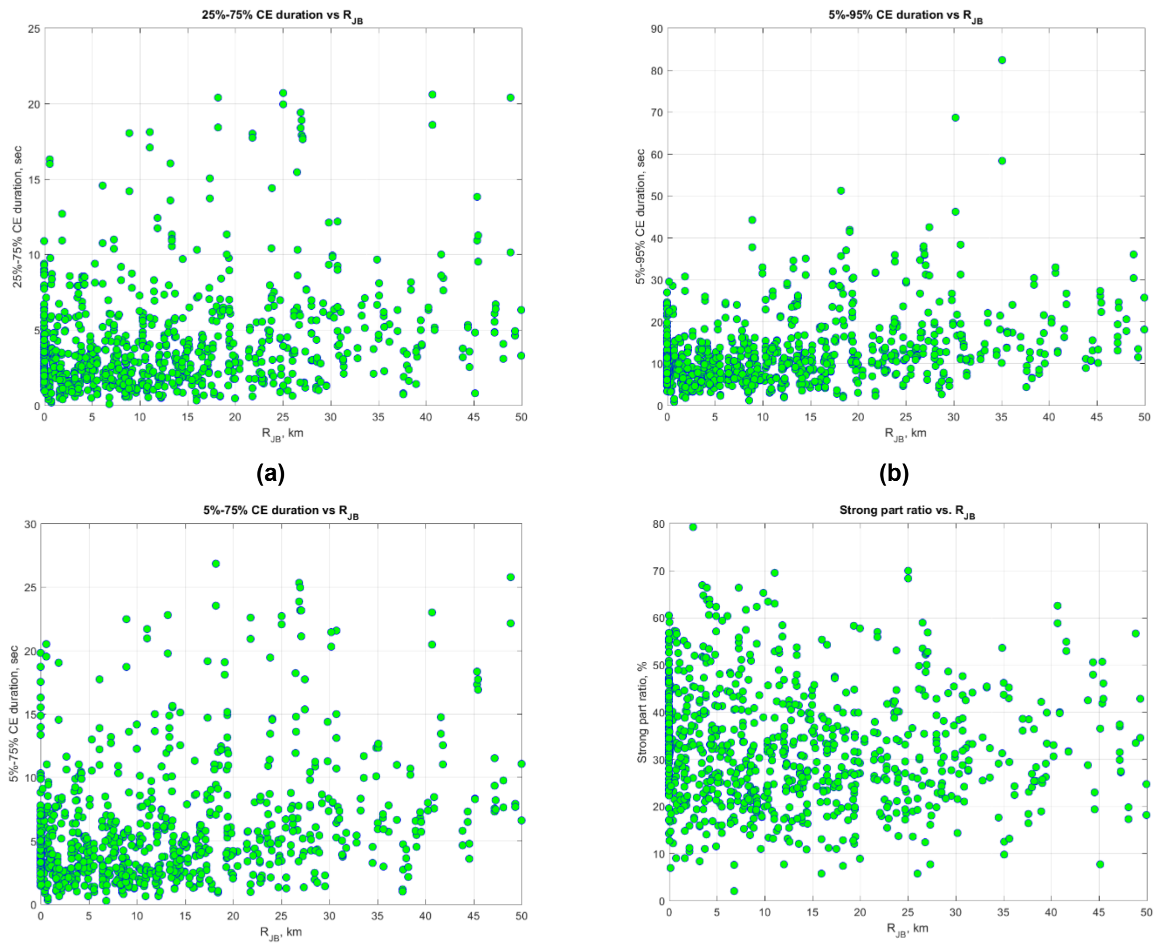

(c) (d)

Figure 2.5 **Cumulative energy-based durations vs. R_{JB}: (a) 25%-75%; (b) 5%–95%; (c) 5%–75%; and (d) strong-part duration ratio.**

Table 2.2 Duration-related parameters

Duration parameter	Mean	COV (%)	Notes
Bracketed duration	10.64 sec	77.7	Needs to meet 20 sec or exceed*
$D_{5–95}$	12.82 sec	67.6	
$D_{5–75}$	6.09 sec	78.5	
$D_{25–75}$	4.26 sec	82.9	
Strong-part ratio (R_{SP})	32.51 %	38.9	Needs to meet 30% or exceed *

* IEEE Std 693-2005 [IEEE 2005] and IEEE P693/D16 [IEEE693 WG 2017].

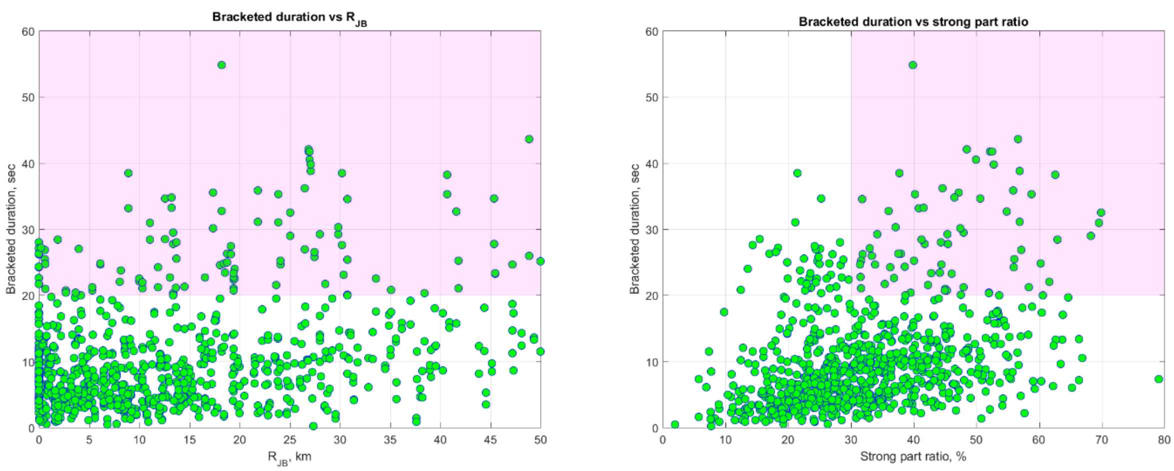

(a) (b)

Figure 2.6 Duration-related thresholds required by IEEE693: (a) threshold for IEEE693 duration; and (b) thresholds for IEEE693 duration and strong-part duration ratio (*R_{SP}*).

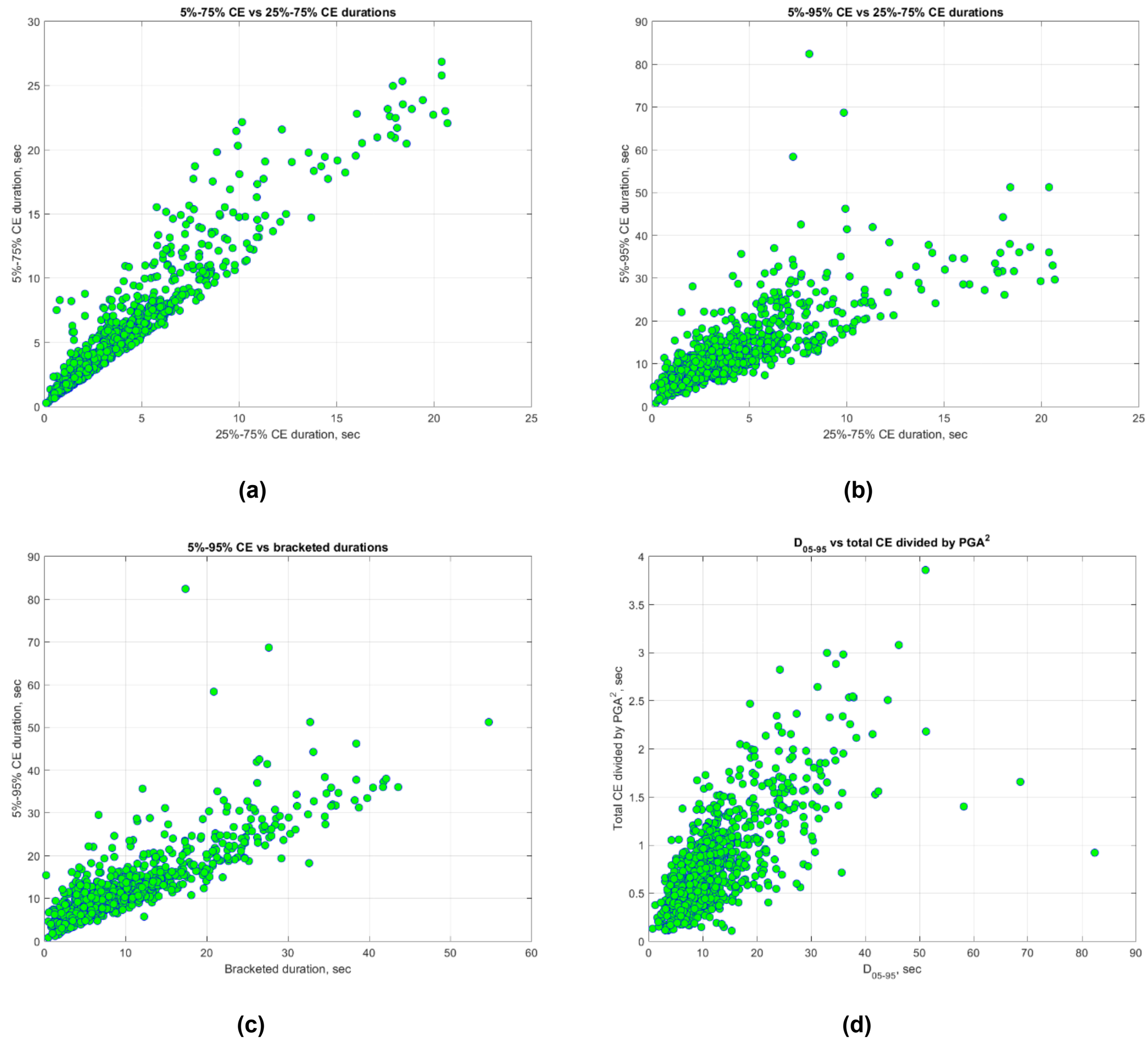

Figure 2.7 **Correlation between duration parameters: (a) $D_{5\text{–}75}$ vs. $D_{25\text{-}75}$: (b) $D_{5\text{–}95}$ vs. $D_{25\text{-}75}$; (c) $D_{5\text{–}95}$ vs. bracketed duration; and (d) total CE divided by PGA2 vs. $D_{5\text{–}95}$.**

2.2.5 Cycle Counting Related Parameters

As one of the IM parameters, a number of cycles exceeding 70% of the peak value—the so-called number of high cycles—was computed for each strong motion in the set; see Figure 2.8(a). The number of high cycles in the single-degree-of-freedom (SDOF) response [Takhirov et al. 2004] with mean and mean-plus-one-deviation is presented in Figure 2.8(b).

The number of cycles in the SDOF response with 2% damping in a seismic qualification time history was recommended to meet or exceed two cycles for the range of frequencies from 0.73 Hz to 12.45 Hz [Takhirov et al. 2004]. The current study on a larger dataset with default damping of 5% shows that this recommendation of having two or more cycles in the test or analysis time history response can be limited to the frequency range from 2.5 Hz to 12.45 Hz; see Figure 2.9. The fewer number of cycles is related to the fact that the system with a higher damping will experience a fewer number of cycles. Therefore, the requirement of having two high cycles in the SDOF response can be too conservative for seismic evaluation of substation equipment with a new default damping value of 5%. A summary of high-cycle counting conducted for the set of the 410 records is presented in Table 2.3.

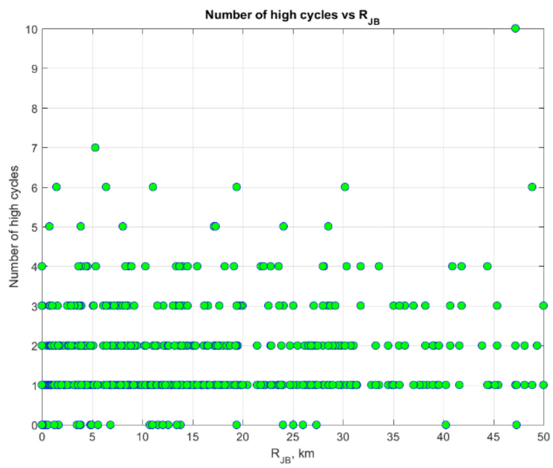

(a)

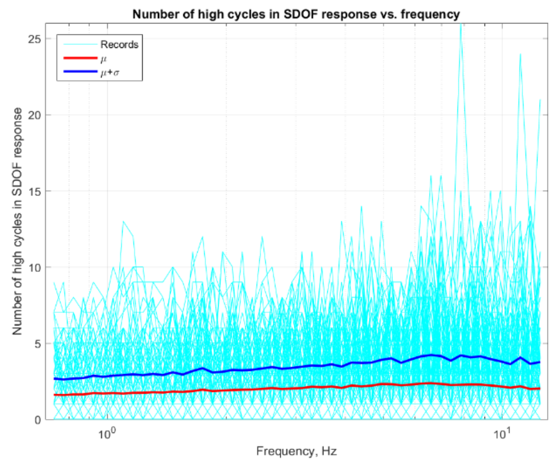

(b)

Figure 2.8 Cycle counting parameters of strong motions: (a) number of high cycles, and (b) number of cycles in SDOF response.

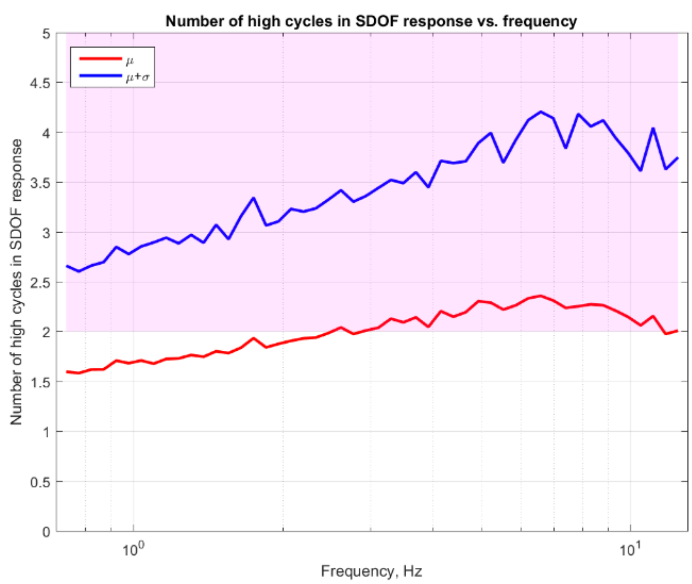

Figure 2.9 Threshold of minimum two cycles in the SDOF response specified in IEEE693 is satisfied starting at about 2.5 Hz.

Table 2.3 Summary of high cycles

Cycle counting parameter	Mean	COV (%)	Notes
Number of high cycles	1.55	68.6	Independent of scaling

2.2.6 Spectral Proximity to IEEE693 Spectrum and Spectral Average

Another parameter is used to characterize the proximity of the spectral shape of each strong-motion record to that of the IEEE693 spectrum. A cumulative distance of spectral accelerations to the IEEE693 spectrum, D_{SA}, was defined as follows:

$$D_{SA} = \sqrt{\left[\sum \left(K_S S_i - S_i^{\mathrm{IEEE}}\right)^2\right]} \tag{2.1}$$

where S_i is a spectral acceleration of the strong motion at frequency f_i; S_i^{IEEE} is a spectral value on the IEEE693 spectrum at the same frequency f_i; and K_S is a scaling factor of the strong motion.

This distance is estimated at a 1/24$^{\text{th}}$ octave resolution, and scaling factor K_S is calculated when the cumulative distance is at its minimum value. The latter is valid when:

$$dD_{SA} / dK_S = 0 \tag{2.2}$$

Equation (2.2) can be resolved as follows:

$$K_S = \sum \left(S_i S_i^{\mathrm{IEEE}}\right) \Big/ \left[\sum \left(S_i\right)^2\right] \tag{2.3}$$

Therefore, for each strong-motion record a scaling factor that best fits the IEEE693 spectrum can be identified from Equation (2.3), and the cumulative distance at the best fit can be calculated from Equation (2.1); see Figure 2.10.

Both K_S and D_{SA} were computed for each record from the dataset and the results presented in Figure 2.11. As presented in Figure 2.11(a), K_S has a strong correlation to PGA whereas D_{SA} does not, as shown in Figure 2.11(b).

Similar to the study conducted by Pacific Gas & Electric Co. (PG&E) [PG&E 1988], another parameter was used in the study presented herein. It was based on a spectral average from 2.5 Hz to 8.0 Hz, S_a^{aver}. This average was selected to assess a spectral demand of each strong-motion record that is not affected by low-pass and high-pass filters commonly used for conditioning raw acceleration records. This range of frequencies, from 2.5 Hz to 8.0 Hz, covers a portion of the spectral plateau of the IEEE693 spectrum and is roughly centered around the peaks of spectral plots of the strong motions included in the set and their mean; see Figure 2.12.

The spectral average S_a^{aver} was calculated for all strong motions. The results are presented in Figure 2.13 and show correlations of this average with PGA and K_S. Table 2.4 contains a summary of spectral proximity parameters and spectral average.

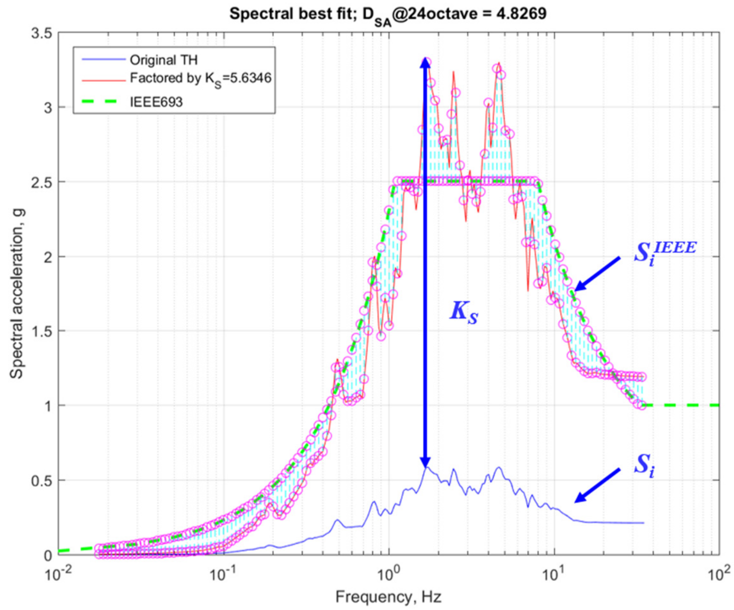

Figure 2.10 Example of scaling to best fit the IEEE693 spectrum.

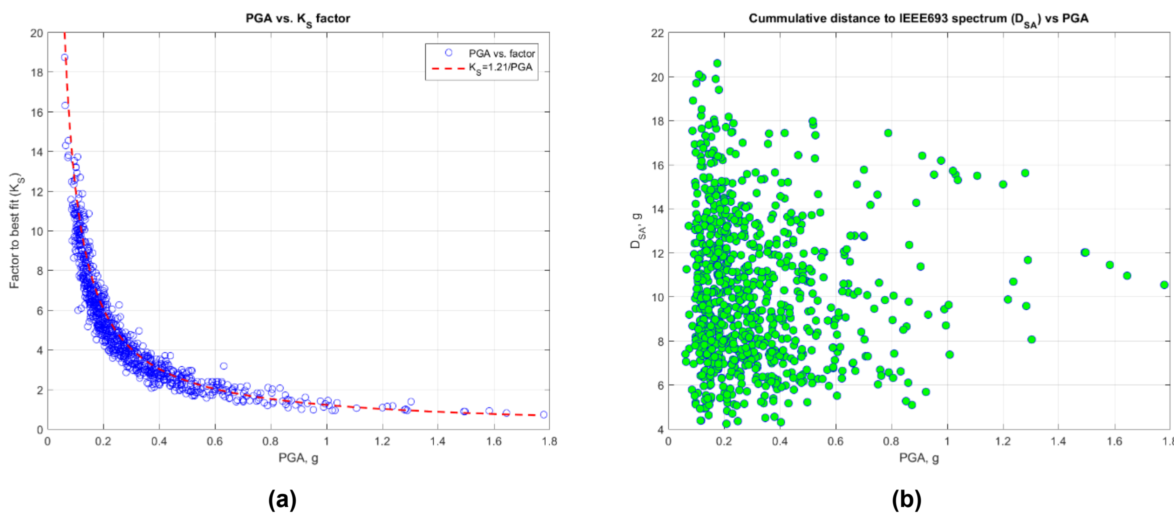

Figure 2.11 Parameters of best fit to IEEE693 spectrum: (a) strong correlation of K_S and PGA; and (b) cumulative distance to IEEE693 spectrum, D_{SA}, vs. PGA.

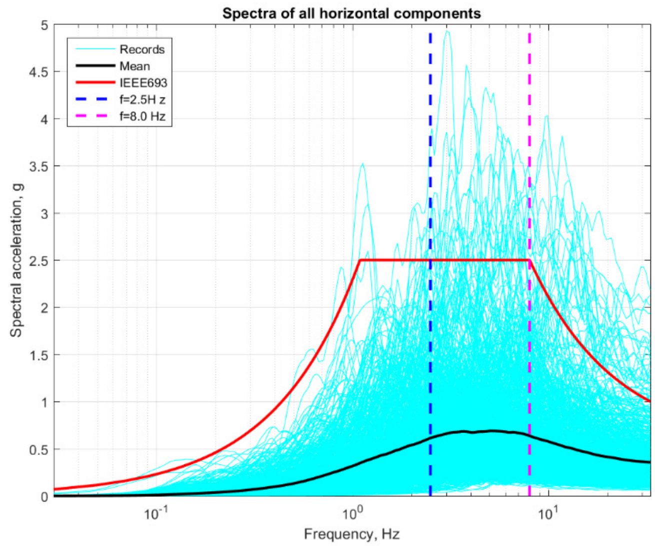

Figure 2.12 Spectral range for spectral average S_a^{aver} calculation.

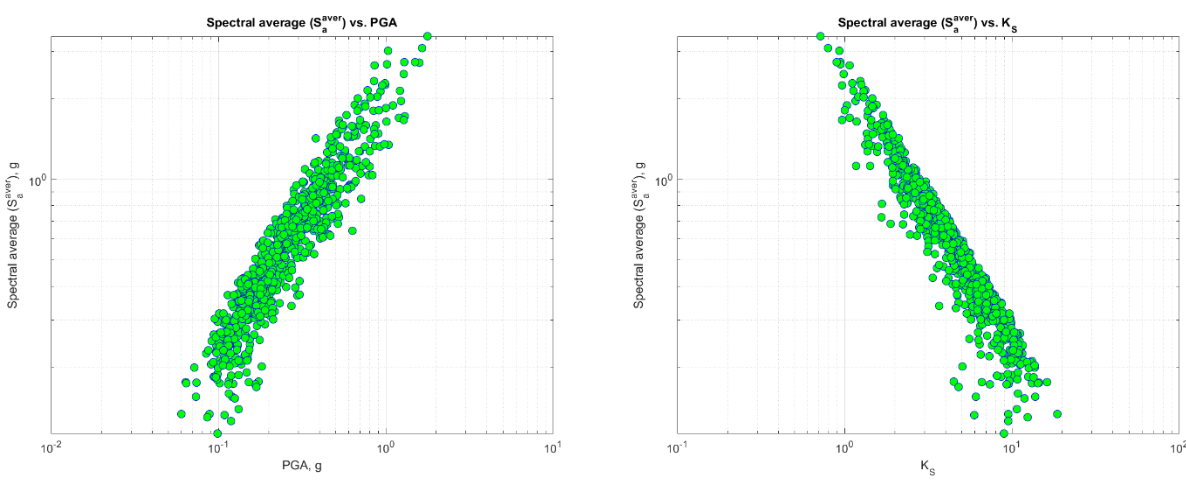

(a) (b)

Figure 2.13 Correlations of spectral average with PGA and K_S: (a) strong correlation of S_a^{aver} with PGA; and (b) strong correlation of S_a^{aver} with K_S.

Table 2.4 Summary of spectral proximity parameters and spectral average

Parameter	Mean	COV (%)	Description
D_{SA}	10.25g	32.3	Distance to IEEE693 spectrum at best fit
K_S	5.17	56.3	Best fit scaling
S_a^{aver}	0.67g	70.2	Spectral average from 2.5 Hz to 8 Hz

2.2.7 Spectral Accelerations

Spectral accelerations for all crustal records are presented in Figure 2.14. The spectral plots show that some components of the records exceed the IEEE693 spectrum. Spectral accelerations of some individual components exceed the IEEE693 spectral plateau by a factor of two or so; see Figure 2.14.

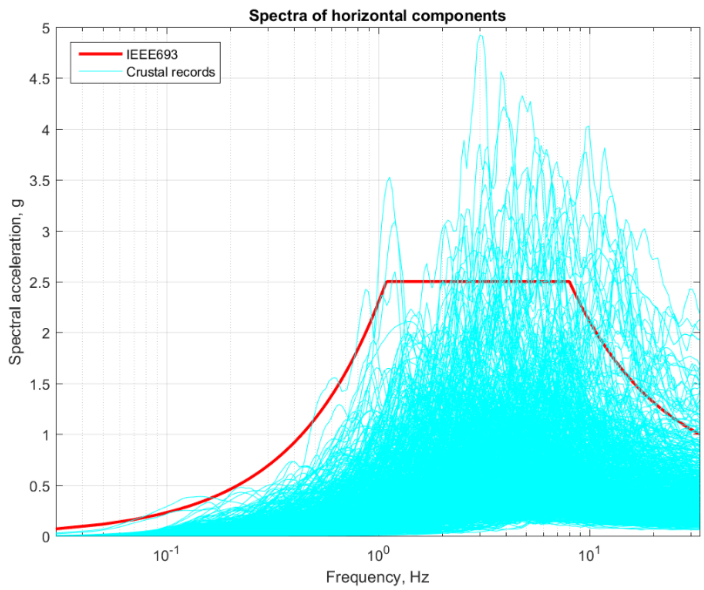

Figure 2.14 Unscaled spectra vs. IEEE693 spectrum anchored at 1*g*.

2.2.8 RotD50 Spectral Accelerations

The main objective of this section is to investigate instances in which some individual components of the strong motions exceed the IEEE693 spectrum as shown in Figure 2.14 and to demonstrate that the IEEE693 spectrum and the associated seismic qualification procedure represent a conservative approach for testing and analysis.

The analysis of the strong-motion records show that some horizontal components of the strong motions can exceed the IEEE693 High Performance Level spectrum anchored at 1g (5% critical damping), as presented in Figure 2.14. This creates a false impression that this result does not correlate with results of a parallel study [Mazzoni et al. 2017]. The latter study clearly demonstrated that the IEEE693 spectrum represents a conservative approach for testing and analysis. The discussion below elaborates on this issue.

The ground motion prediction equations (GMPEs) of the recent NGA-West2 database [Campbell and Bozorgnia 2013] and including the recent results by Mazzoni et al. [2017] are based on the utilization of RotD50 values of PGA, PGV, and spectral accelerations. In the case of the spectral accelerations, RotD50 is calculated as follows [Boore 2012]:

1. Project the two as-recorded horizontal time series into azimuth AZ;
2. For each period/frequency, compute spectral acceleration (S_A), store AZ, S_A pairs in an array;

3. Increment AZ by $\Delta\alpha$ ($\Delta\alpha = 1°$) and repeat first two steps until AZ =180°;
4. Sort array over S_A values; and
5. RotD50 is the median value of the array.

This procedure is followed for all strong motions in the set of 410 records; see the example provided in Figure 2.15. In addition, an average of S_A from 2.5 Hz to 8 Hz, S_a^{aver}, is calculated for each horizontal component and RotD50. This average was used in the PG&E study [1988] to assess a potential structural response while minimizing the effects of low-pass and high-pass filters on the spectral demand of each time history. In many cases, the average spectral acceleration of the RotD50 can be lower than that of the largest component. For this particular example, the average spectral acceleration of the RotD50 is 19% lower than that for one of the individual components; see Figure 2.15(d).

When the entire set is considered, the difference between average spectral acceleration from 2.5 Hz to 8.0 Hz for each component and that for the RotD50 can be quite different; it can be as high as 40% as shown in Figure 2.16(a). Nevertheless, the average spectral acceleration of the RotD50 is generally below the spectral accelerations at the IEEE693 spectrum's plateau for the exception of some records; see Figure 2.16(b). These records were obtained from those stations located in a close proximity to the source (within 5 km), as shown in Figure 2.17.

The spectral plots for the records with an average spectral acceleration of RotD50 in close proximity or exceeding 2.5*g* are presented in Figure 2.18. Since all of them were recorded in close proximity to the source, this large value for the average spectral acceleration of the RotD50 is most likely associated with the near-source effects.

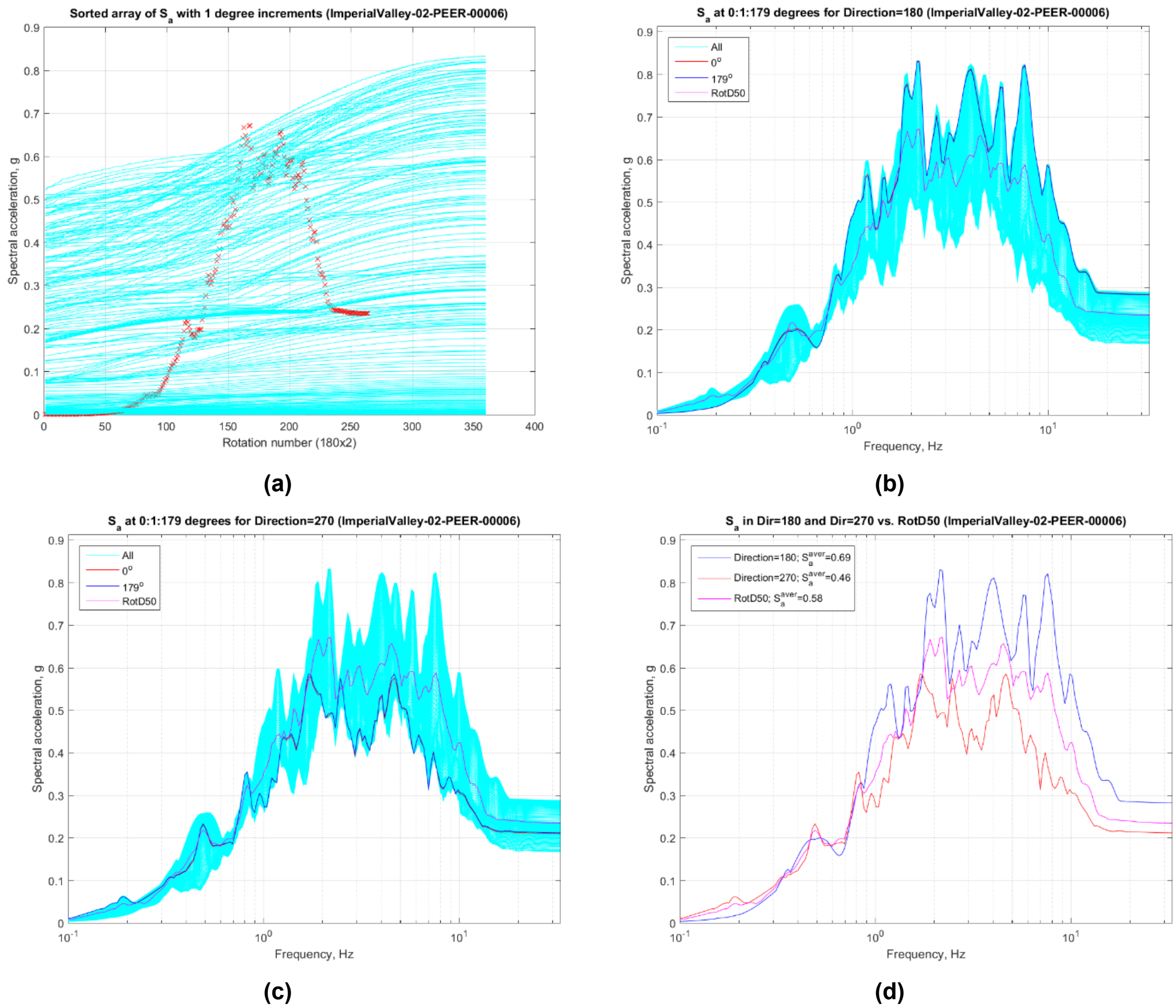

Figure 2.15 **Example of a RotD50 calculation for PEER-0006 (El-Centro) record: (a) median values of the sorted array; (b) S_A values for all rotations (direction = 180°); (c) S_A values for all rotations (direction = 270°); and (d) S_A in directions 180° and 270° vs. RotD50.**

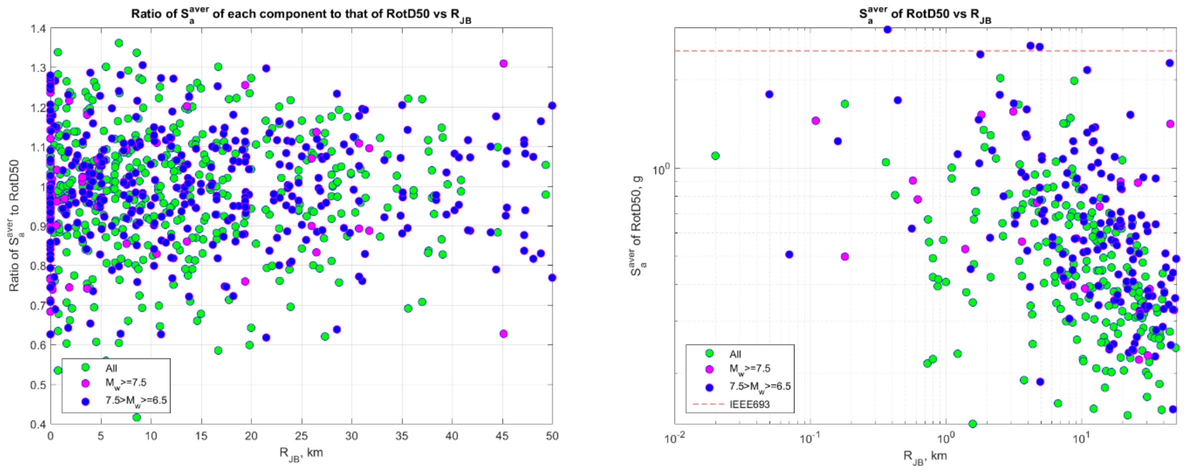

(a) **(b)**

Figure 2.16 Average spectral acceleration from 2.5 Hz to 8 Hz for each horizontal component of the set and RotD50: (a) ratio of average spectral acceleration of each component to that of RotD50; and (b) average spectral acceleration of RotD50.

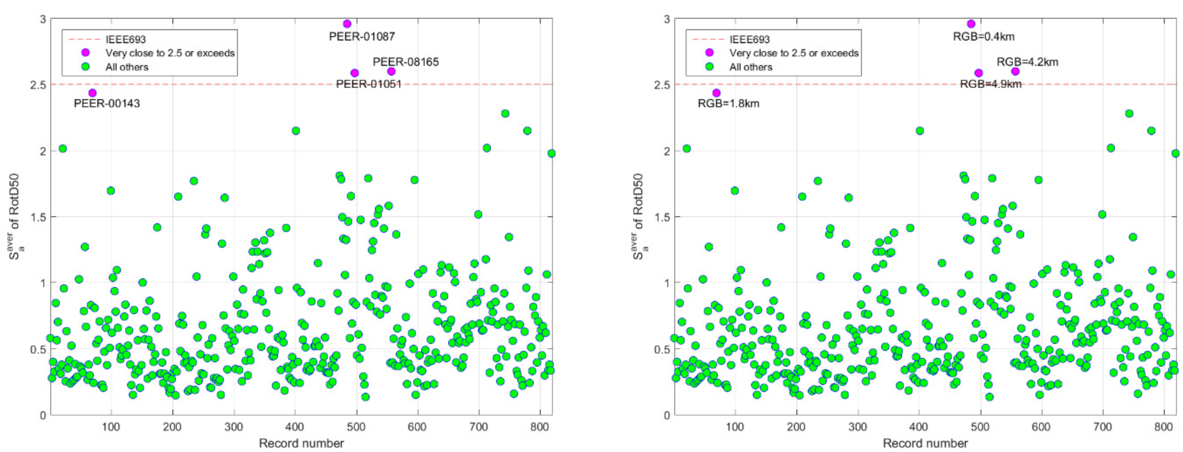

(a) **(b)**

Figure 2.17 Records with an average spectral acceleration of RotD50 in close proximity or exceeding 2.5*g*: (a) PEER record numbers; and (b) R_{JB} of the records.

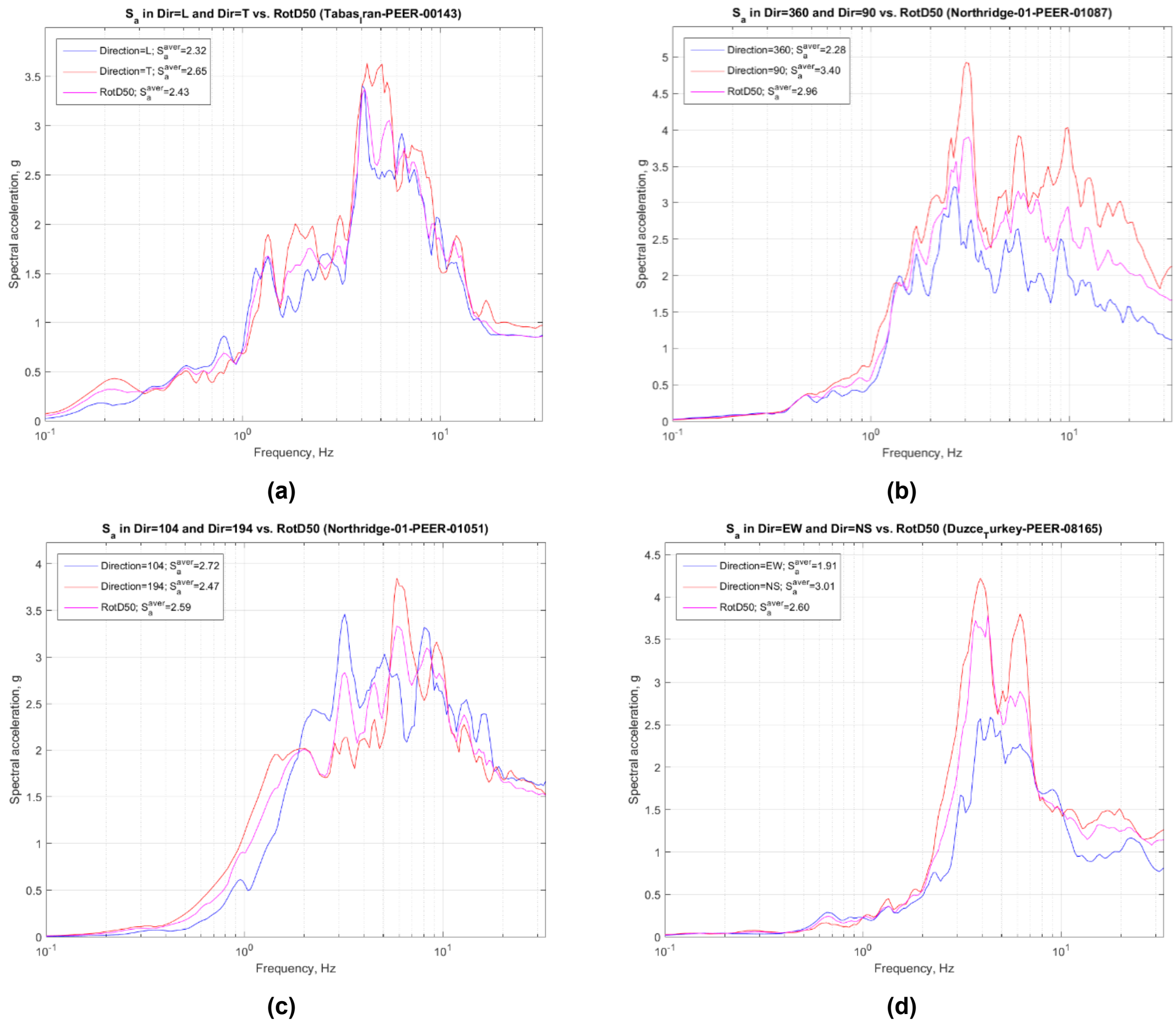

Figure 2.18 Spectral plots of the records with an average spectral acceleration of RotD50 in close proximity or exceeding 2.5*g*: (a) PEER Record No. 00143 (R_{JB} = 1.8 km); (b) PEER Record No. 01087 (R_{JB} = 0.4 km); (c) PEER Record No. 01051 (R_{JB} = 4.9 km); and PEER Record No. 08165 (R_{JB} = 4.2 km);

While S_a^{aver} for the RotD50 spectral accelerations does not exceed the spectral acceleration on the plateau by a large factor, the RotD50 accelerations at some frequencies can still exceed the IEEE693; see Figure 2.19. A comparison between Figure 2.14 and Figure 2.19 demonstrate that the RotD50 spectra are generally lower than those of individual components.

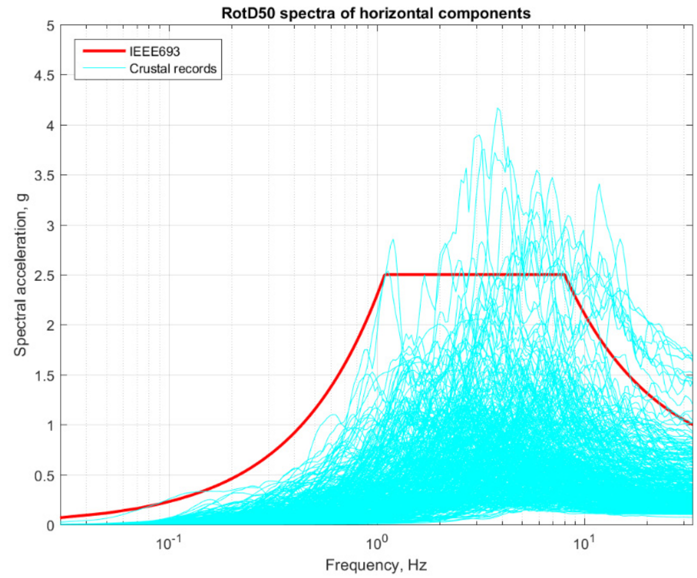

Figure 2.19 RotD50 spectra for all records.

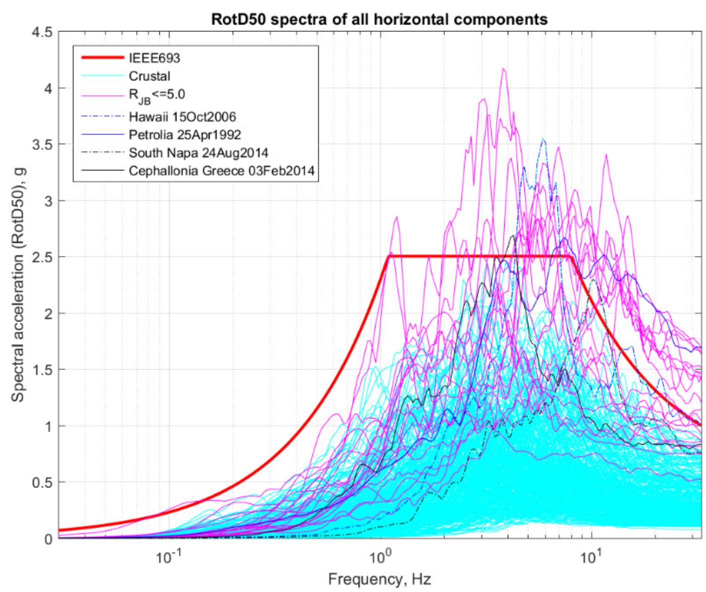

Figure 2.20 RotD50 spectra for all records (near-fault records are shown in magenta).

As identified earlier, the majority of all crustal RotD50 spectra exceeding the IEEE693 spectrum are from records obtained in close proximity to the source; see Figure 2.20. Only three records with no near-fault effects exceeded the IEEE693 spectra as shown in Figure 2.21. They amount to 1.5% of all crustal records with $R_{JB} > 10$ km (212 records). Note that these records do not exceed the IEEE693 spectrum by a large margin.

When compared at 1/24 octave resolution, the RotD50 spectral accelerations of several strong motions exceeded the IEEE693 spectrum; see Figure 2.22(a). These strong-motion records amount to 6% of the total number of crustal strong motions included in the study; see Figure 2.22(b). The latter histogram shows the distribution of records with the maximum ratio of RotD50 spectral acceleration at each frequency to the corresponding IEEE693 spectral value, e.g., the number of records with the maximum RotD50 spectral acceleration from 0.8 to 0.6 of the IEEE693 spectrum is 42.2%; see the second column blue in the plot. The magenta columns show the number of records exceeding the IEEE693, and the total percentage of those records is presented in the title of the plot.

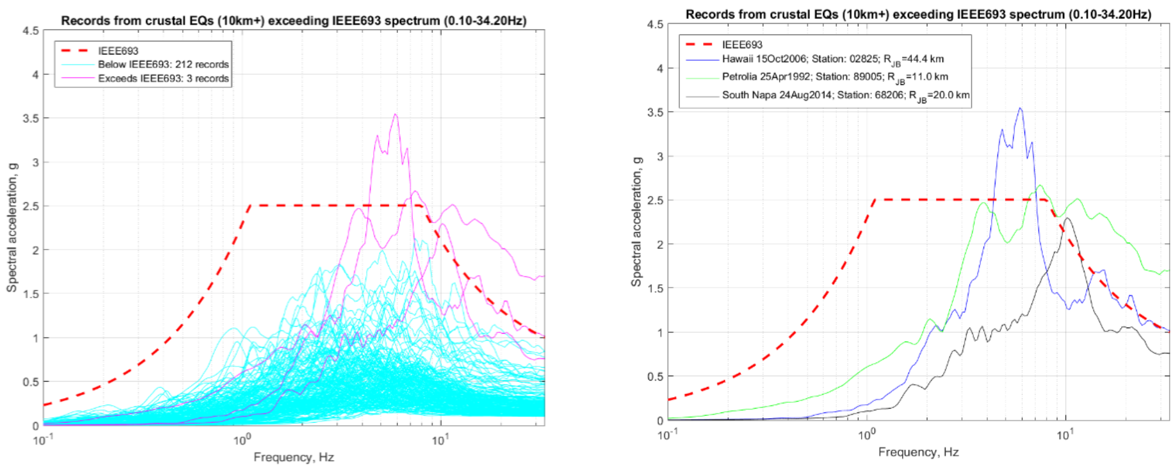

(a) **(b)**

Figure 2.21 Records where R_{JB} > 10 km exceed the IEEE693 spectrum: (a) all records with R_{JB} > 10 km; (b) records with R_{JB} > 10 km exceeding the IEEE spectrum.

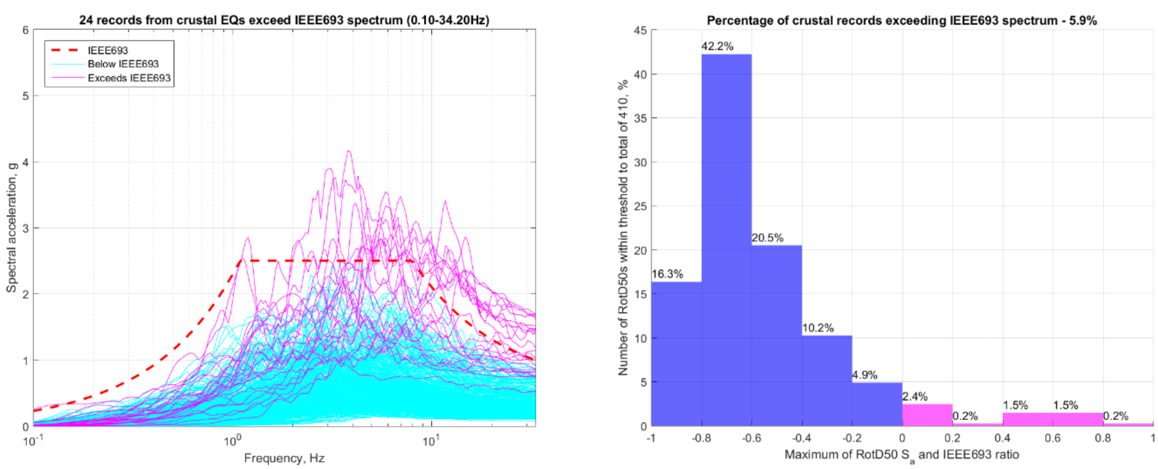

(a) **(b)**

Figure 2.22 RotD50 spectral accelerations for all crustal records and their proximity to the IEEE693 spectrum: (a) RotD50 exceeding the IEEE693; and (b) number of records exceeding the IEEE693 (magenta).

The IEEE Std 693-2005 [IEEE 2005] requires that both horizontal components of the IEEE693-spectrum-compatible strong motion need to envelope the IEEE693 spectra and very limited deviation is allowed. As shown in Figure 2.23, this results in a RotD50 that is very close to each individual component. Since each horizontal component envelopes the IEEE693, the average RotD50 spectral acceleration is greater than the spectral acceleration at the IEEE693 spectrum's plateau.

In conclusion, although the average spectral accelerations of some individual components of the strong motions may exceed the IEEE693 spectrum, the average RotD50 spectral accelerations are generally below the IEEE693's spectrum's plateau with the exception of a few records with near-fault effects. The IEEE693's enveloping requirement adds another level of conservatism to ensure that S_a^{aver} of the RotD50 of the IEEE693-spectrum-compatible time histories exceeds S_a^{aver} of the RotD50 for almost all of the historic crustal records. In addition, having the same target response spectrum in both horizontal directions causes the RotD50 spectral accelerations of the IEEE693-spectrum-compatible time histories to exceed the IEEE693. The latter adds another level of conservatism.

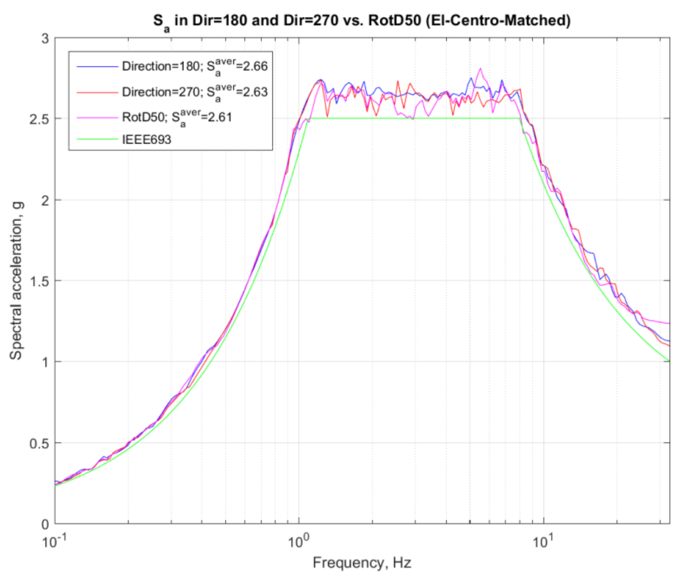

Figure 2.23 RotD50 calculation for El-Centro record modified to envelope IEEE693 (procedure from Abrahamson [1992] was used).

2.3 STRONG-MOTION RECORDS FOR SUBDUCTION AND EASTERN U.S. TYPE SEISMIC EVENTS

The set of crustal earthquakes discussed above was compared to that from subduction and eastern U.S.-type events. In order to conduct this comparison an additional two sets were selected and analyzed in the same way as the main set of records from the crustal events.

2.3.1 Dataset Selection: Subduction Type Records

Due to the specifics of the subduction zone earthquakes (i.e., some of them happened offshore), the majority of the records were obtained at locations farther away than the threshold of 50 km established for the set of crustal earthquakes. A set of records was selected from the PEER NGA West-2 database [PEER 2016] and the CESMD database [2016].

The databases were searched using the following criteria:

1. The horizontal distance of the station to rupture (R_{JB}) is less than 450 km; when R_{JB} was not known it is substituted by epicentral distance;
2. A strong-motion record has all three components;
3. Magnitude of the seismic event is greater than 5;
4. PGA of the recorded motion is 0.1*g* or greater in one of the horizontal directions;
5. Aftershocks are excluded;
6. The number of records is limited to 15 (except for the 2011 Tohoku event); and
7. Only records from seismic stations that are representative of free-field site conditions based on Campbell and Bozorgnia [2013] definition were selected.

A final list of the selected earthquake records is presented in Table 2.5 that consists of 134 records from five events. A set of subduction records with 15 records per event requirement was selected from this list. The subduction set consists of 65 records from the same 5 events.

Table 2.5 Subset of strong records from subduction type events.

Earthquake Name	Year	Magnitude	Mechanism	No of records	Source
Chile 16Sep2015 (Illapel earthquake)	2015	8.3	Subduction	5	CESMD
Iniskin 24Jan2016 (Alaska)	2016	7.1	Strike Slip*	15	CESMD
Japan 07Apr2011 (Miyagi earthquake)	2011	7.1	Subduction	15	CESMD
Japan 11Mar2011 (Tohoku earthquake)	2011	9.0	Subduction	75[!]	CESMD
Chile 27Feb2010 (Offshore Bio-Bio)	2010	8.8	Subduction	15	CESMD

* Inside the subducting Pacific Plate (AEC, 2015); [!]Limited to 15 in the subduction set

2.3.2 Dataset Selection: Eastern U.S. Records

The online PEER NGA East-2 database [2016] and the number of strong-motion records is much less than that in the PEER NGA-West2. During preparation of this report, the PEER NGA-East2 project was still ongoing and the so-called NGA Flatfile for the database was not yet available. Hence, the online database was searched using the following criteria:

1. The horizontal distance of the station to rupture (R_{JB}) is less than 138 km; when R_{JB} was not known it is substituted by epicentral distance;
2. A strong-motion record has all three components;
3. Magnitude of the seismic event is greater than 4;
4. PGA of the recorded motion is 0.1*g* or greater in one of the horizontal directions;
5. Aftershocks are excluded; and

6. Only records from seismic stations that are representative of free-field site conditions based on the Campbell and Bozorgnia [2013] definition were selected.

The search resulted in two records that were obtained during the M_W 5.8 2011 Central Virginia earthquake on August 23, 2011. A final list of the selected earthquakes is presented in Table 2.6.

Table 2.6 Subset of strong motions from eastern U.S.

Earthquake Name	Year	Magnitude	Mechanism	No of records	Source
Central Virginia, 23 August, 2011	2011	5.8	TBD	2	PEER NGA-East2

2.3.3 Major Intensity Measures of Datasets (PGA, PGV, and M_W)

The major IMs for all strong-motion records were computed: PGA and PGV versus R_{JB} are presented in Figure 2.24(a) and Figure 2.24(b). As shown in the plots, the attenuation of the PGA and PGV for the subduction records may be quite different from that for crustal records. It can be related to (1) local amplifications due to the geological characteristics of the site and/or (2) by the subsequent triggering of new earthquakes by the major event.

Although PGD is too sensitive to the low-cut filters used in the data processing to be a stable IM of ground shaking [Boore and Atkinson 2007], PGD are presented in Figure 2.25(a) to show the upper limit that is important for seismically isolated equipment. The distribution of the station proximity to the rupture versus M_W of the seismic event is presented in Figure 2.25(b).

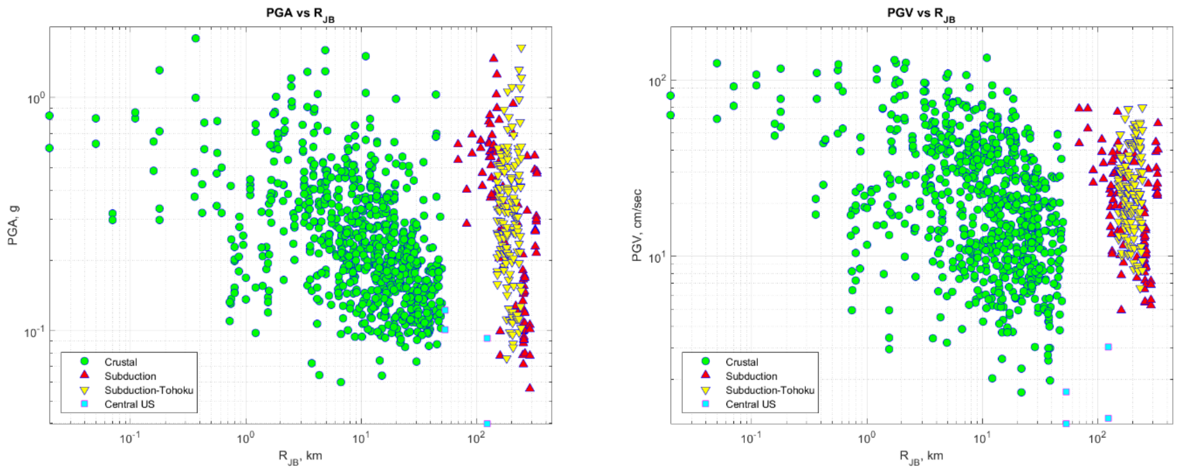

(a) (b)

Figure 2.24 (a) PGA and (b) PGV versus horizontal distance to rupture (R_{JB}).

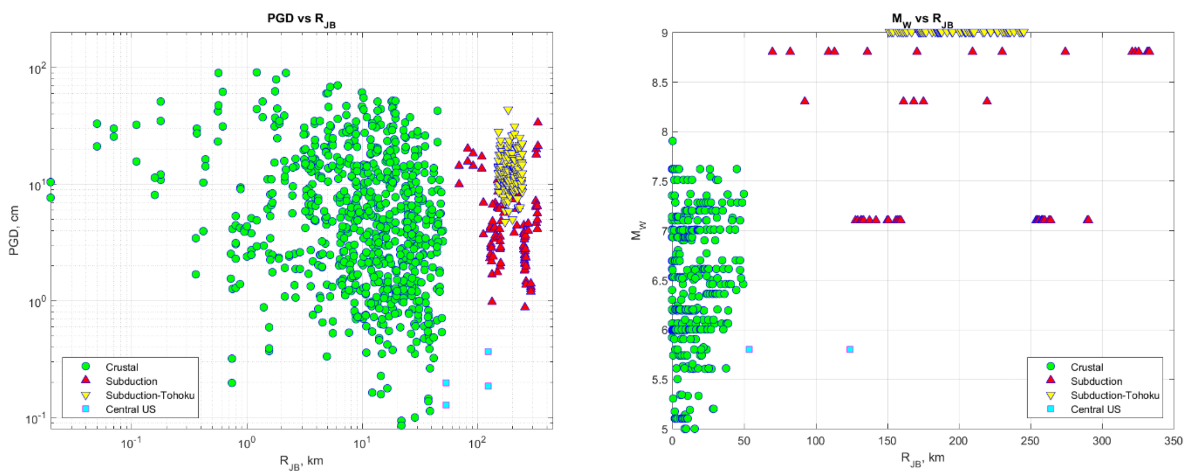

(a) (b)

Figure 2.25 (a) PGD and (b) M_W versus horizontal distance to rupture (R_{JB}).

2.3.4 Root Mean Square Acceleration and Cumulative Energy

The RMS acceleration and CE calculations are discussed in detail in Appendix A. The RMS acceleration and the total CE for the set are presented in Figure 2.26. The plots in Figure 2.26(a) show that there is a strong linear correlation in a log-log scale between total CE and RMS acceleration, especially for the 2011 Tohoku seismic event. The latter is related to the total duration of the records, which was about the same for all records. For the same value RMS acceleration, the total CE for subduction zone earthquakes is much higher than that for crustal events. The total CE of the subduction zone records attenuates much slower than that for the crustal seismic events; see Figure 2.26(b). In the case of the 2011 Tohoku event, some of these records exceed the maximum total CE of the crustal set by a factor of three or so as shown in Figure 2.26(b).

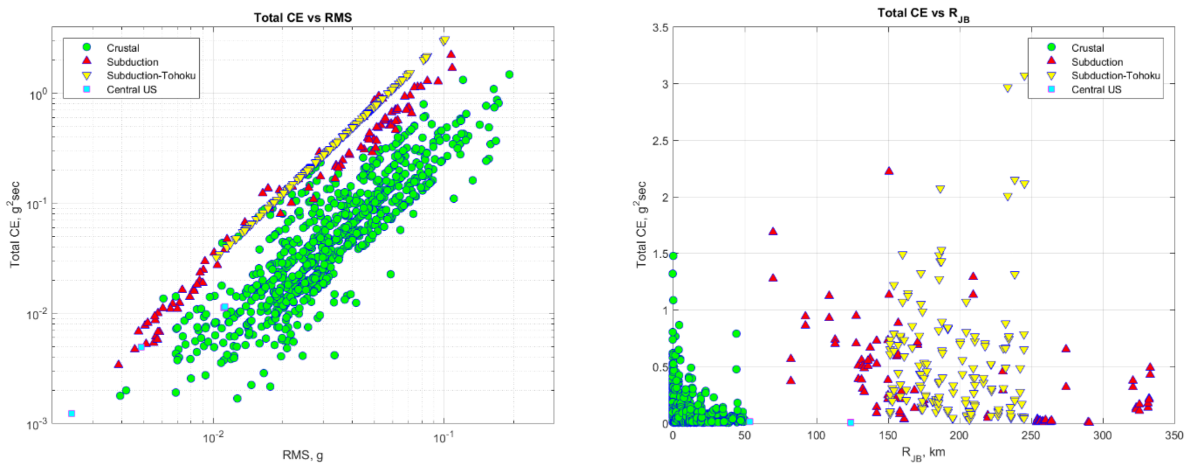

(a) (b)

Figure 2.26 Total cumulative energy vs. (a) root mean square acceleration and (b) *R_{JB}*.

2.3.5 Duration Parameters

The IEEE Std 693-2005 [IEEE 2005] and IEEE P693/D16 [IEEE693 WG 2017] require that the bracketed duration of the strong-motion time history used for qualification testing and analysis meets or exceeds 20 sec; see Figure 2.27(a). In addition, the IEEE Std 693-2005 [IEEE 2005] and its current draft version IEEE P693/D16 [IEEE693 WG 2017] require that a strong-part ratio of the time history is at 30% and greater. Both these thresholds are presented in Figure 2.27(b). In both plots, the magenta colored region indicates a zone where the IEEE693 requirements are satisfied.

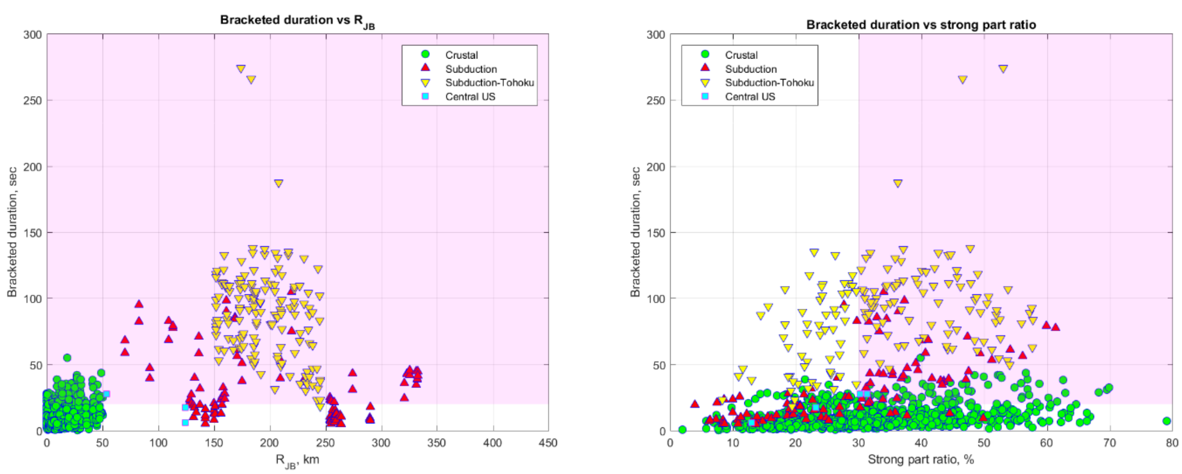

(a) (b)

Figure 2.27 Duration-related thresholds specified in IEEE693: (a) threshold for IEEE693's bracketed duration; and (b) thresholds for IEEE693's strong-part ratio and bracketed duration.

Note that all duration-related parameters of the subduction type earthquakes are much greater than the corresponding ones for crustal earthquakes, which is to be expected. This is valid for the bracketed duration [shown in Figure 2.27(a)] and all CE-based durations $D_{25–75}$, $D_{5–95}$, and $D_{5–75}$ presented in Figures 2.28(a), 2.28(b), and 2.28(c), respectively. In contrast, the strong-part ratio for subduction events is about the same as that for crustal type earthquakes as shown in Figure 2.28(d). A summary of duration-related parameters is presented in Table 2.7 that lists mean values and coefficients of variations for each parameter.

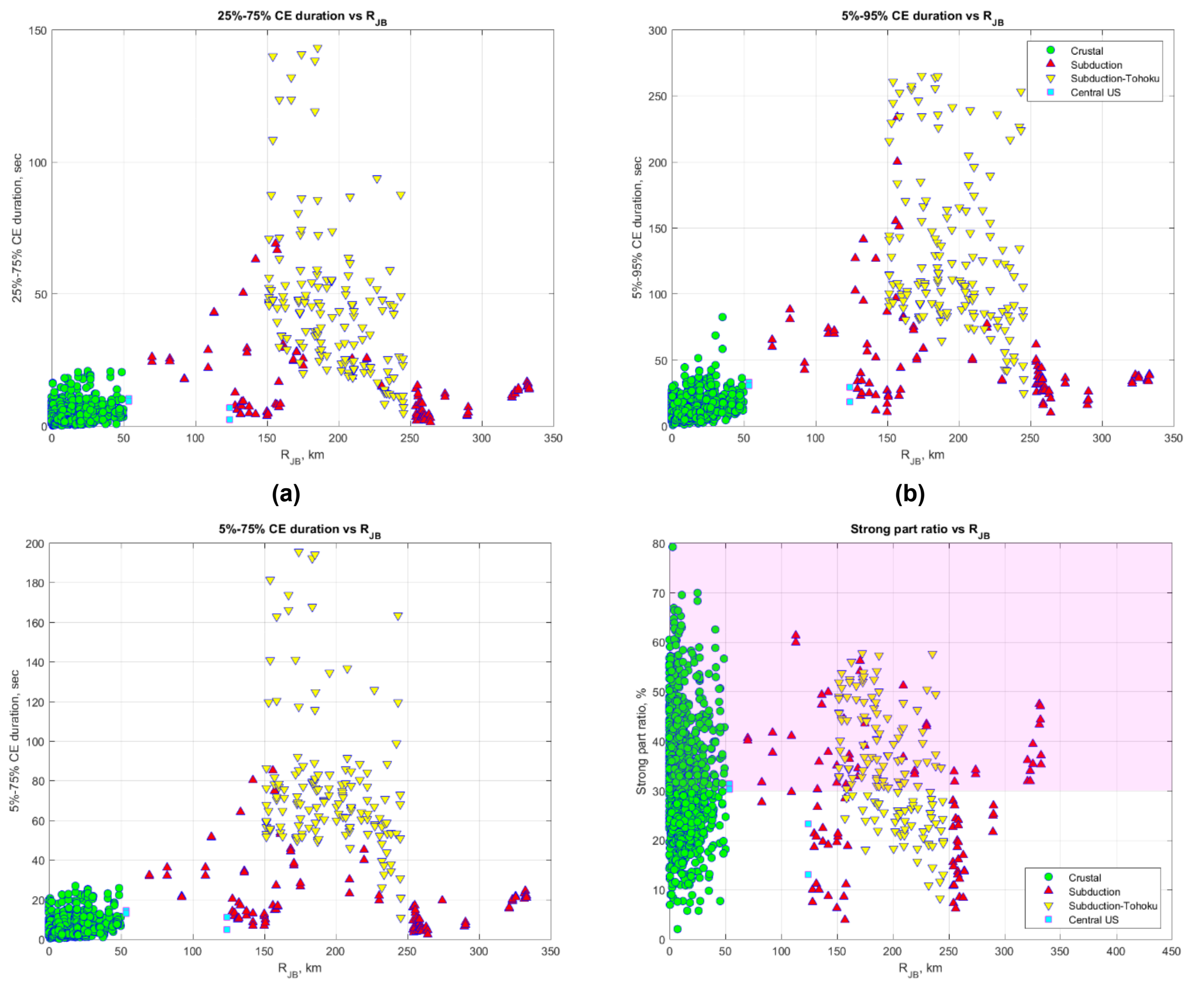

Figure 2.28 **Cumulative energy-based durations: (a) 25%–75% CE duration vs. R_{JB}; (b) 5%–95% CE duration vs. R_{JB}; (c) 5%-75% CE duration vs. R_{JB}; and (d) strong-part ratio vs. R_{JB}.**

Table 2.7 Duration related parameters for subduction events (up to 15 records per event).

Duration parameter	Mean	COV (%)	Note
Bracketed duration	46.12sec	76.5	Needs to meet 20 sec or exceed*
$D_{5\text{–}95}$	73.50 sec	84.0	
$D_{5\text{–}75}$	35.93 sec	101.7	
$D_{25\text{–}75}$	25.47 sec	108.4	
Strong-part ratio	31.34 sec	44.1	Needs to meet 30% or exceed *

*IEEE Std 693-2005 [IEEE 2005] and IEEE P693/D16 [IEEE693 WG 2017].

2.3.6 Cycle Counting Related Parameters

As one of the IM parameters, a number of cycles exceeding 70% of the peak value—the so-called number of high cycles—was computed for each strong motion in the subduction and eastern U.S. sets. The number of high cycles of the subduction set is about the same as that of the crustal set as presented in Figure 2.29(a). The number of high cycles in the SDOF response with mean and mean-plus-one-deviation is presented in Figure 2.29(b). As expected, the number of high cycles in the SDOF response for subduction records is higher than those for the crustal records. It exceeds the limit of two cycles set the by the IEEE Std 693-2005 [IEEE 2005] (see the magenta region in the plot).

A summary of high-cycle counting conducted for the set of 65 subduction records is presented in Table 2.8. The mean number of high cycles (2.44) for subduction-zone events exceeds that of the crustal events (1.55).

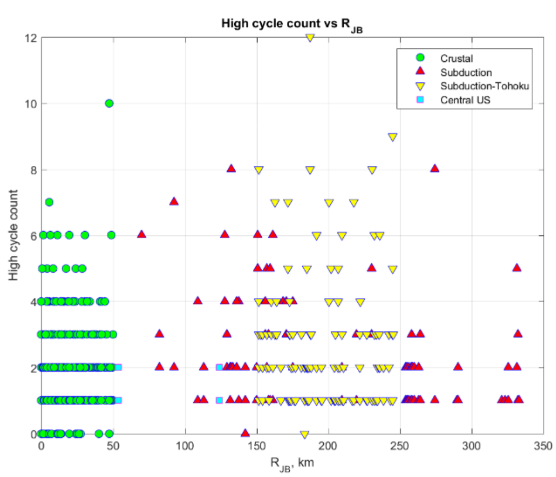

(a)

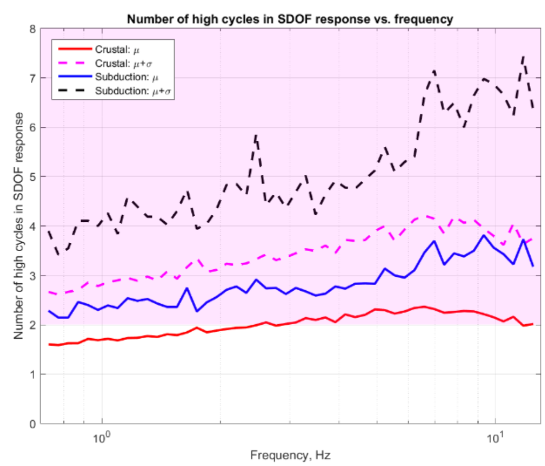

(b)

Figure 2.29 Cycle counting parameters of strong motions: (a) number of high cycles; and (b) number of cycles in SDOF response.

Table 2.8 Summary of high cycles

Cycle counting parameter	Mean	COV (%)	Note
Number of high cycles	2.44	70.0	Independent of scaling

2.3.7 Spectral Proximity to IEEE693 Spectrum and Spectral Average

Both K_S and D_{SA} were computed for each record from the subduction dataset. The results are presented in Figure 2.30. Since the eastern U.S. records were recorded far away from a source of a moderate earthquake, one of the records from eastern U.S. requires the largest scaling factor to best fit the IEEE693 spectrum anchored at 1.0*g* as shown in Figure 2.30(a). In contrast, the majority of subduction-zone records require a relatively small best fit factor, which can be as low as five. As presented in Figure 2.30(b), the cumulative distance to the IEEE693 spectrum at best fit for all subduction records is within the maximum of 20.6 obtained for that of crustal earthquakes.

Figure 2.31 shows that the best fit factor, K_S, is inversely proportional to PGA, as was noticed earlier in regard to the crustal records. For smaller PGAs, a larger best fit factor is required, which is to be expected. The spectral acceleration average from 2.5 Hz to 8.0 Hz was calculated for all records (including subduction and eastern U.S.) with the results presented in Figure 2.32. A summary of average and coefficients of variations for the subduction type records is presented in Table 2.9.

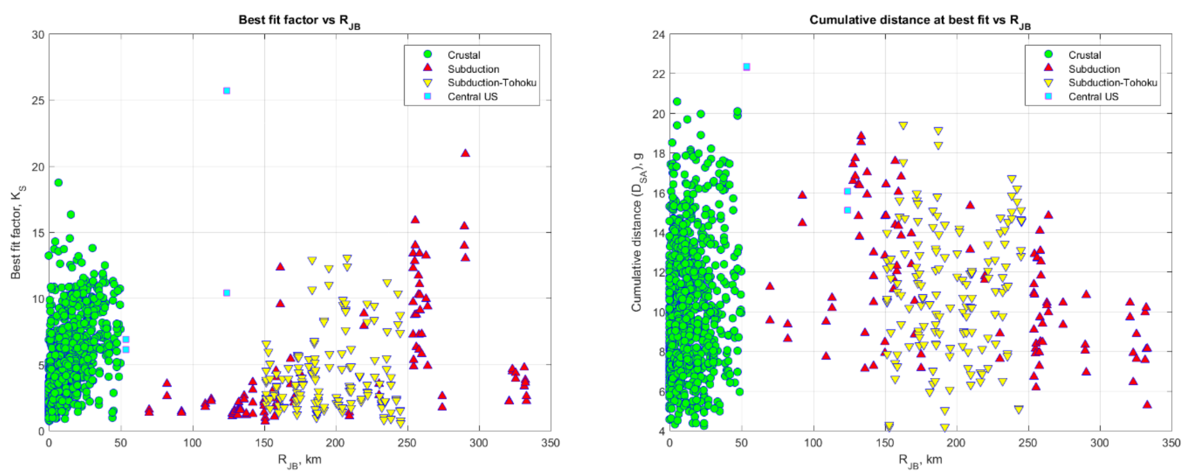

(a) (b)

Figure 2.30 Parameters of best fit to IEEE693 spectrum: (a) K_S vs. R_{JB}; and (b) Cumulative distance, D_{SA}, vs. R_{JB}.

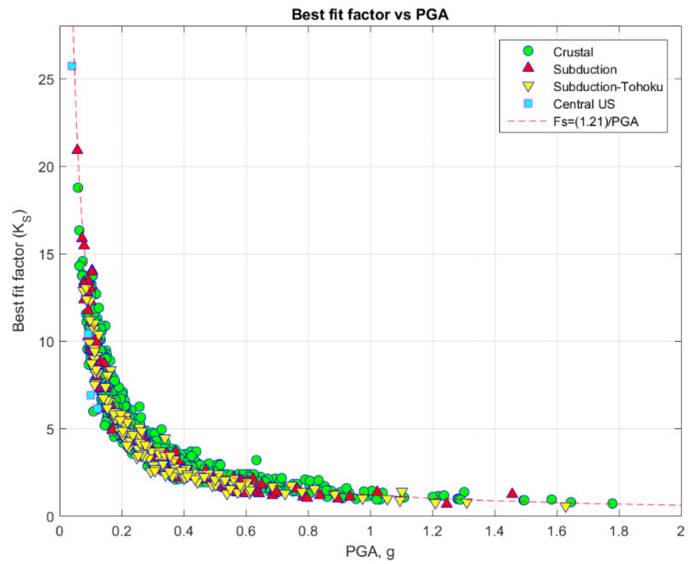

Figure 2.31 Best fit factor is closely approximated by F_S = 1.21/PGA.

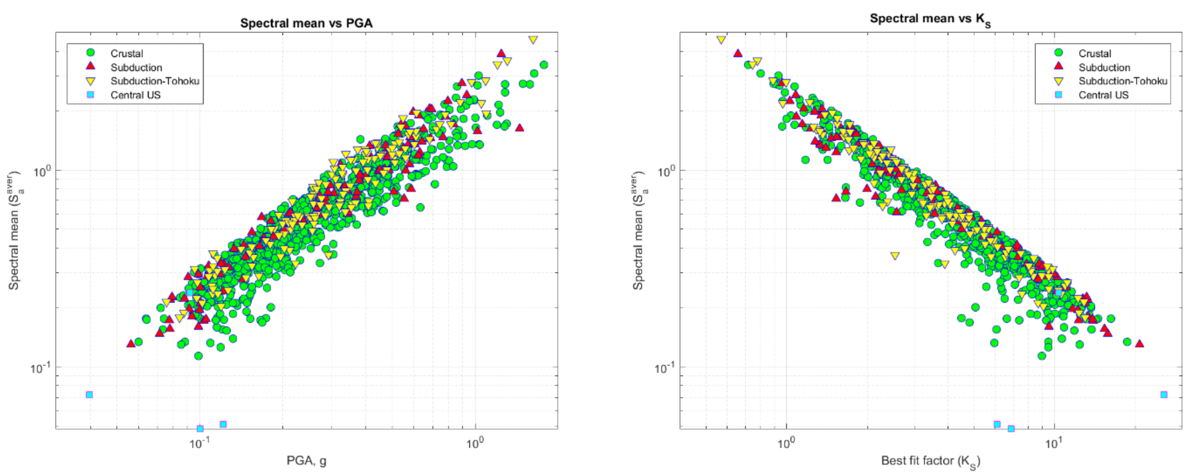

(a) **(b)**

Figure 2.32 Correlations of spectral average with PGA and K_S: (a) strong correlation of S_a^{aver} with PGA; and (b) strong correlation of S_a^{aver} with K_S.

Table 2.9 Summary of spectral proximity parameters and spectral average (subduction type records).

Parameter	Mean	COV (%)	Description
D_{SA}	11.21*g*	30.0	Distance to IEEE693 spectrum at best fit
K_S	4.69	84.7	Best fit scaling
S_a^{aver}	0.88*g*	68.4	Spectral average from 2.5 Hz to 8 Hz

2.3.8 Spectral Accelerations

Spectral accelerations for crustal, subduction, and eastern U.S. records are presented in Figure 2.33. The spectral plots show that the subduction type records can exceed the IEEE693 spectrum. Spectral acceleration of a single component of the 2011 Tohoku earthquake exceeds the IEEE693 spectral plateau by a factor of 3 or so as presented in Figure 2.33.

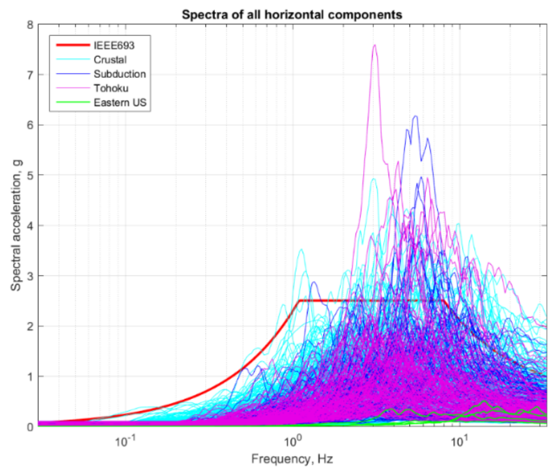

Figure 2.33 Spectra vs. IEEE693 spectrum anchored at 1*g*.

2.3.9 RotD50 Spectral Accelerations

The objective of this section is to investigate the case when some individual components of the strong motions exceed the IEEE693 spectrum as shown in Figure 2.33. When the subduction set is considered, the difference between average spectral acceleration from 2.5 Hz to 8.0 Hz for each component and that for the RotD50 can be quite different, and can be close to 40% or so as shown in Figure 2.34(a). Nevertheless, the average spectral acceleration of the RotD50 is generally below the spectral accelerations at the IEEE693 spectrum's plateau with the exception of some records; see Figure 2.34(b). The records with S_a^{aver} of the RotD50 exceeding 2.5*g* are shown by the diamonds in Figure 2.34(a). The RotD50 spectral accelerations are much lower than the spectral accelerations of individual horizontal components; see Figure 2.35.

When compared at 1/24 octave resolution, the RotD50 spectral accelerations of several strong motions exceed the IEEE693 spectrum as presented in Figure 2.36(a). These strong-motion records amount to 16.9% of the total number of subduction strong motions included in the study as presented in Figure 2.36(b). The latter histogram shows the distribution of records with a maximum ratio of the RotD50 spectral acceleration at each frequency to the corresponding IEEE693 spectral value. For example, the number of records with a maximum RotD50 spectral acceleration from 0.8 to 0.6 of the IEEE693 spectrum is 21.5% (the second blue column in the plot). The magenta columns show the number of records exceeding the IEEE693, and the total percentage of those records is presented in the title of the plot.

In conclusion, subduction-zone records may contain more demanding spectral accelerations than those for the crustal earthquakes. This result is well correlated to the results in the recent companion study [Mazzoni et al. 2017], which concluded that the subduction-zone earthquake records have a smaller margin in high frequencies with respect to the High PL IEEE693 spectrum. The increased demand can be related to the subsequent smaller earthquakes following the major rupture and/or local amplifications of the sites due to basin or other geological effects.

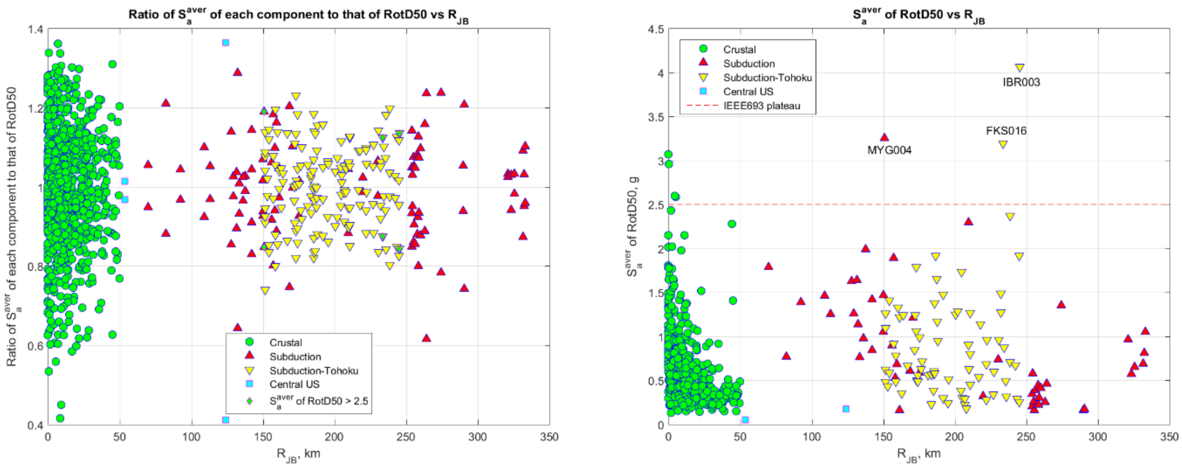

(a) (b)

Figure 2.34 Average spectral acceleration from 2.5 Hz to 8 Hz for each horizontal component of the records and RotD50: (a) ratio of average spectral acceleration of each component to that of RotD50; and (b) average spectral acceleration of RotD50.

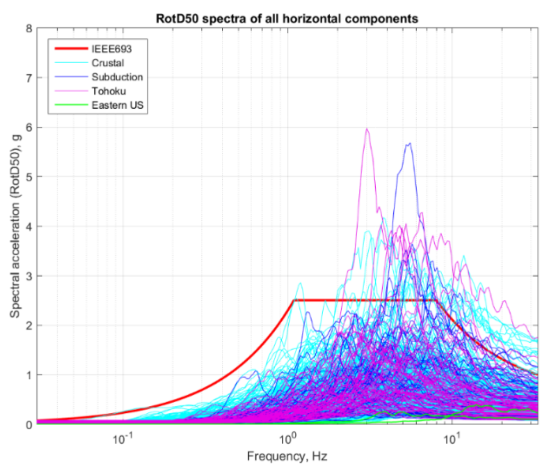

Figure 2.35 RotD50 spectra vs. IEEE693 spectrum anchored at 1*g*.

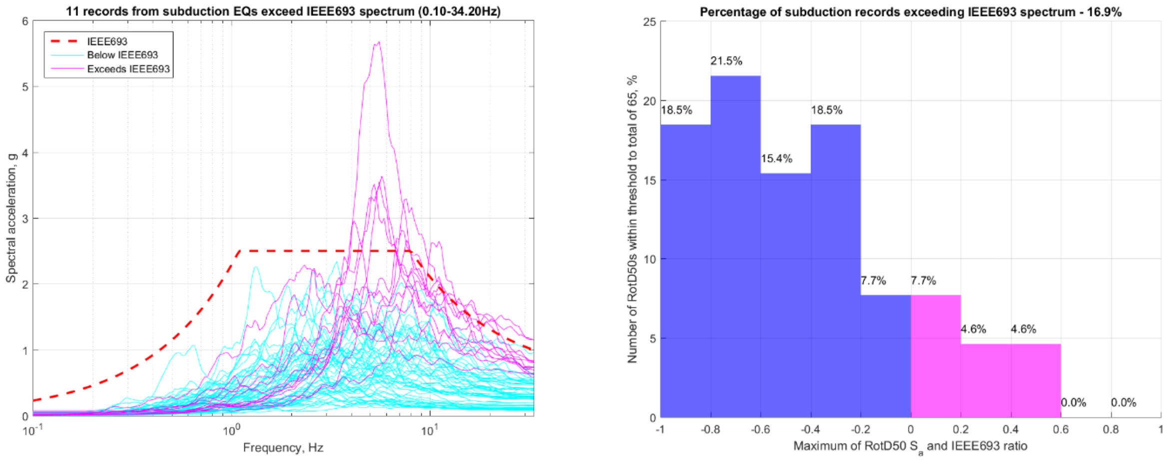

(a) (b)

Figure 2.36 Subduction records with RotD50 spectral accelerations exceeding IEEE693: (a) RotD50 exceeding the IEEE693; and (b) number of records exceeding IEEE693.

2.4 VERTICAL TO HORIZONTAL COMPONENT RATIO (CRUSTAL AND SUBDUCTION)

The RotD50 spectral accelerations were used in determining the vertical to horizontal ratio estimate. The current version of the IEEE Std 693-2005 [IEEE 2005] states that the spectrum of the vertical component shall be at 80% of the horizontal spectrum. This section contains a discussion related to this factor of 80%. For simplicity, it is called V2H factor. This factor is calculated as a ratio of the vertical spectral accelerations at each frequency to the corresponding RotD50 spectral accelerations.

2.4.1 V2H Factor: Crustal Type Records

The V2H factors for all crustal records considered in the study is presented in Figure 2.37(a). The mean and mean plus one standard deviation is presented in Figure 2.37(b). The latter plot shows that the mean value of the ratio meets the IEEE693 expectations up to about 7.2 Hz. The factor has a maximum value of 1.25 at 16.1 Hz.

Next, the strong-motion records with a relatively large PGA were identified and selected based on the following condition: the RotD50 spectral acceleration at the largest frequency of 35.2 Hz was considered an effective PGA of the record in the horizontal direction. A subset was selected based on the condition that the effective PGA (the RotD50 spectral acceleration at 35.2 Hz) is more than 0.2*g*. The corresponding plots are presented in Figure 2.38. The mean of the V2H factor still satisfies the IEEE693 statement up to 6.6 Hz, with the peak value of 1.35 at 16.6 Hz.

The V2H factor for the records without near-fault effects and high PGA has a much better correlation with the IEEE693 requirement as presented in Figure 2.39. The mean value of the V2H factor stays below 0.8 up to 8.1 Hz and has a maximum value of 1.12 at 16.1 Hz.

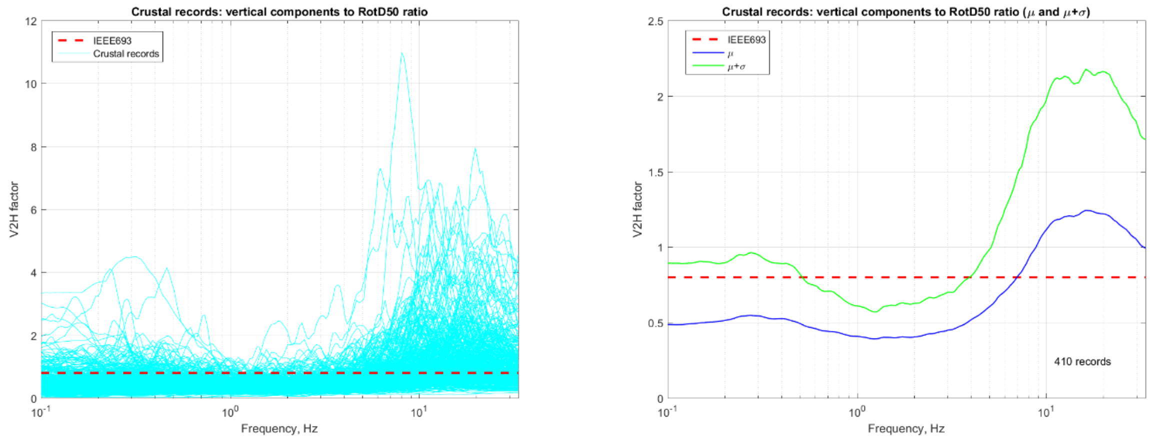

(a) (b)

Figure 2.37 V2H factor for all crustal records: (a) V2H factors for individual records; and (b) mean and mean plus one standard deviation.

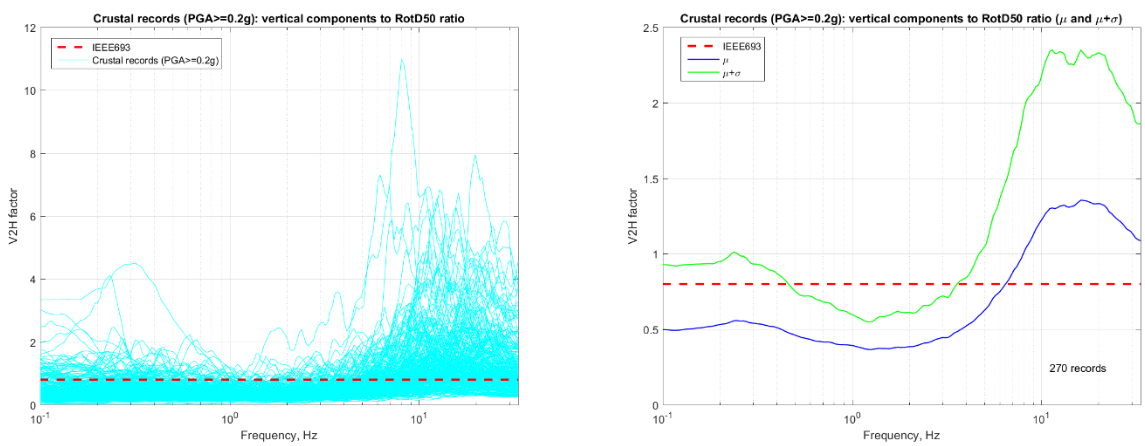

(a) (b)

Figure 2.38 V2H factor for crustal records with effective horizontal PGA meeting and exceeding 0.2*g*: (a) V2H factors for individual records; and (b) mean and mean plus one standard deviation.

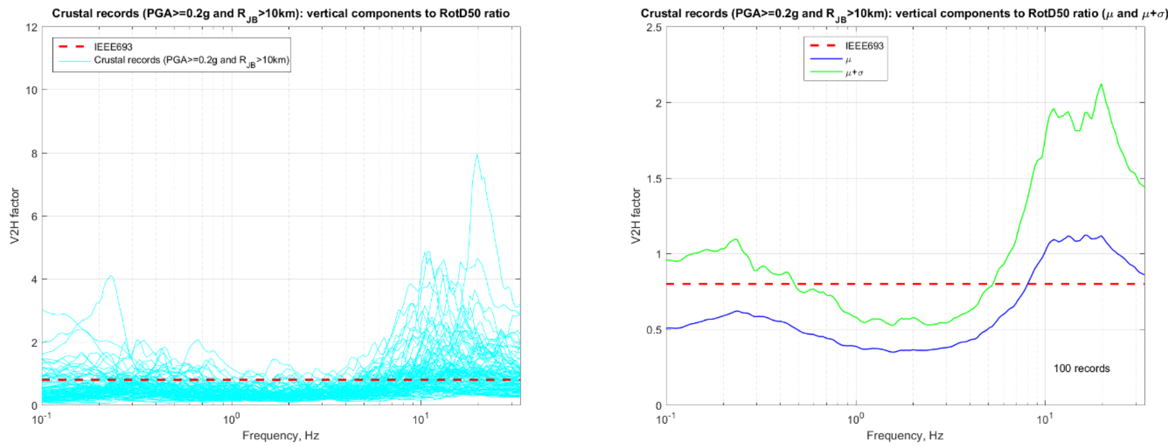

(a) **(b)**

Figure 2.39 V2H factor for crustal records with effective horizontal PGA meeting and exceeding 0.2*g* and R_{JB} > 10 km: (a) V2H factor for individual records; and (b) mean and mean plus one standard deviation.

2.4.2 V2H Ratio: Subduction Type Records

The V2H factor for the subduction records is quite different from that for crustal records as presented in Figure 2.40. It exceeds the threshold of 0.8 in low and high-frequency ranges. The mean value of the V2H factor stays below 0.8 from 0.3 Hz to 12.8Hz and after 20.1 Hz. It has a maximum value of 1.20 at 0.1 Hz. The latter frequency is the lowest frequency of the frequency range considered in the study.

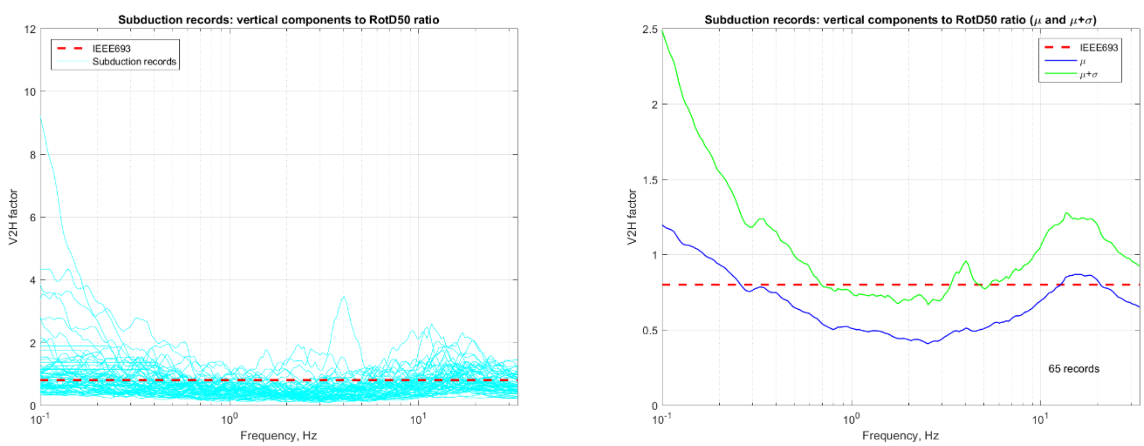

(a) **(b)**

Figure 2.40 V2H factor for subduction records: (a) V2H factor for individual records; and (b) mean and mean plus one standard deviation.

2.4.3 V2H Factor: All Records

The V2H factors for all crustal and subduction records are presented in Figure 2.41. Two subsets of crustal records are also added to the plot. Since the IEEE693 High Performance spectrum was developed based on the crustal records without the near-fault effects and with relatively large PGA, the corresponding curve (shown in green) is the most representative for the V2H factor assumed in the IEEE Std 693-2005 [IEEE693 2005]. As noted earlier, the mean value of the V2H factor for these records stays below 0.8 up to 8.1 Hz and has a maximum value of 1.12 at 16.1 Hz.

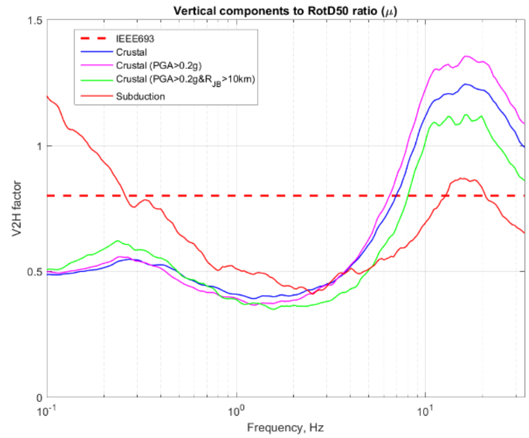

Figure 2.41 V2H factor for crustal and subduction records.

2.5 SEED MOTION SELECTION AND IEEE693-SPECTRUM-COMPATIBLE TIME HISTORIES

Based on an analysis of the strong-motion parameters discussed in the previous sections, several records were selected as the seed motions for subsequent modifications in order to turn them into IEEE693-spectrum-compatible strong-motion time histories. The spectral matching is performed at 5% damping, in accordance with IEEE P693/D16 [IEEE693 WG 2017]. To preserve the non-stationary feature of the historic records, the spectral matching was performed in a time domain. The matching procedure in the time domain is a FORTRAN implementation of the algorithm developed by Abrahamson [1992]. The procedure was updated in 2005 [Hancock et al. 2006]. In the 2005 version of the procedure (RspMatch2005), additional wavelets are sometimes needed to prevent a divergence of the solution. Since these wavelets sometimes have limited success in ensuring a solution convergence, another update in 2009 was undertaken [Al Atik and Abrahamson 2010] that resulted in the newer version called RspMatch2009. An improved method for the generation of a spectrum-compatible acceleration time series was added into the procedure. An improved tapered cosine wavelet was developed for the adjustment of recorded ground motions resulting in an acceleration time series that has no drift in the corresponding velocity and displacement profiles. As a result, the new method did not require a baseline correction of the adjusted record after each pass. The application of the new wavelet ensured stability and convergence of the spectral matching solution. This updated version of the procedure was utilized in this study.

In addition, three 3-component synthetic strong-motion time histories compatible with IEEE693 requirements were generated to have an option of using strong-motion time histories generated from a set of harmonics. SimQke-1 [Gasparini, 1976; Vanmarcke 1976] was used in generation of these synthetic strong-motion time histories. SimQke-1 is a FORTRAN-based program that generates a synthetic time history, the spectrum of which matches the target spectrum. The same parameters were computed for all IEEE693-spectrum-compatible strong-motion time histories and were compared to those of the set.

2.5.1 Seed Motions Selection: Crustal Records

The main approach in selecting the seed motions is to choose records based on the high values of parameters that are independent of scaling while maintaining the lowest possible values for the best fit factor (K_S) and the distance to IEEE693 spectrum at best fit (D_{SA}). The latter helps to select a seed motion that is "naturally" close to the IEEE693 spectrum and does not require excessive scaling with a relatively small cumulative distance from the IEEE693 spectrum. A schematic representation of this approach is presented in Figure 2.42. The schematic diagram shows the sets of parameters that should intersect where the seed motions are. The parameters are sorted in a way that is the most beneficial in the selection of a robust record, i.e., K_S and D_{SA} are increasing in a direction pointing away from the sets' intersection, and all other parameters are increasing toward the point of the intersection.

Note that the IEEE Std 693-2005 and P693/D16 requirements [IEEE 2005] on the bracketed duration and the strong-part ratio will control the selection. As a result of this selection approach, four 3-component records were selected as seed motions as presented in Table 2.10. The major selection parameters are presented in Table 2.11.

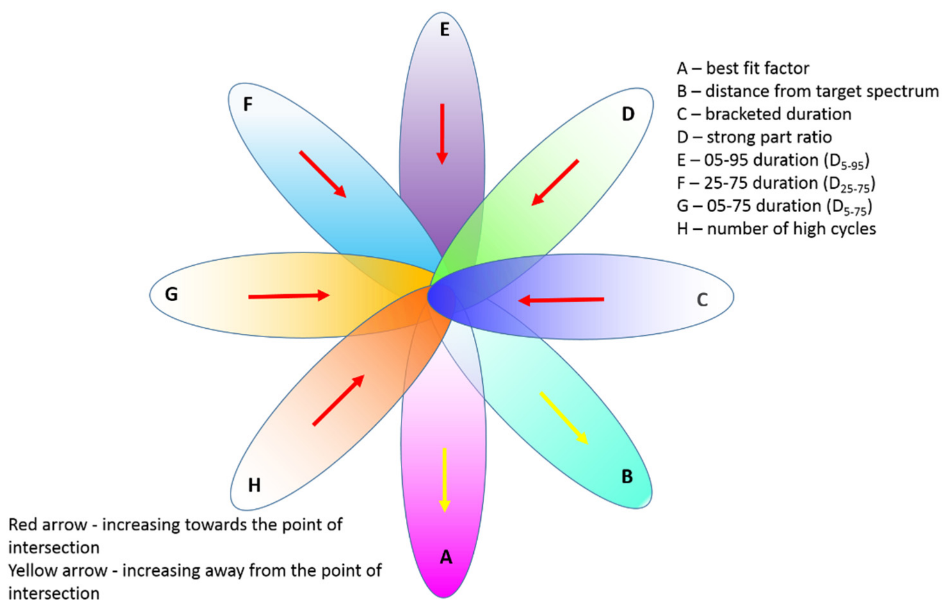

Figure 2.42 Schematic diagram of seed motion selection approach.

Table 2.10 Four 3-component records selected based on the parameter analysis.

Earthquake	Year	Magnitude	Record ID (database)
Imperial Valley-02 (El Centro)	1940	6.95	RSN0006 (PEER NGA-West2)
Landers, CA	1992	7.28	RSN0864 (PEER NGA-West2)
Chi-Chi, Taiwan	1999	7.62	RSN1503 (PEER NGA-West2)
El Mayor-Cucapah, Mexico	2010	7.20	RSN5827 (PEER NGA-West2)

Table 2.11 Duration and scaling related parameters of the selected seed motions.

Earthquake record	Duration (sec)	Strong-part ratio (R_{SP})	Factor K_S	Distance to IEEE693, D_{SA}
RSN0006 (PEER NGA-West2) from 1940 El Centro, CA	24.68	44.4%	3.93	5.71
	24.81	60.3%	5.63	4.83
	12.18	35.1%	5.71	11.51
RSN0864 (PEER NGA-West2) from 1992 Landers, CA	28.40	62.9%	4.52	7.64
	30.96	69.5%	4.17	7.04
	29.94	71.0%	4.31	6.91
RSN1503 (PEER NGA-West2) from 1999 Chi-Chi, Taiwan	26.82	57.1%	2.10	6.56
	25.43	56.1%	2.38	5.94
	22.48	37.5%	3.51	6.53
RSN5827 (PEER NGA-West2) from 2010 El Mayor-Cucapah, Mexico	33.21	41.5%	2.39	6.26
	34.76	46.5%	2.67	7.52
	32.37	60.0%	0.89	16.05

Parameters of Seed Motions from Crustal Records. The bracketed duration versus strong-part ratio for all strong-motion records compared to those for the selection is presented in Figure 2.43. The magenta shade reflects the IEEE Std 693-2005 and P693/D16 requirements [IEEE 2005].

The best fit parameters K_S and D_{SA} for the selected motions are presented in Figure 2.44. The cyan shade shows the thresholds established in this study. As presented in the plots, the best fit factor, K_S, is less than 6 or less than 32% of the set's maximum and D_{SA} is less than 8*g*, which is about 39% of the set's maximum value. Note that the minimum value of D_{SA} for the entire set was 4.24*g*. Other duration-related parameters are presented in Figure 2.45. As shown in the plots, the following thresholds were satisfied: $D_{5\text{–}95}$, $D_{5\text{–}75}$, and $D_{25\text{–}75}$ durations of the selected records are longer than 24 sec, 12 sec, and 10 sec, respectively. The cyan shade shows the thresholds established in this study. The RMS acceleration, total CE and average spectral acceleration S_a^{aver} of the selected records versus those of the entire set are presented in Figure 2.46.

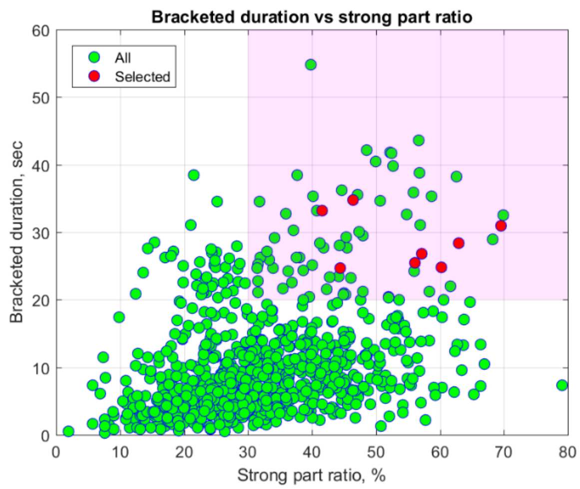

Figure 2.43 Bracketed duration vs. strong-part ratio.

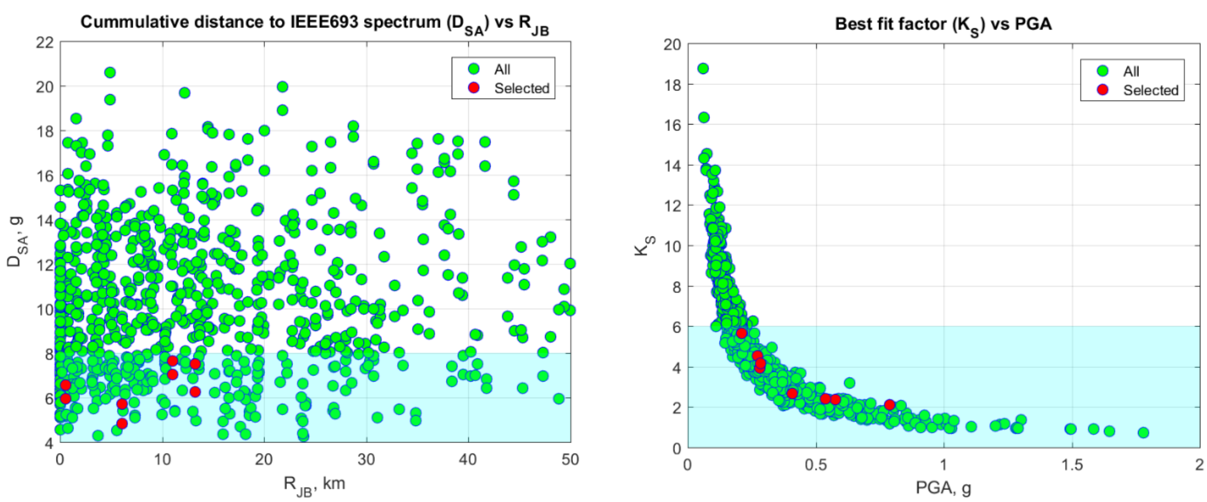

(a) (b)

Figure 2.44 Best fit parameters of selected records vs. those for the set: (a) *D_{SA}* is less than 8*g* (less than 39% of maximum): and (b) *K_S* is less than 6 (less than 32% of maximum).

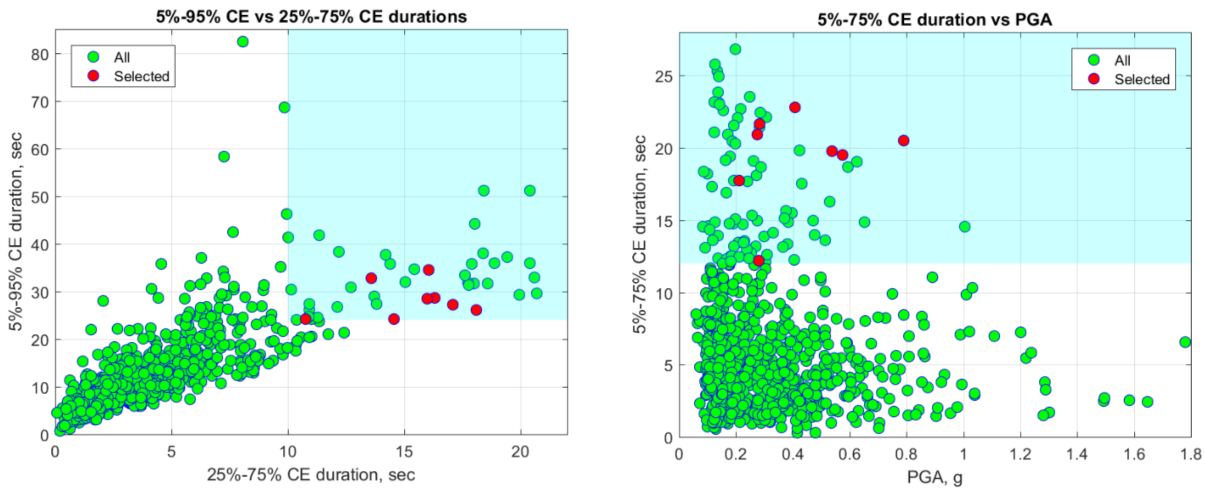

(a) **(b)**

Figure 2.45 Duration-related parameters of selected records vs. those for the set: (a) $D_{5–95}$ is more than 24 sec and $D_{25–75}$ is more than 10 sec; and (b) $D_{5–75}$ is more than 12 sec.

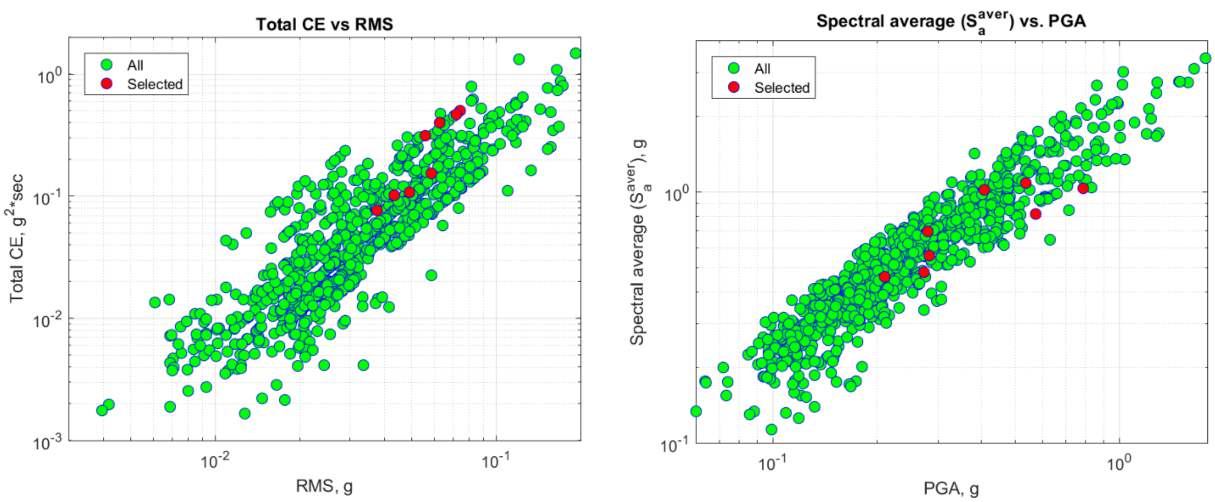

(a) **(b)**

Figure 2.46 The RMS acceleration, total cumulative energy, and average spectral acceleration S_a^{aver} of selected records vs. those for the set: (a) RMS acceleration and total CE; and (b) spectral average S_a^{aver}.

2.5.2 Seed Motions Selection: Subduction Records

The same approach in the selection of the seed motions from the subduction records was followed. A schematic representation of this approach is discussed earlier and presented in Figure 2.42. This schematic diagram shows the sets of parameters that should intersect where the seed motions are. The parameters are sorted in a way that is the most beneficial in a selection of a robust record, i.e., K_S and D_{SA} are increasing in a direction pointing away from the intersection and all other parameter are increasing toward the intersection point. Note that the IEEE Std 693-2005 and P693/D16 requirements [IEEE 2005] on the bracketed duration and the strong-part ratio will control the selection. As a result of this selection approach, a single 3-component record was selected as a seed motion as presented in Table 2.12. The major selection parameters are presented in Table 2.13.

Table 2.12 Three three-component records selected based on the parameter analysis.

Earthquake	Year	Magnitude	Epicenter (km)	Record ID (database)
Chile, February 27, 2010	2010	8.8	69.7	CONSTITUCIONS/N4598 (CESMD)

Table 2.13 Duration and scaling related parameters of the selected seed motions.

Earthquake record	Duration (sec)	Strong-part ratio (R_{SP})	Factor K_S	Distance to IEEE693, D_{SA}
CONSTITUCIONS/N4598 Chile, February 27, 2010	58.76	40.65%	1.57	11.25
	68.15	40.05%	1.35	9.56
	53.65	36.82%	4.31	6.91

2.5.3 IEEE693-Spectrum-Compatible Time Histories Generated from Seed Motions

To preserve the non-stationary feature of the historic seed records, the spectral matching procedure was performed in a time domain. The matching procedure is a FORTRAN implementation of the algorithm developed by Abrahamson [1992]. Note that the TestQke4IEEE [Takhirov el al. 2004] was matched to the IEEE693 spectrum at 2% and 5% of critical damping with the subsequent final match to a 2% damped spectrum. In contrast, the seed motions in this study were matched to a 5% damped spectrum only. As a result, an excellent spectral matching with about ±7% tolerance was achieved for the wide frequency range from 0.13 Hz to 33.3 Hz for all nonstationary time histories.

Each seed motion was matched to the target IEEE693 spectrum by using both wavelet options, the so-called Model 6 and Model 7 [Al Atik and Abrahamson 2010]. The use of the tapered cosine wave as an adjustment function in Model 6 has the advantage of preserving the non-stationary character of the acceleration time histories. However, this adjustment function introduces drift to the velocity and displacement time histories. As a result, it requires applying an additional baseline correction to the adjusted acceleration. Model 7 utilizes a wavelet with a modified taper, the Gaussian taper, so the adjustment wavelet is smooth and continuous. As a result, the wavelet ends with zero velocity and displacement, and no drift appears in the velocity and displacement time histories of the adjusted ground motion. The matched time histories were checked to ensure that both bracketed duration and the strong-part ratio meet and exceed the threshold values established by the IEEE Std 693-2005 and P693/D16.

2.5.4 IEEE693-Spectrum-Compatible Synthetic Time Histories

Three 3-component synthetic strong-motion time histories compatible with IEEE693 requirements were generated in order to have an option of using time histories generated from a set of harmonics. SimQke-1 [Gasparini 1976; Vanmarcke 1976] was used in the generation of these synthetic strong-motion time histories. SimQke-1 is a FORTRAN-based program that generates a synthetic time history, the spectrum of which matches the target spectrum.

The matching was performed at a 5% damping. Since the tolerance between the target spectrum and the acceleration spectra had quite large variations, a total of 399 synthetic strong-motion time histories were generated. Nine time histories with the best match to the target spectrum were selected. The main criterion for adequate matching was to limit the variations from the target spectrum to about ±7% in the wide range of frequencies from 0.13 Hz to 33.3 Hz at 1/24 octave resolution. In many cases the spectra of time histories generated by SimQke significantly exceeded this tight tolerance threshold. To address this issue, all synthetic time histories were subsequently matched to the same target response spectrum. The latter matching was performed in a time domain by utilizing RspMatch09. One of the typical results of this approach is presented in Figure 2.47.

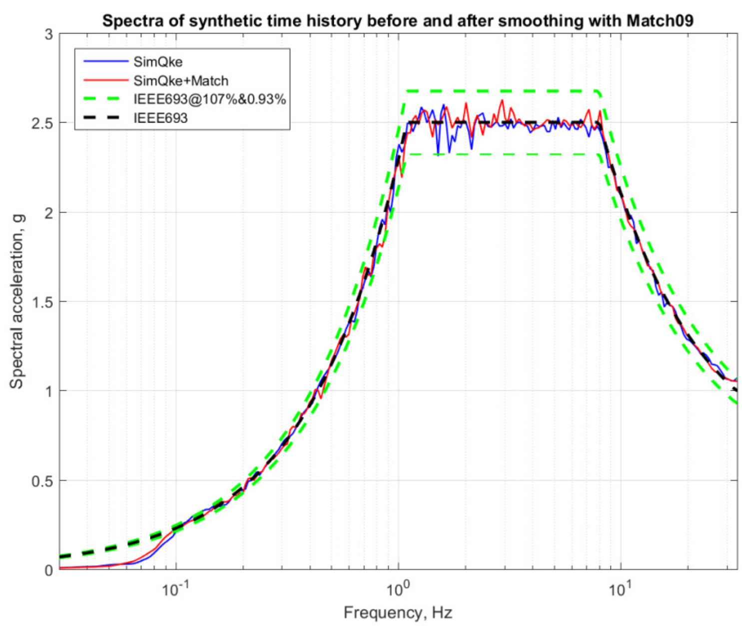

Figure 2.47 Spectra of synthetic time history (SQ-009.acc) before and after subsequent matching in a time domain by RspMatch09.

2.5.5 Resultant IEEE693-Spectrum-Compatible Time Histories

The following naming convention was adopted. The name of the IEEE693-spectrum-compatible time history starts from "TestQke4IEEE5", where 5 stands for the 5% damping. The name ends with a number preceded by a dash. This is a sequential number of the time history. This study developed eight three-component time histories. The first five were generated from the seed motions and the last three are synthetic strong motions as presented in Table 2.14.

The resultant time histories are presented in Figures 2.48–2.63. The plots are organized as follows. The first group of plots shows the acceleration time history and spectral plot for each component. For example, Figure 2.48 shows the acceleration time history and the spectral accelerations for the TestQke4IEEE5-1. The second group of plots shows the change of the Power Spectral Density (PSD) in time compared to the acceleration time history. These plots show the variation of the frequency content of each component in time. For example, Figure 2.49 shows the acceleration time histories and the PSD variations in time for each component of the TestQke4IEEE5-1.

Table 2.14 List of IEEE693-spectrum-compatible time histories developed in the study.

Seed motion, if any	Earthquake type	Name of IEEE693-spectrum-compatible time history
El-Centro, CA (1940)	Crustal	TestQke4IEEE5-1
Landers, CA (1992)	Crustal	TestQke4IEEE5-2
Chi-Chi, Taiwan (1999)	Crustal	TestQke4IEEE5-3
El Mayor-Cucapah, Mexico (2010)	Crustal	TestQke4IEEE5-4
CONSTITUCIONS/N4598 Chile, February 27, 2010	Subduction	TestQke4IEEE5-5
NA (synthetic)	NA	TestQke4IEEE5-6
NA (synthetic)	NA	TestQke4IEEE5-7
NA (synthetic)	NA	TestQke4IEEE5-8

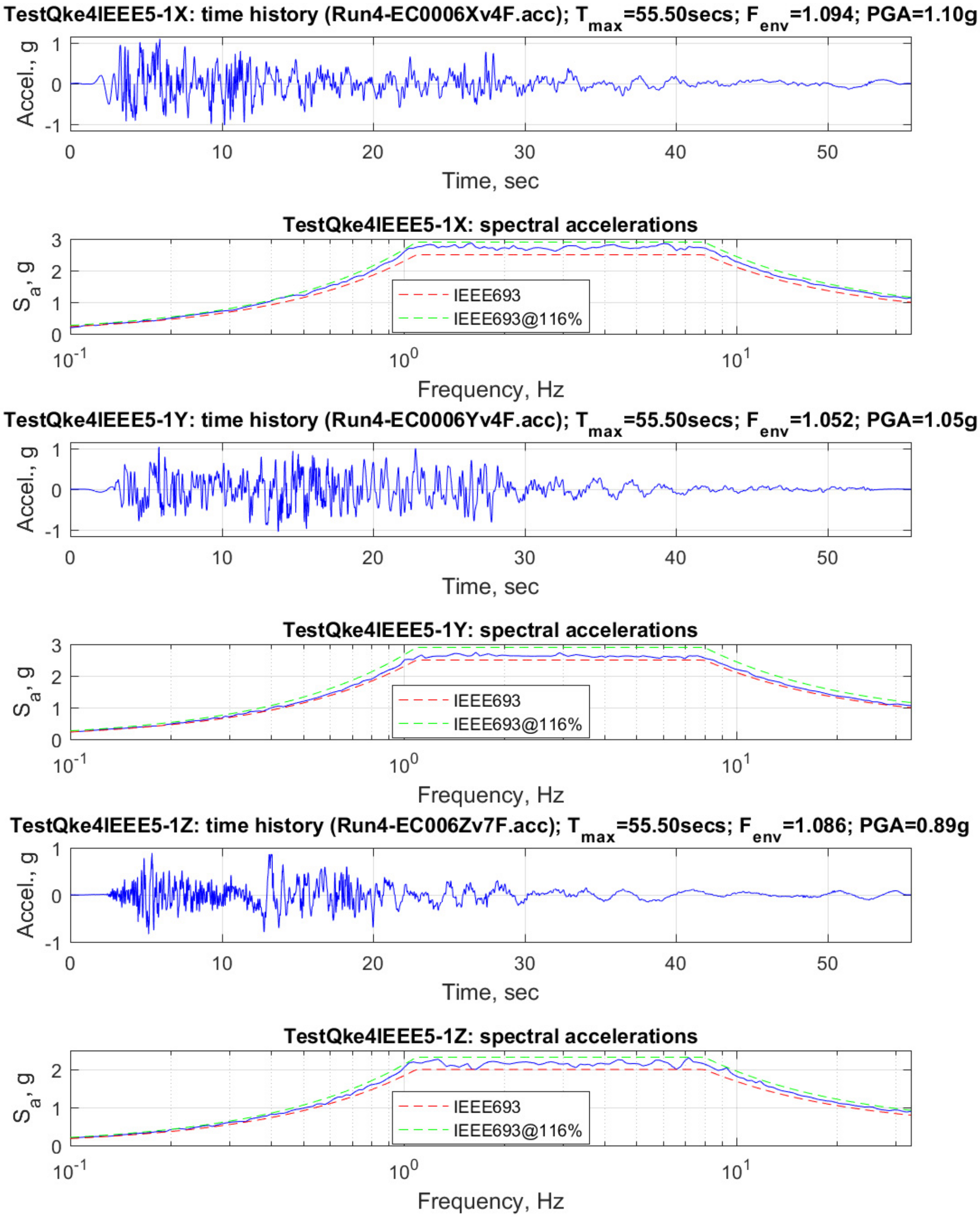

Figure 2.48 **IEEE693-spectrum-compatible time history matched to IEEE693 spectrum at 5% damping (TestQke4IEEE5-1 matched from 1940 El-Centro seed record).**

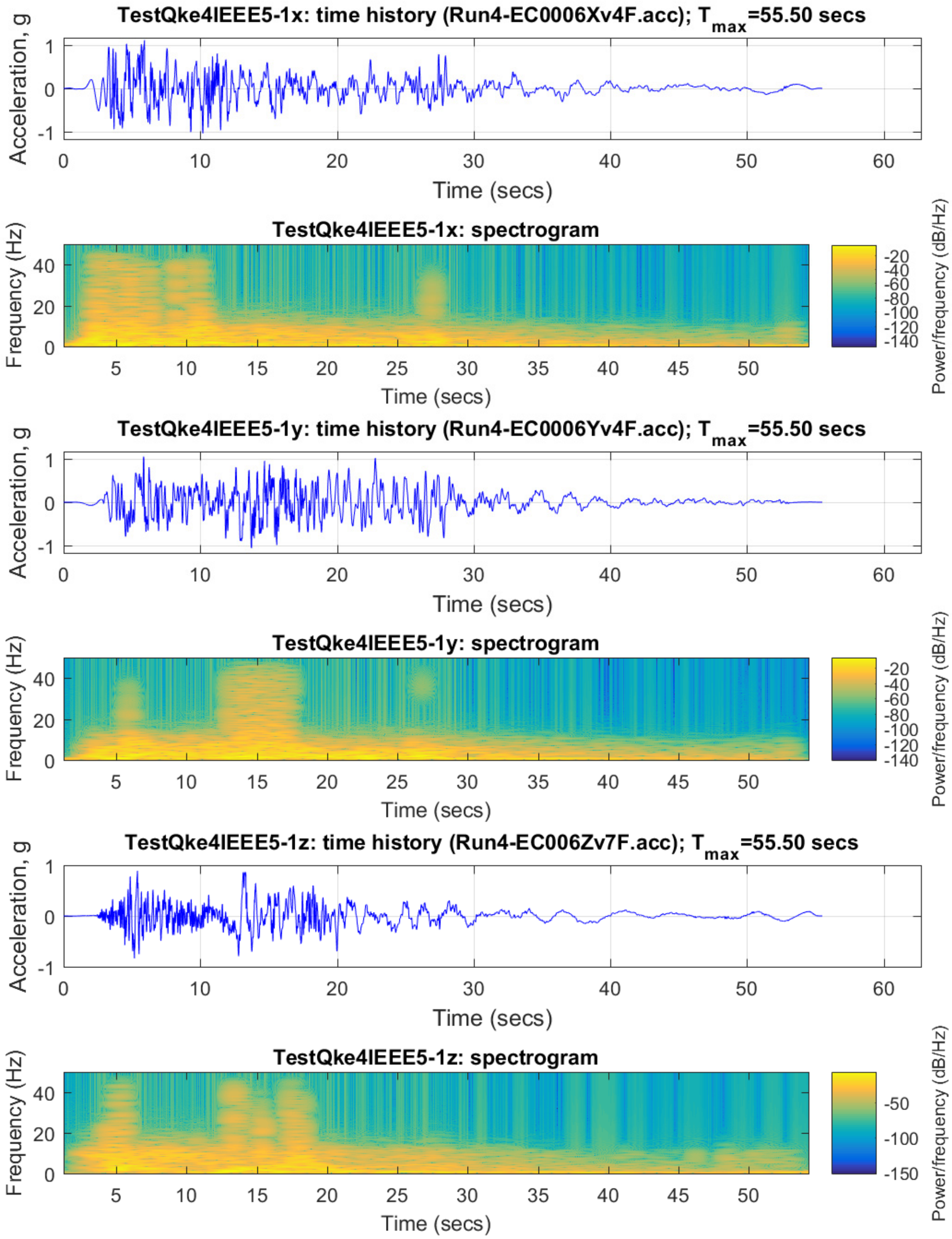

Figure 2.49 Variation of the Power Spectral Density in time (TestQke4IEEE5-1).

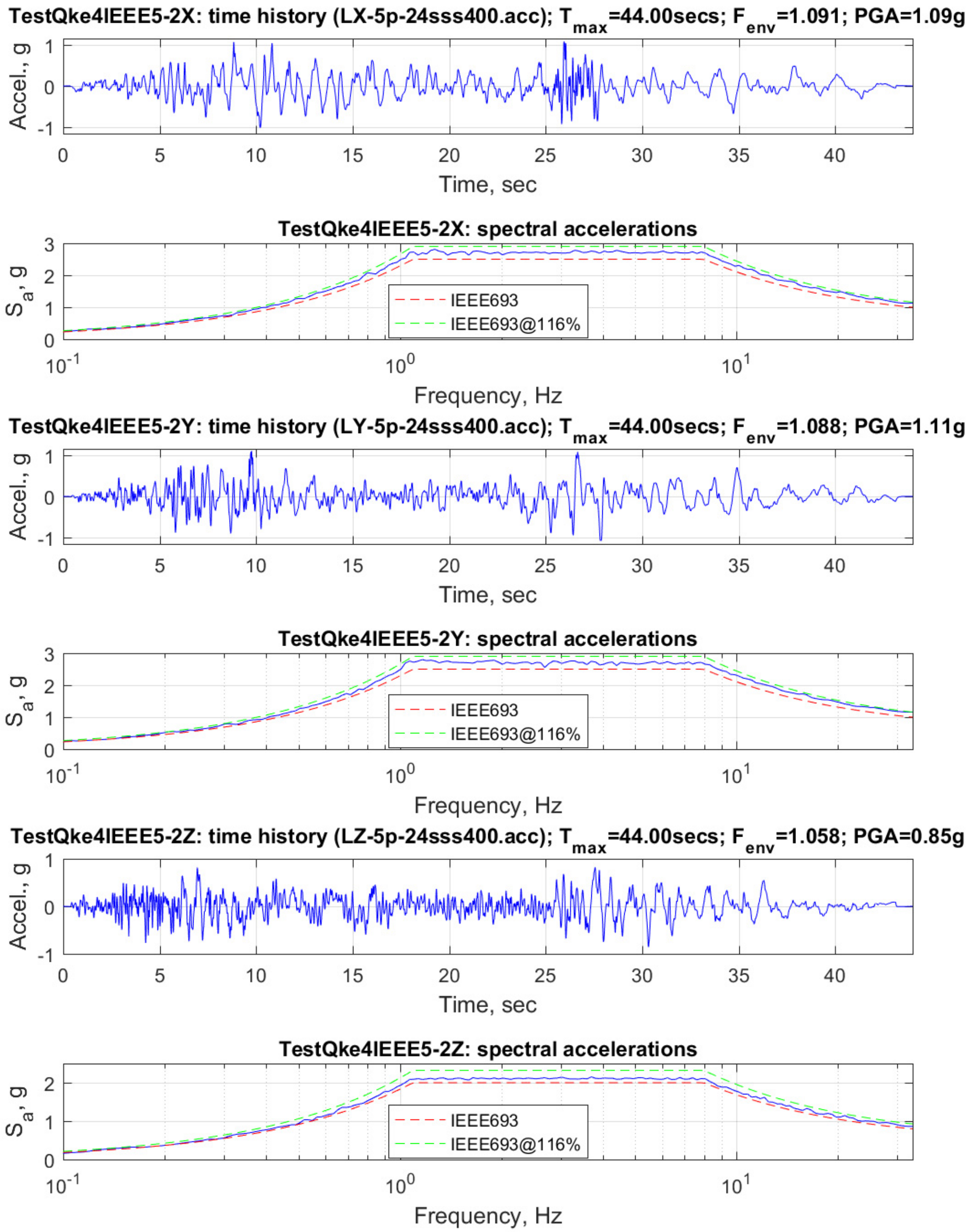

Figure 2.50 **IEEE693-spectrum-compatible time history matched to IEEE693 spectrum at 5% damping (TestQke4IEEE5-2 matched from 1992 Landers seed record).**

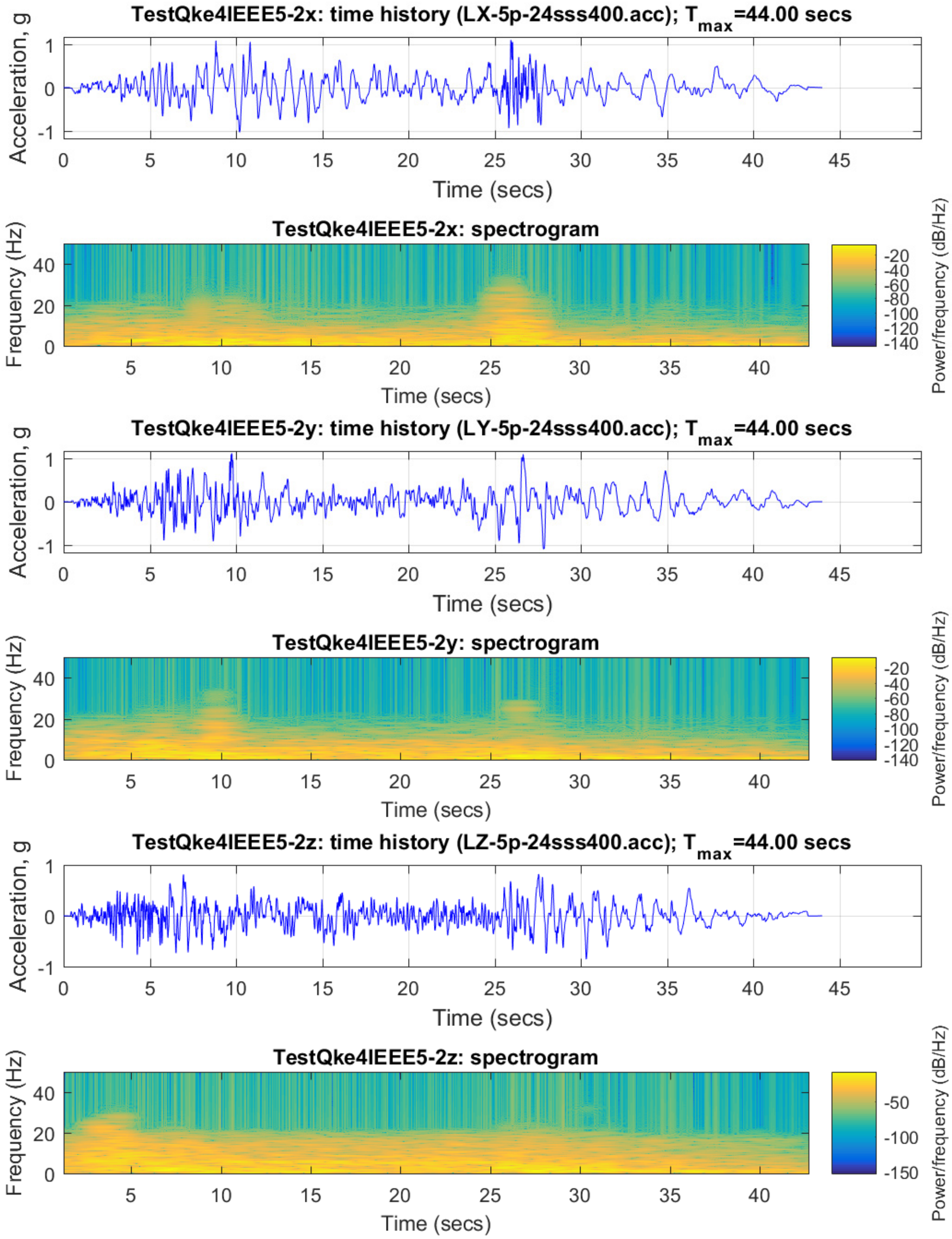

Figure 2.51 Variation of the Power Spectral Density in time (TestQke4IEEE5-2).

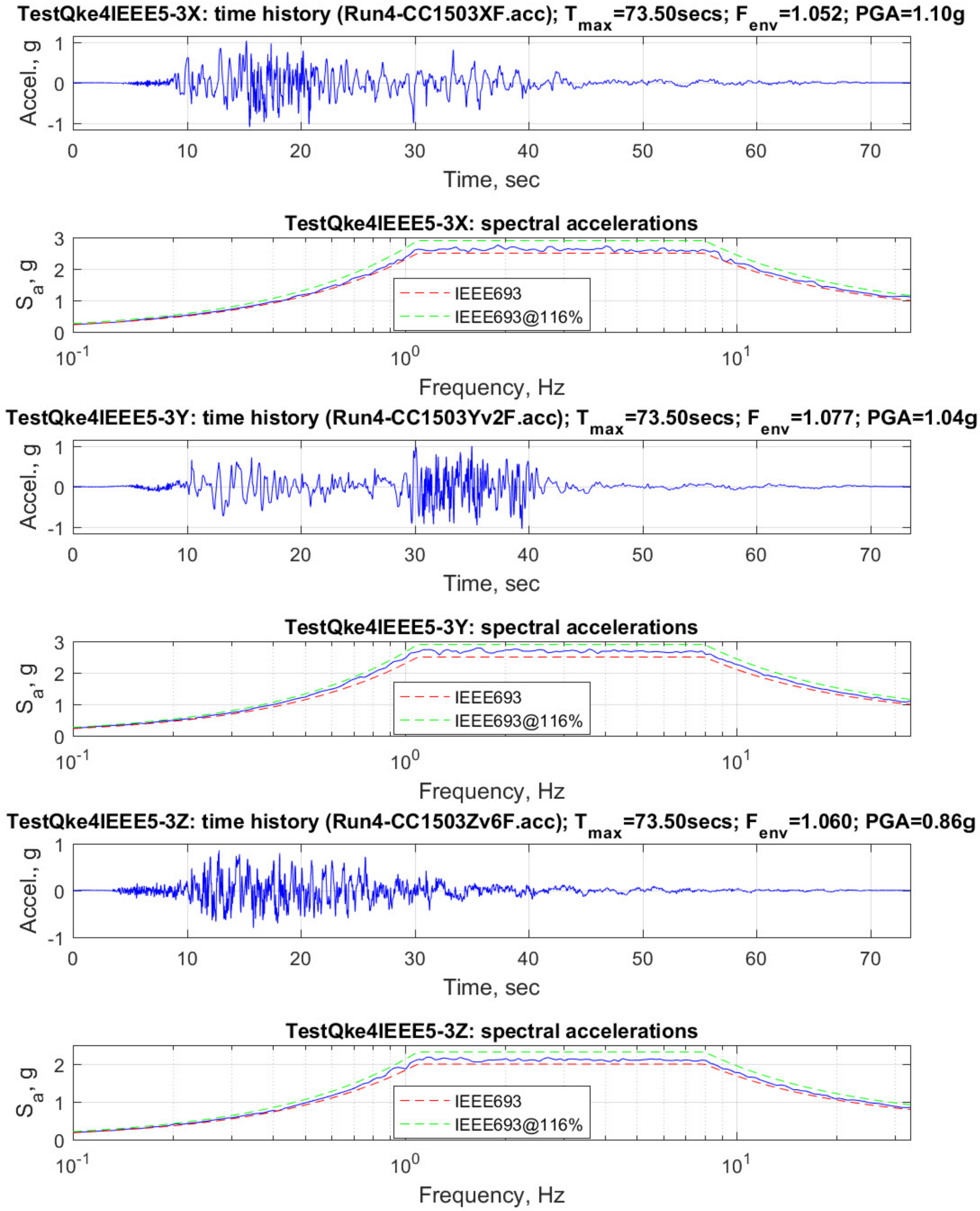

Figure 2.52 **IEEE693-spectrum-compatible time history matched to IEEE693 spectrum at 5% damping (TestQke4IEEE5-3 matched from 1999 Chi-Chi seed record).**

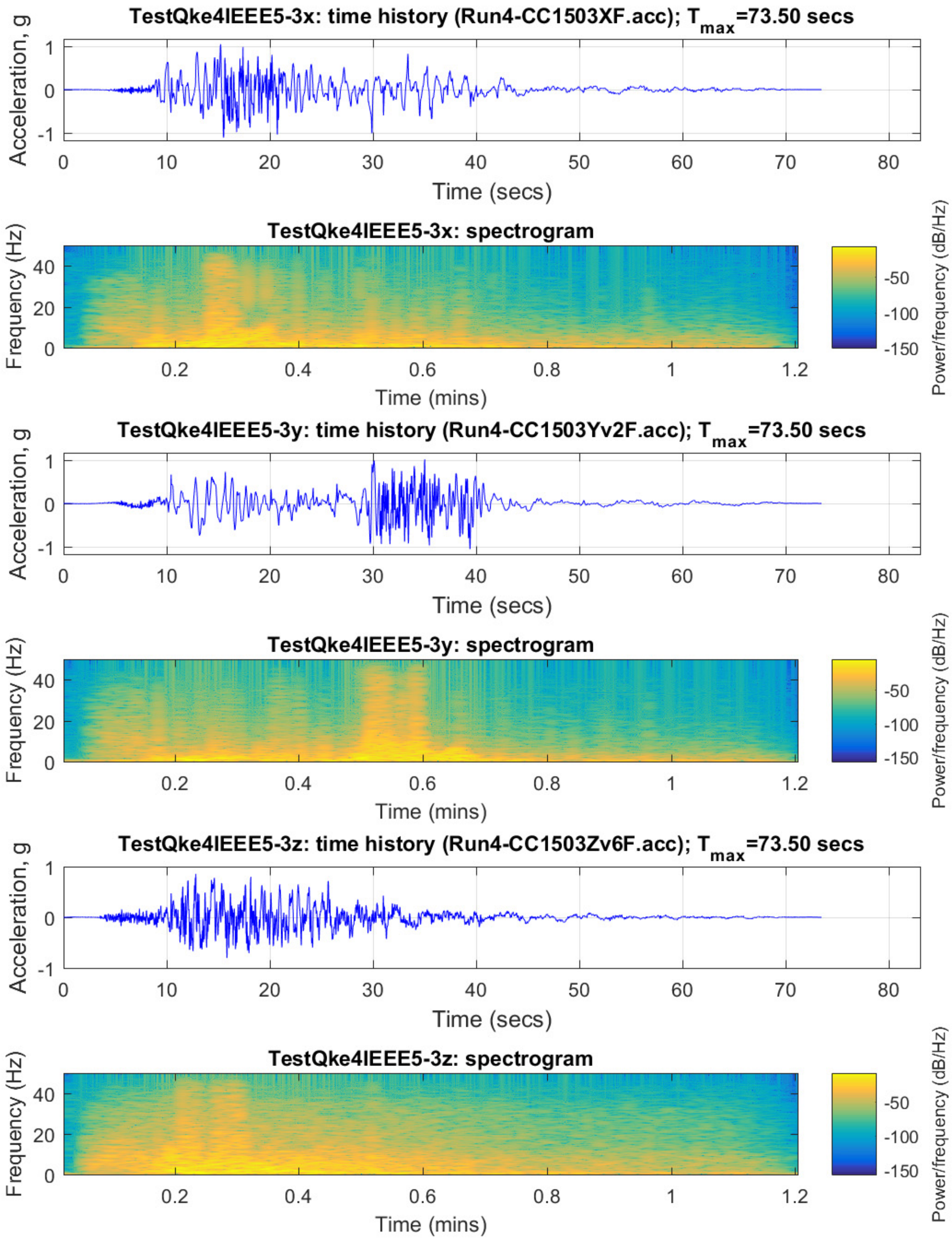

Figure 2.53 Variation of the Power Spectral Density in time (TestQke4IEEE5-3).

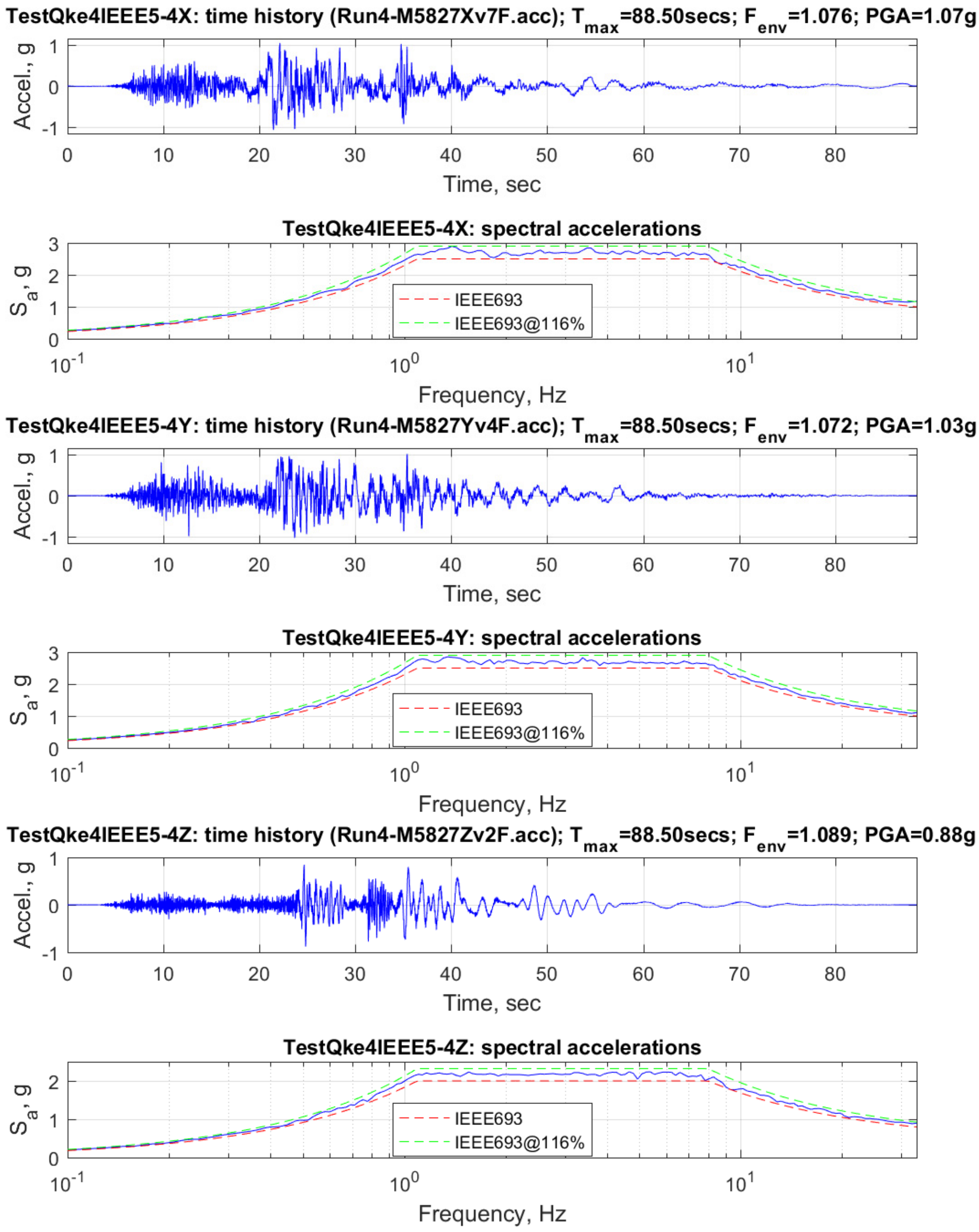

Figure 2.54 **IEEE693-spectrum-compatible time history matched to IEEE693 spectrum at 5% damping (TestQke4IEEE5-4 matched from 2010 El Mayor-Cucapah seed record).**

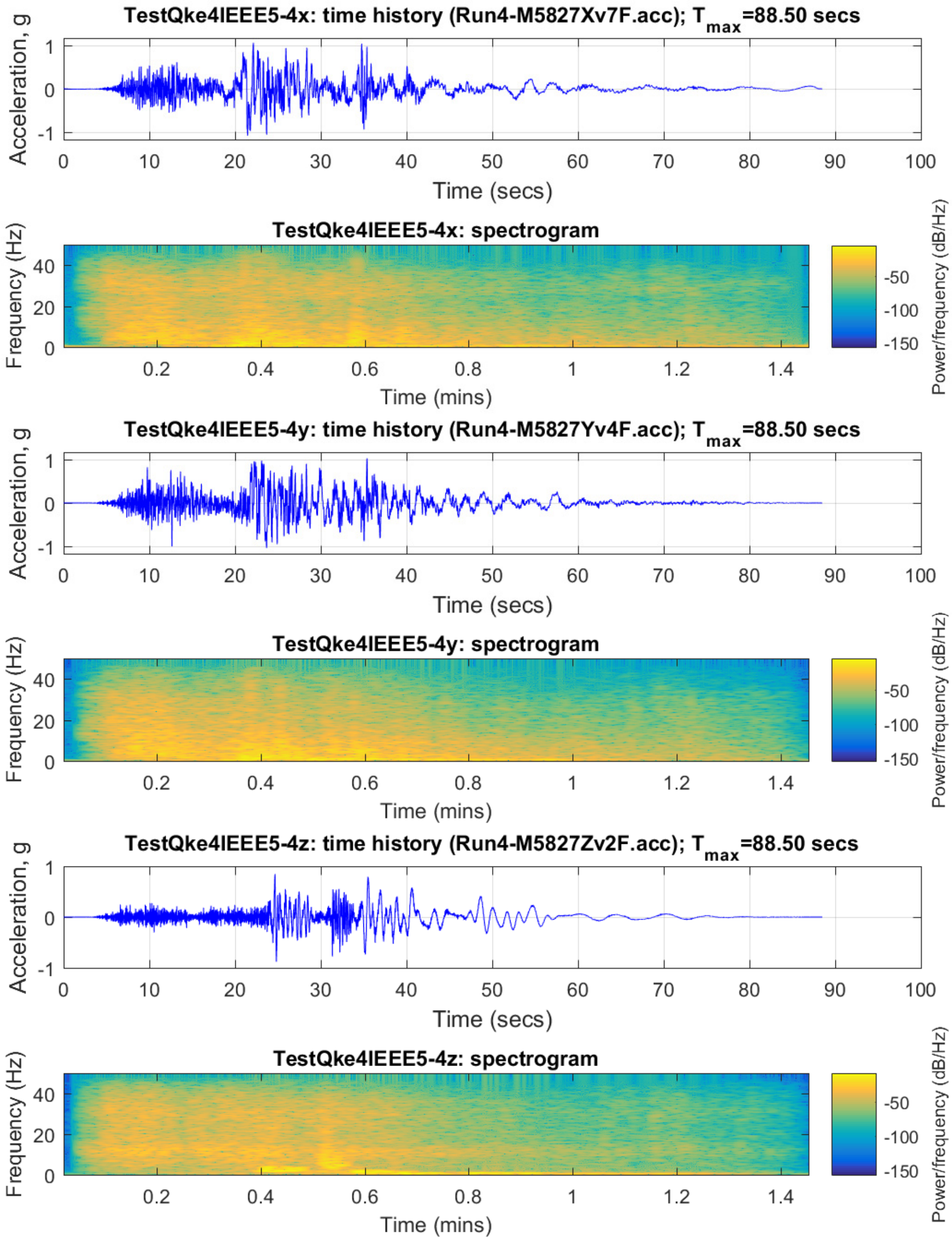

Figure 2.55 Variation of the Power Spectral Density in time (TestQke4IEEE5-4).

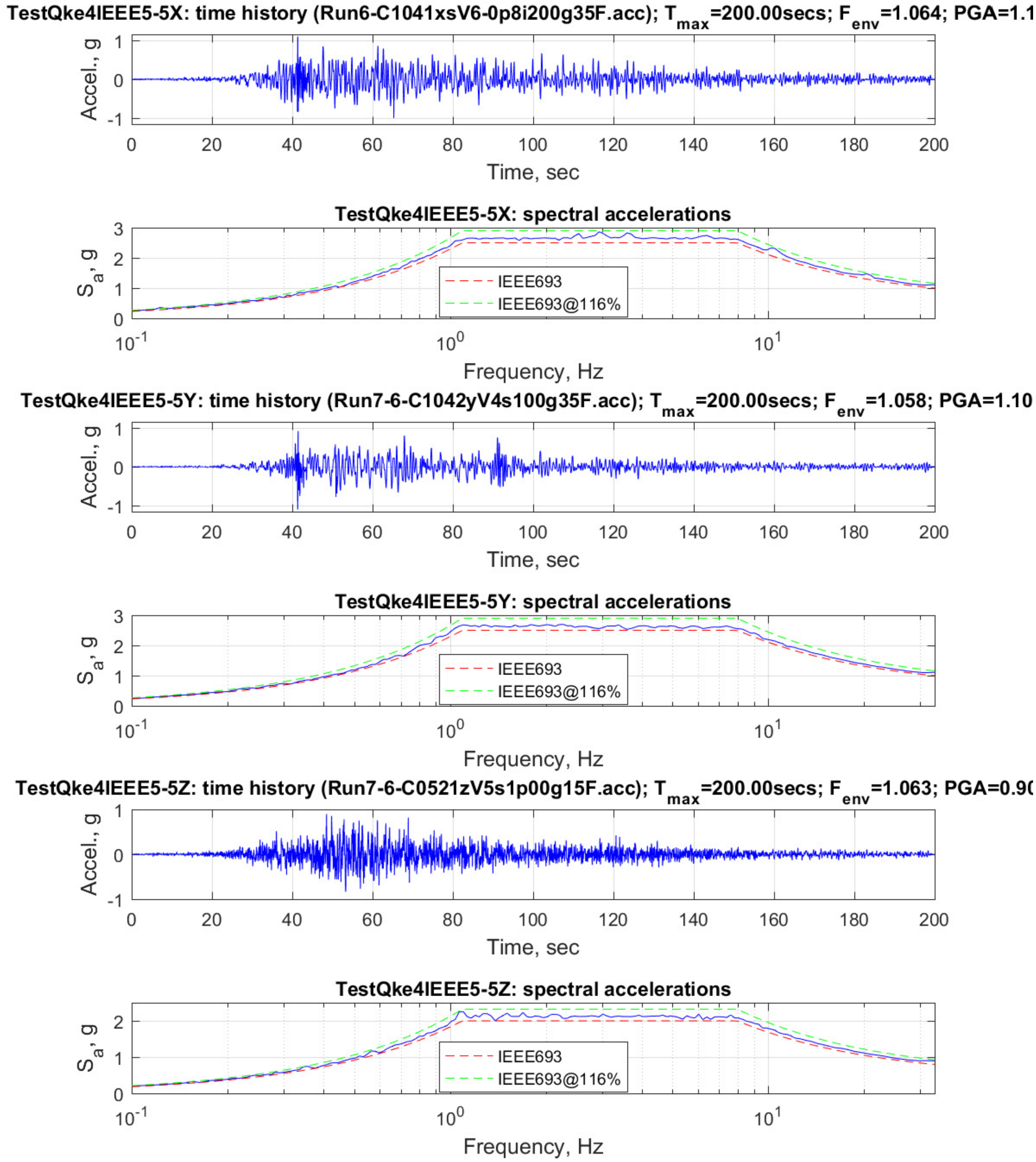

Figure 2.56 IEEE693-spectrum-compatible time history matched to IEEE693 spectrum at 5% damping (TestQke4IEEE5-5 matched from subduction seed record).

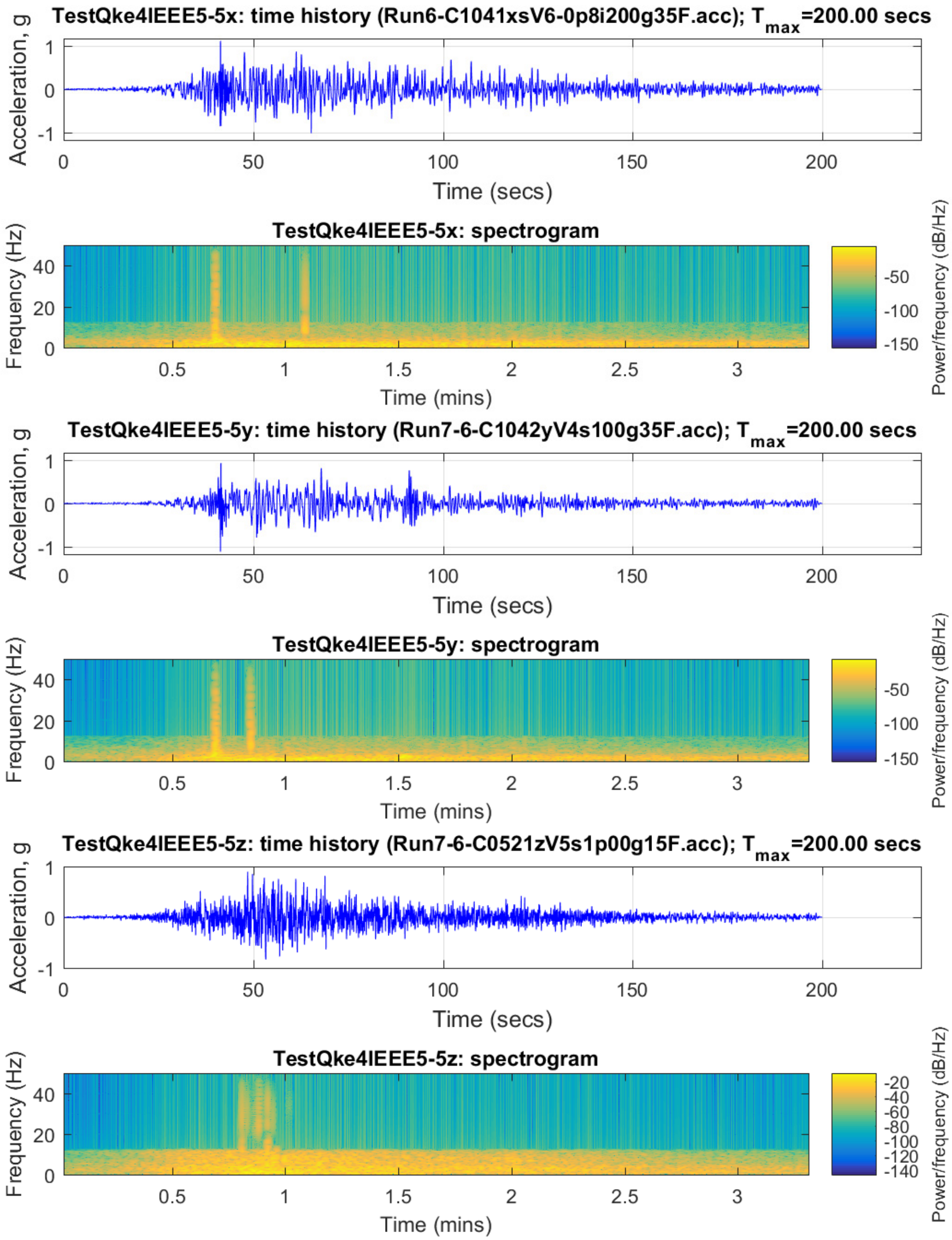

Figure 2.57 Variation of the Power Spectral Density in time (TestQke4IEEE5-5).

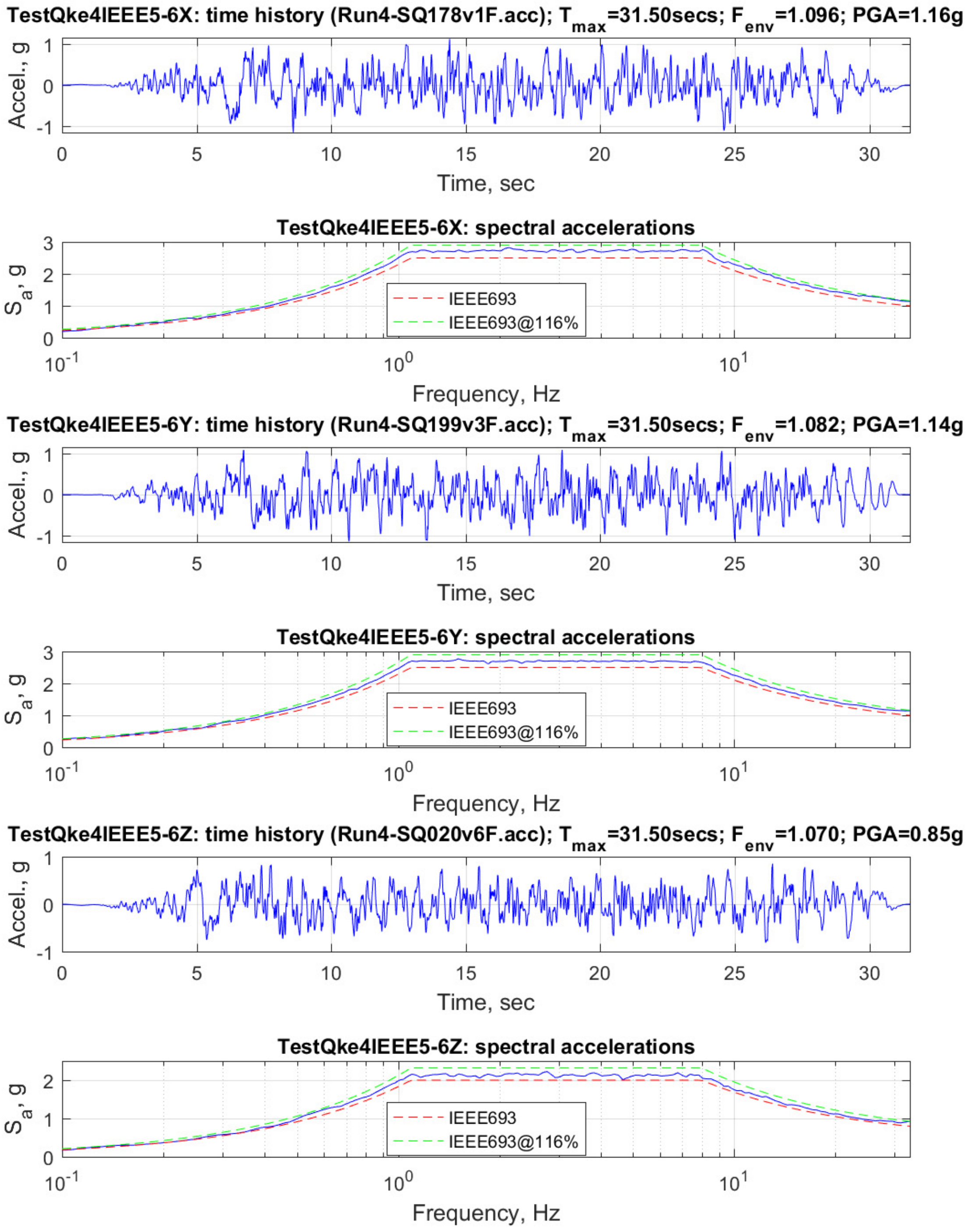

Figure 2.58 IEEE693-spectrum-compatible time history matched to IEEE693 spectrum at 5% damping (TestQke4IEEE5-6, synthetic).

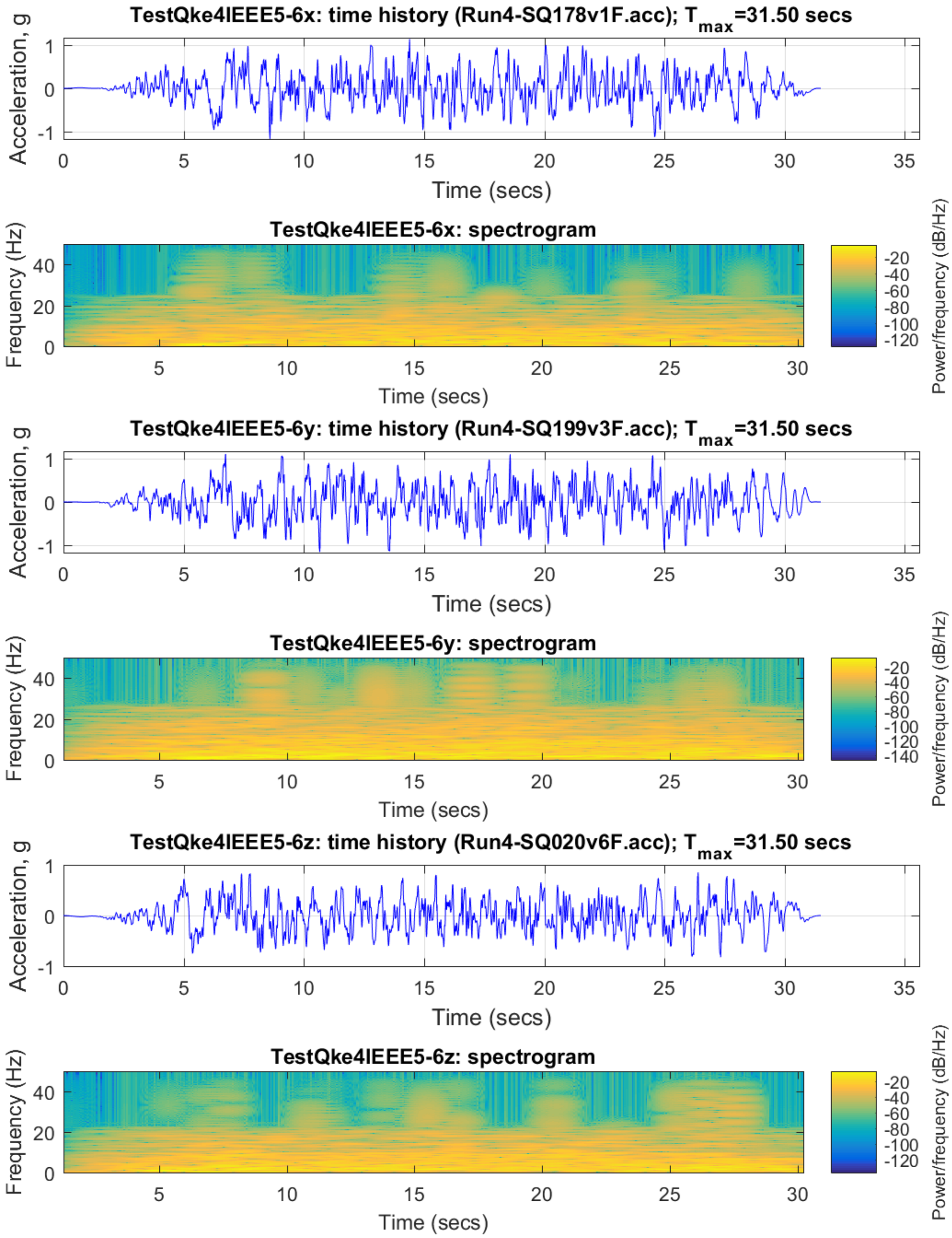

Figure 2.59 Variation of the Power Spectral Density in time (TestQke4IEEE5-6).

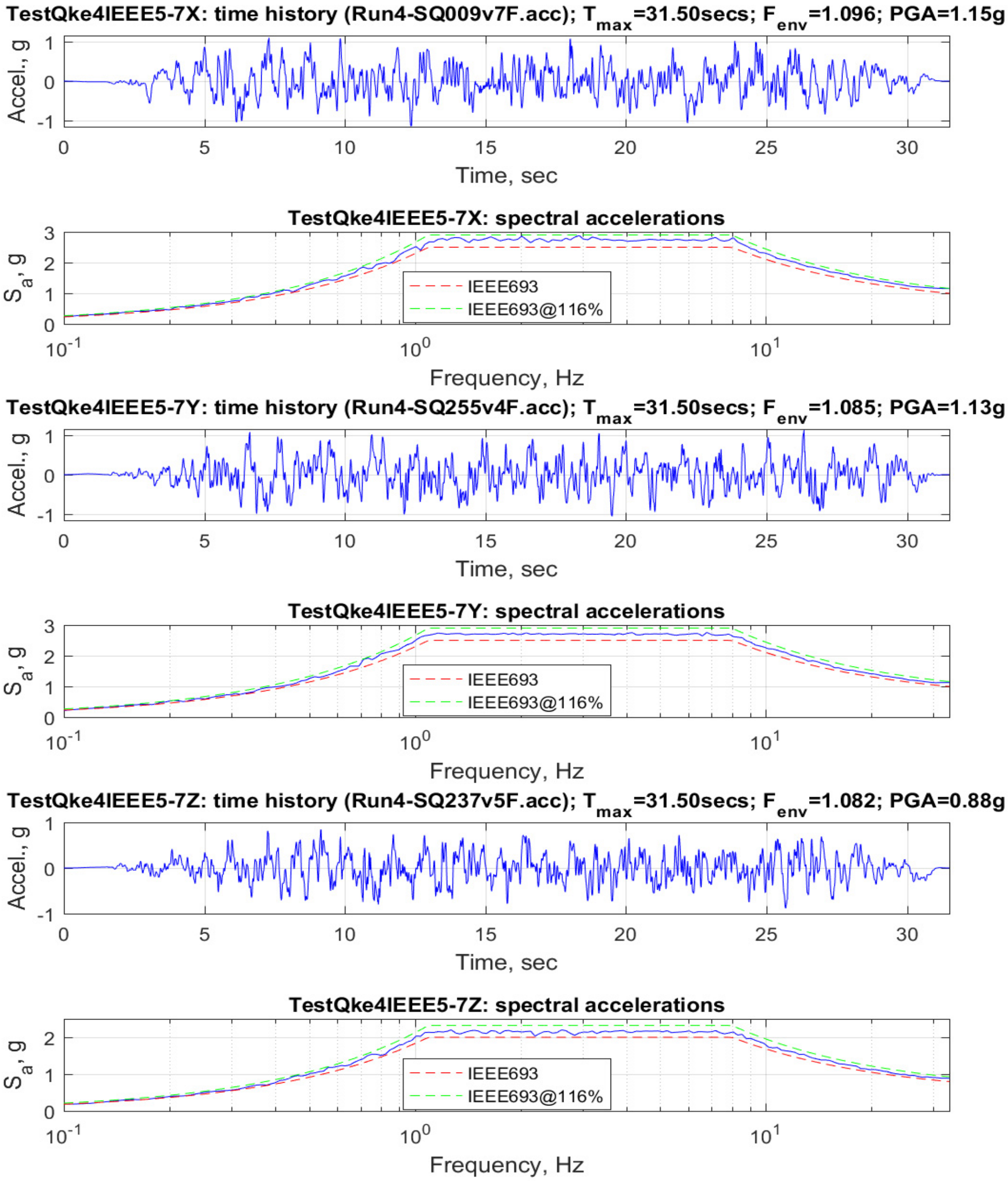

Figure 2.60 IEEE693-spectrum-compatible time history matched to IEEE693 spectrum at 5% damping (TestQke4IEEE5-7, synthetic).

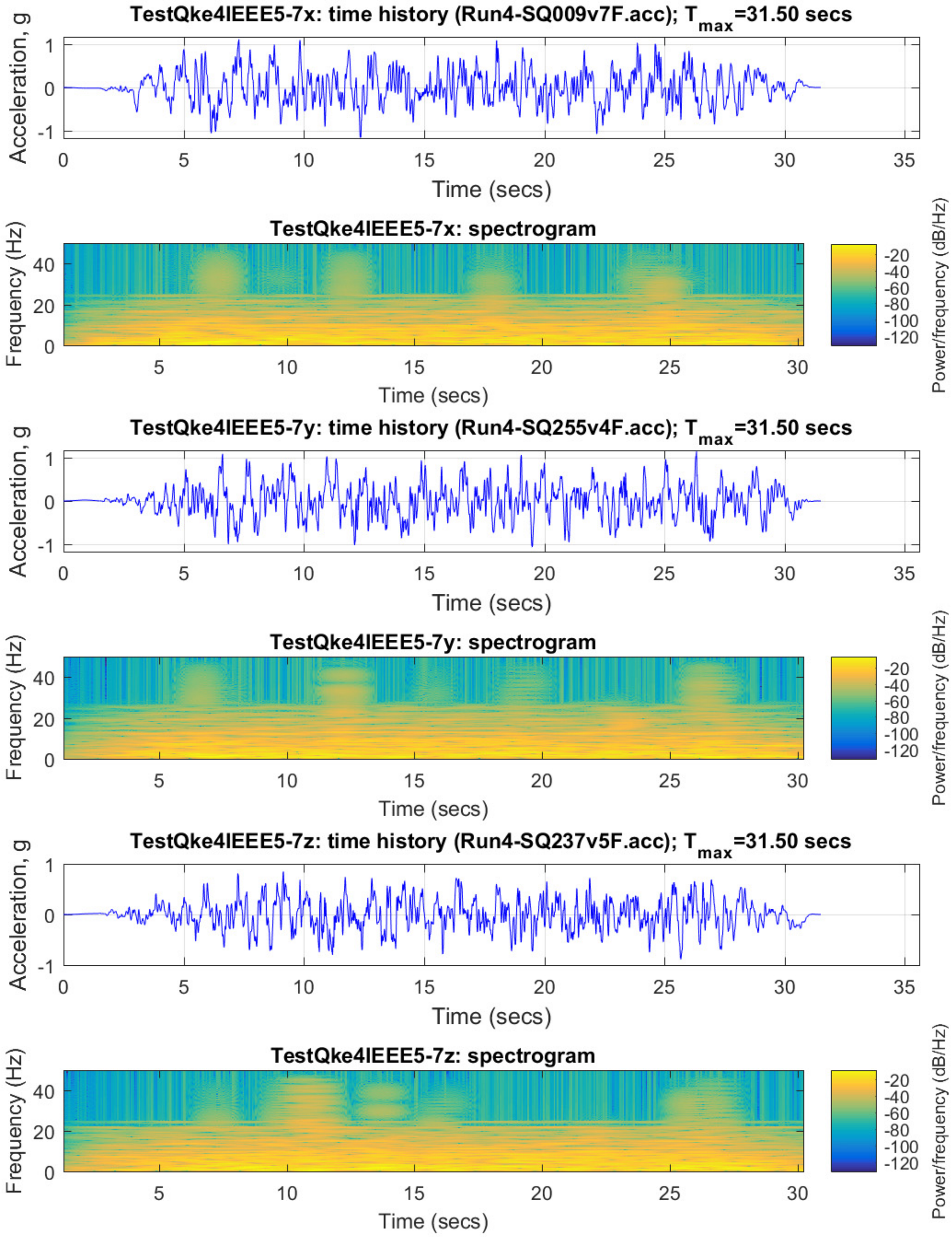

Figure 2.61 Variation of the Power Spectral Density in time (TestQke4IEEE5-7).

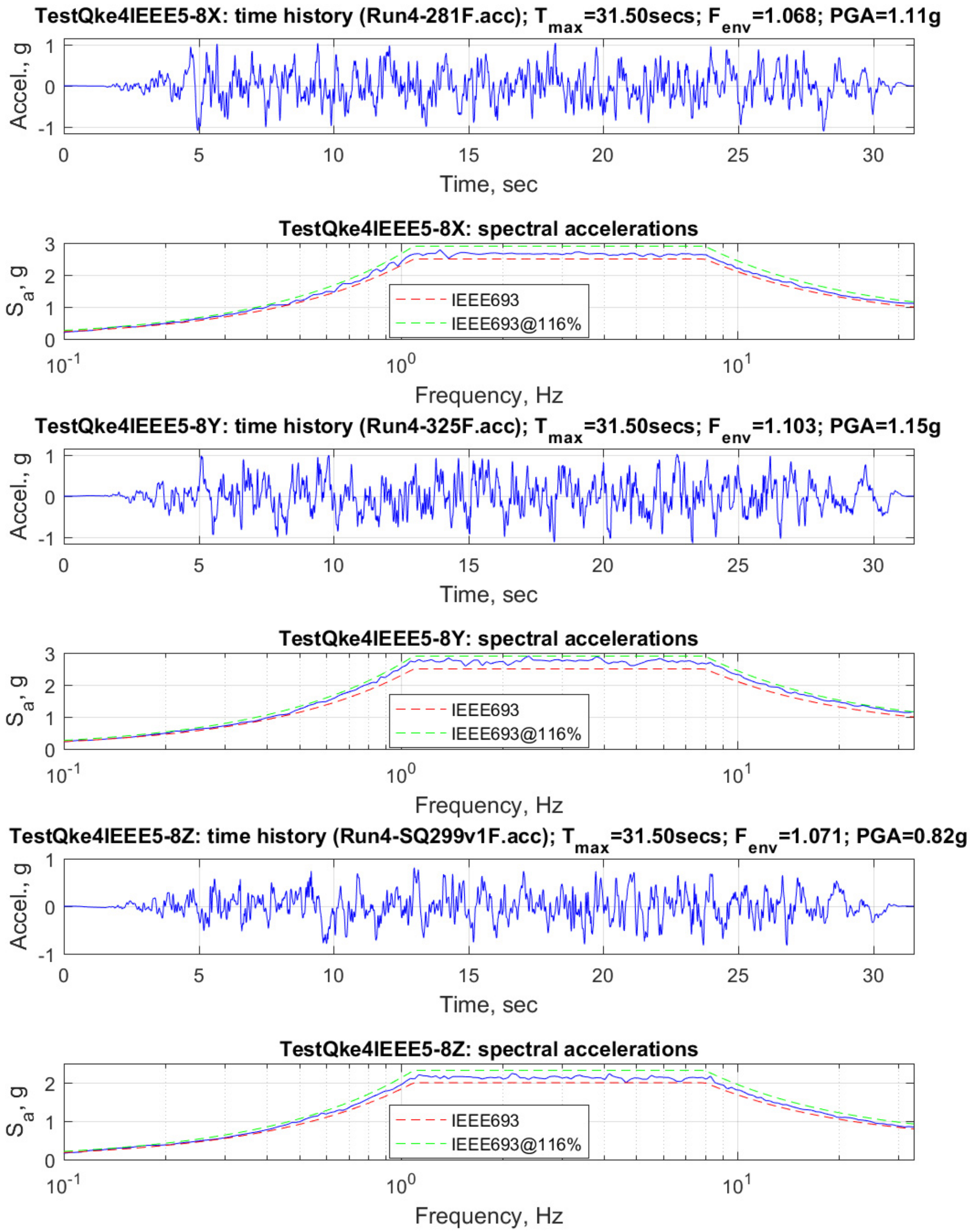

Figure 2.62 **IEEE693-spectrum-compatible time history matched to IEEE693 spectrum at 5% damping (TestQke4IEEE5-8, synthetic).**

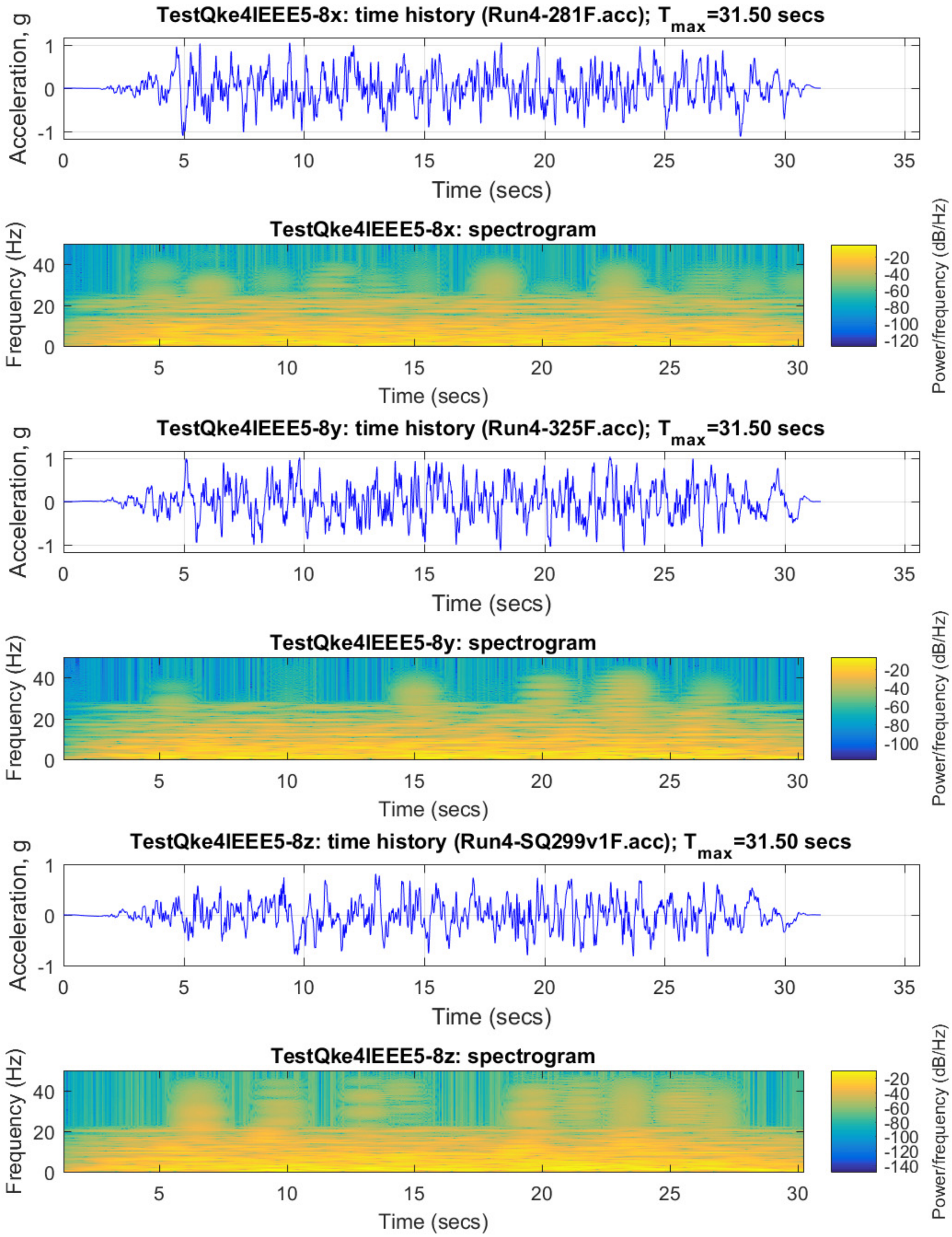

Figure 2.63 Variation of the power spectral density in time (TestQke4IEEE5-8).

All resultant time histories have spectra closely enveloping the IEEE693 from 0.13 Hz to 33.3 Hz as presented in Figure 2.64. At 1/24th octave resolution all spectral accelerations meet and exceed the IEEE693 spectrum and they stay within 16% of the target spectrum. In the case of the 1/12th octave frequency resolution, this tolerance above the target response spectrum is limited by 15%.

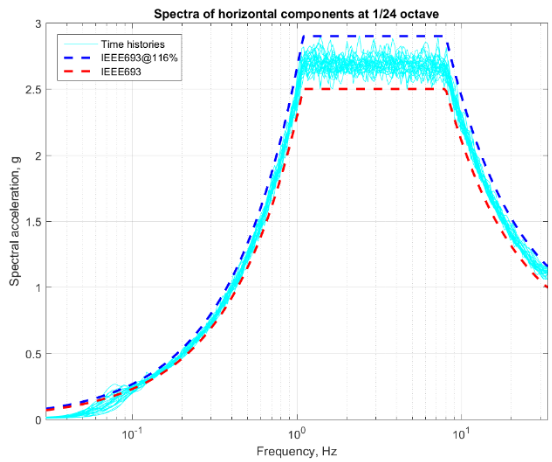

(a)

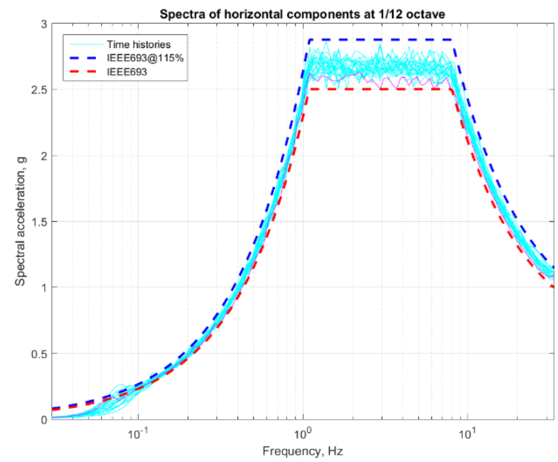

(b)

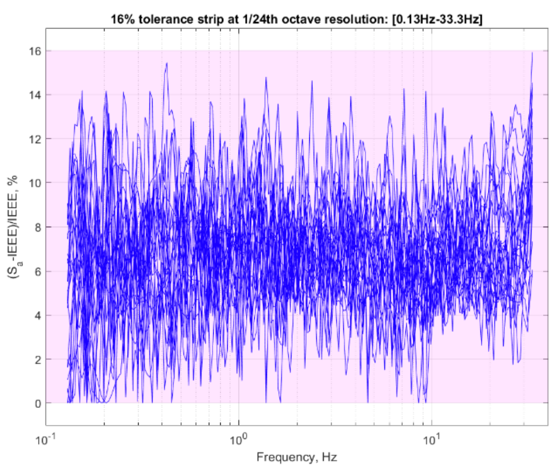

(c)

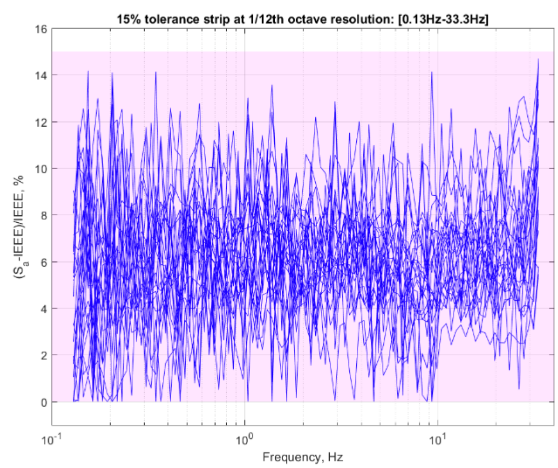

(d)

Figure 2.64 The resultant time histories have spectra closely enveloping the IEEE693 from 0.13 Hz to 33.3 Hz: (a) all spectra fit into a 16% strip above the IEEE693 High PL at 1/24 octave resolution; (b) all spectra fit into a 15% strip above the IEEE693 High PL at 1/12 octave resolution; (c) (S_a-IEEE)/IEEE ratio at 1/24 octave; and (d) (S_a-IEEE)/IEEE ratio at 1/12 octave.

The strong-part ratio and bracketed duration of all IEEE compatible records exceed the minimum requirements of the IEEE Std 693-2005 [IEEE 2005] and P693/D16 as presented in the two top plots of Figure 2.65. The total CE is presented in the third plot from the top. The cycle count does not fall below one cycle as shown in the fourth plot from the top. The factor at best fit (K_S) is very close to unity as presented in the fifth plot from the top. Because of the close match to the IEEE693 spectrum, the cumulative distance (D_{SA}) from the target spectra at best fit is very small and does not exceed 0.7 as shown in the bottom plot.

The number of high cycles in the SDOF response is presented in Figure 2.66. The magenta dashed line is a threshold specified in IEEE693 [IEEE 2005]. Since the number of high cycles in the SDOF response is expected to be less for systems with higher damping, the number of cycles for the 5% damped systems is less than the threshold of two cycles established by the IEEE Std 693-2005 [IEEE 2005] for the 2% damped systems. This was observed earlier in the study of the historic records. Based on the results of this study and because IEEE P693/D16 [IEEE693 WG 2017] requires the spectrum matching to be performed at 5% instead of 2% damping, the requirement on the number of high cycles in the SDOF response has been eliminated from the draft standard.

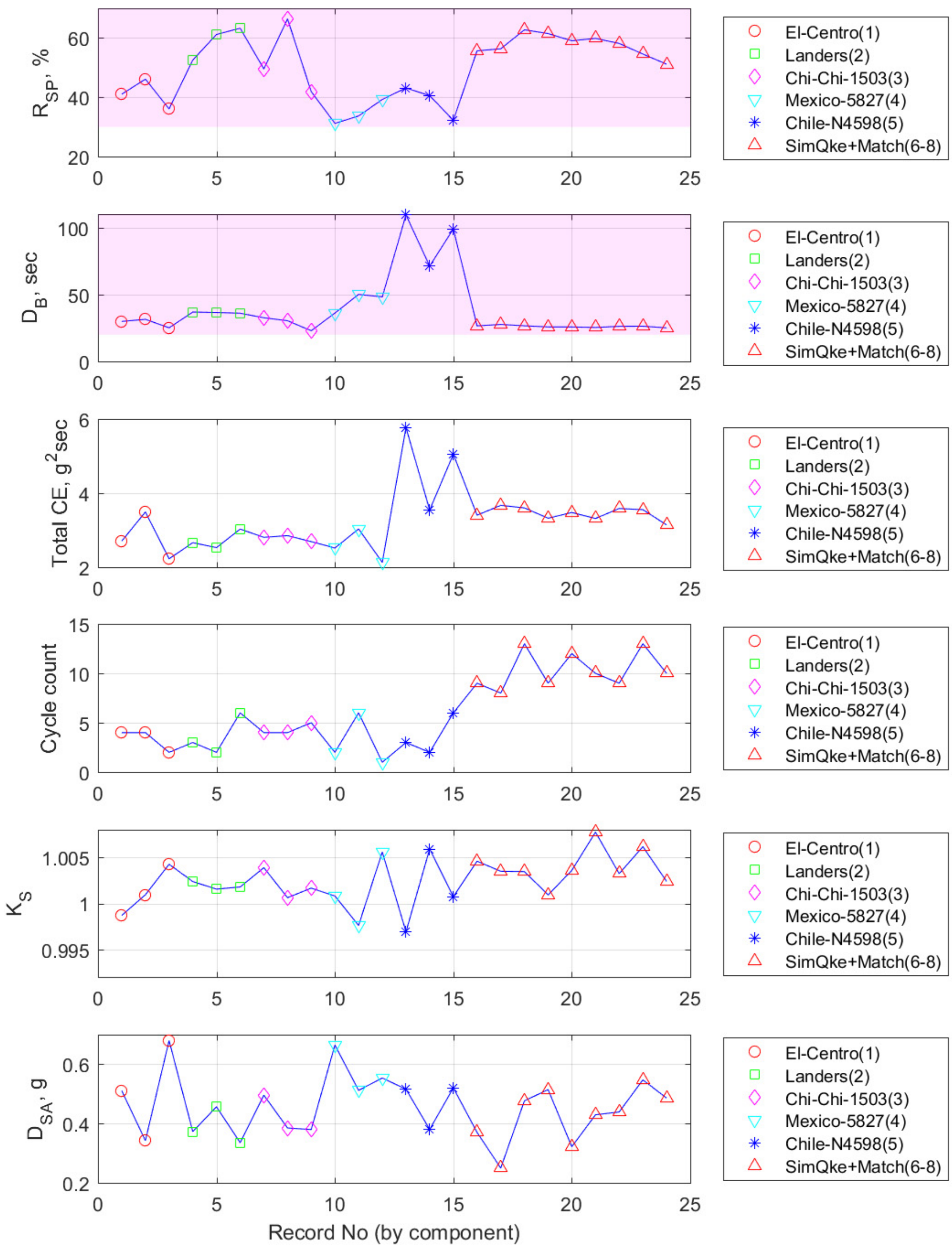

Figure 2.65 Major parameters of the IEEE693-spectrum-compatible time histories.

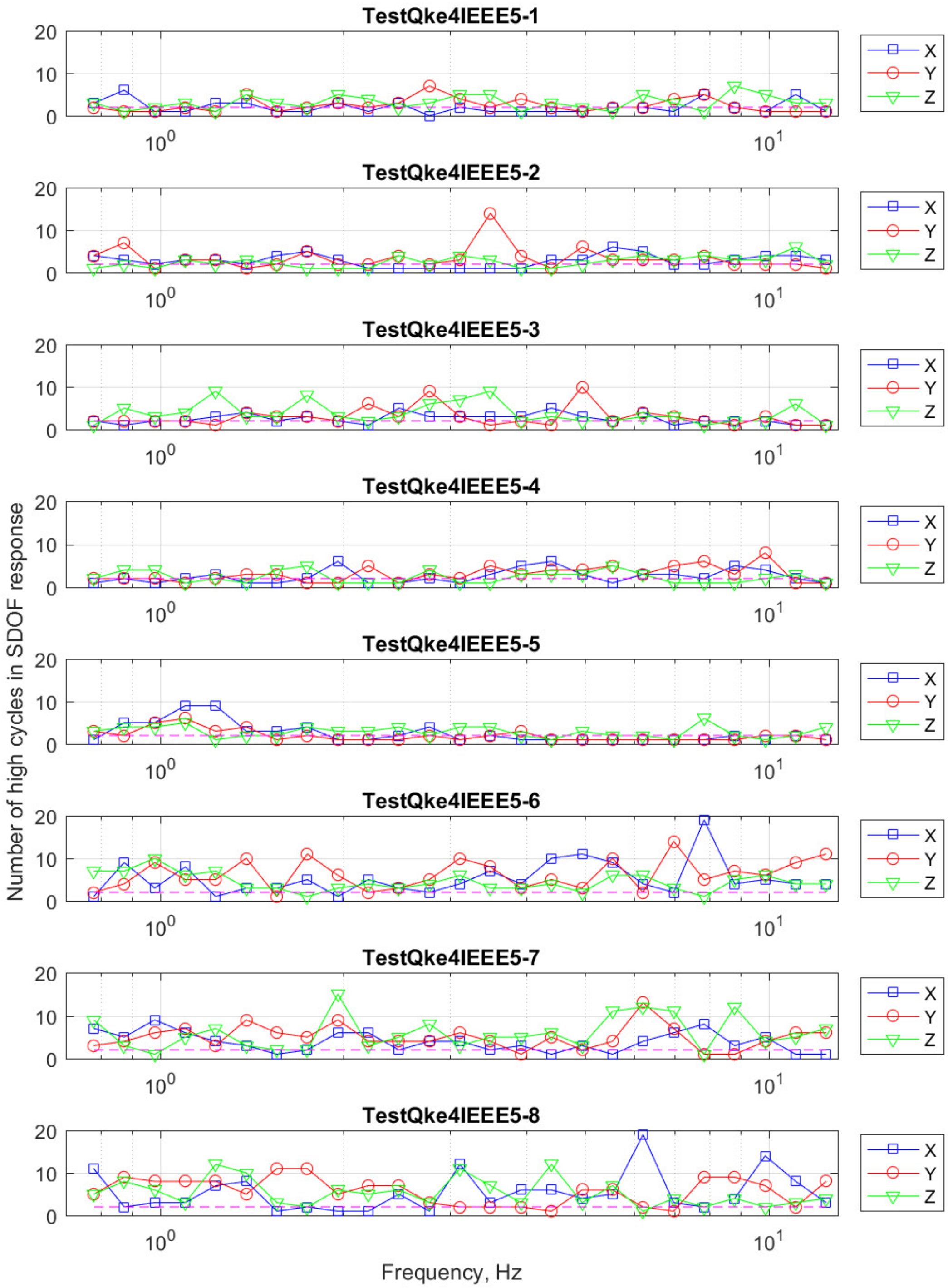

Figure 2.66 Number of cycles in the 5%-damped SDOF response (magenta is a threshold specified in IEEE Std 693-2005 [IEEE 2005]).

2.5.6 Filtered Versions of TestQke4IEEE5

Since enveloping of the IEEE693 spectrum starts from 0.13 Hz, all time histories developed herein impose large displacement demand. While this is acceptable for analysis, the time histories need to be filtered to meet the limitations of the existing shaking tables. The limitations of the major shaking tables worldwide is presented in Table 2.15. It is selected from the world list of shaking tables [Wikipedia 2017] by limiting the selection to 3D and 6D shaking tables and uniaxial shaking tables with long stroke. The displacement limitations of the shaking tables that are listed in Table 2.15 are going to control the filtering requirements. They are combined in several groups and summarized in Figure 2.67.

The validation tests of the time histories began at the uni-axial shaking table at the University of California, Berkeley, with a stroke capacity of ±31.5 in. and peak velocity of 100 in./sec. The time histories were filtered to accommodate this stroke limitation and all validation tests were successful [Takhirov et al. 2017a; 2017b]. In addition to that, several testing laboratories worldwide were approached to validate the time histories on their shaking tables. The list included the following laboratories: the shaking table at Bristol University (Bristol, United Kingdom), shaking table at National Technical University of Athens (Athens, Greece), Clark Testing (Jefferson Hills, Pennsylvania, U.S.), shaking table at PEER-UCB (Richmond, California, U.S.), shaking table at iABG lab (Ottobrunn, Germany), shaking testing at the University of Nevada, Reno (Reno, Nevada, U.S.), the shaking table facility at the State University of New York at Buffalo (New York, U.S.), uni-axial shaking table laboratory at Istanbul Technical University (Istanbul, Turkey), shaking table facility at University of Pavia (Pavia, Italy), and many others. The main concern raised by the laboratories was that the time histories require application of a filtering procedure that can vary from facility to facility, and it would be more convenient for the laboratories and the engineering community to have several filtered options of the time histories suitable for the majority of the shaking tables worldwide.

The filtering procedure used in the past [Takhirov et al. 2004] was utilized herein. The main goal was to develop a complete set for three types of time histories: (1) modified from a record obtained during crustal type earthquake; (2) modified from a record obtained during subduction type earthquake; and (3) synthetically generated time history. The results are presented in Table 2.16, which shows the stroke limitations filtered for and the file names containing the filtered time histories. The complete sets were developed for TestQke4IEEE5-4 (yellow fields), TestQke4IEEE5-5 (orange fields), and TestQke4IEEE5-6 (green fields).

The filtered versions of the time histories can be deployed at the majority of the shaking tables worldwide as presented in Figure 2.68. For example, since the filtered time histories cover many displacement thresholds in horizontal directions up to 30 in., they can be successfully used at more than 90% of the shaking tables worldwide (a sum of two first columns in Figure 2.68 on the left). The filtered versions of the vertical time histories can be used at more than 80% of the shaking tables worldwide (a sum of three first columns in Figure 2.68 on the right).

All time histories including their filtered versions will be posted on the Internet by the IEEE693 Working Group. They can be downloaded free of charge from the following link: http://ewh.ieee.org/cmte/substations/scd0/wgd4/basefile.htm. More information on the filtered versions of the time histories can be found in [Takhirov et al 2017c] and [EPRI 2017].

Table 2.15 A world list of 3D and 6D shaking tables and 1D shaking tables with long stroke.

No	Region	Country	State	Name, location	Size, m	MT	DOF	D_X, mm	D_y, mm	D_z, mm	V_X, mm/s	V_y, mm/s	V_z, mm/s
1	Africa	Algeria	-	CGS Laboratory, Alger	6.1 x 6.1	60	6	±150	±250	±100	±1100	±1100	±1000
2	Africa	South Africa	-	University of Witwatersrand, Johannesburg	4 x 4	10	1	±750	n/a	n/a	±1000	n/a	n/a
3	Asia	China	-	China Academy of Building Research, Beijing	6.1 x 6.1	60	6	±150	±250	±100	±1000	±1200	±800
4	Asia	China	-	Guangzhou University	3 x 3	20	6	±100	±100	±50	±1000	±1000	±1000
5	Asia	China	-	Nanjing University of Technology	3 x 5	15	3	±120	±120	±120	±500	±500	±500
6	Asia	China	-	Tongji University, Shanghai	4 x 4	25	6	±100	±50	±50	±1000	±600	±600
7	Asia	India	Karnataka	IISc, Bangalore	1 x 1	0.5	6	±220	±220	±100	±570	±570	±570
8	Asia	India	Tamil Nadu	Indira Gandhi Centre for Atomic Research(IGCAR), Chennai,Tamil Nadu	3 x 3	10	6	±100	±100	±100	300	300	?
9	Asia	Japan	-	NIED ‘E-Defence’ Laboratory, Miki City	20 x 15	1200	6	±1000	±1000	±500	±2000	±2000	±700
10	Asia	Japan	-	Hazama Corp Ltd.	6 x 4	80	3	±300	±150	±100	±1150	?	?
11	Asia	Japan	-	Ishikawajima Harima Heavy Ind Corp.	4.5 x 4.5	35	6	±100	±100	±67	±750	±750	±500
12	Asia	Japan	-	Kajima Corp. Ltd.	5 x 5	50	6	±200	±200	±100	±1000	±1000	±500
13	Asia	Japan	-	Kumagai-Gumi Corp Ltd	5 x 5	64	6	±80	±260	±50	±600	±1500	±500
14	Asia	Japan	-	NIED (Nat. Inst. for Disaster Prevention)	6 x 6	1100	3	±1000	?	?	±2000	?	?
15	Asia	Japan	-	Public Works Research Institute (PWRI)	8 x 8	300	6	±600	±600	±300	±2000	±2000	±1000
16	Asia	Japan	-	Tokyu Const. Corp.	4 x 4	30	6	±500	±200	±100	±1500	±1000	?
17	Asia	South Korea	-	Korea Institute of Machinery and Metals, Changwon	4 x 4	30	6	±200	±200	±134	±750	±750	±500
18	Asia	Korea	-	Pusan National University	4 x 4	30	6	±300	±200	±150	±1500	±1500	±1000
19	Asia	Taiwan	-	National Center for Research in Earthquake Engineering	5 x 5	50	6	±250	±100	±100	±1000	±600	±500
20	Europe	France	-	Commissariat à l'Energie Atomique et aux Energies Alternatives (CEA), AZALEE	6 x 6	100	6	±125	±125	±100	±700	±700	±700
21	Europe	Germany		iABG, Ottobrunn	4.1 x 3.2	10	6	±125	±125	±50	±430	±530	±260
22	Europe	Greece	-	National Technical University of Athens	4 x 4	10	6	±100	±100	±100	±1000	±1000	±1000
23	Europe	Italy	-	ENEA (Casaccia R. C.) - System 1, Shake Table (1 of 2)	4 x 4	30	6	±125	±125	±125	±500	±500	±500
24	Europe	Italy	-	ENEA (Casaccia R. C.) - System 1, Shake Table (2 of 2)	2 x 2	5	6	±150	±150	±150	±1000	±1000	±1000
25	Europe	Italy	-	CESI S.p.A., Static & Dynamic Testing Laboratories, Seriate (BG)	4 x 4	30	6	±100	±100	±100	±440	±440	±440
26	Europe	Italy		Laboratory of Earthquake engineering and Dynamic Analysis (LEDA) - "Kore" University of Enna (2 shaking tables)	4 x 4	60	6	±400	±400	±250	±2200	±2200	±1500
27	Europe	Italy		Laboratory of Earthquake engineering and Dynamic Analysis (LEDA) - "Kore" University of Enna (dual table)	10 x 4	100	6	±400	±400	±250	±1100	±1100	±750
28	Europe	The Netherlands	-	European Space Agency (ESA) ESTEC Test Centre, Noordwijk	5.5 x 5.5	22.5	6	±70	±70	±70	±800	±800	±800
29	Europe	Portugal	-	Laboratorio Nacional de Engenharia Civil (LNEC), Lisbon	5.6 x 5.6	40	3	±175	±175	±175	±200	±200	±200
30	Europe	Russia	-	Hydroproject Research Institute	5 x 5	50	3	±70	±70	±40	±600	?	?
31	Europe	Spain	-	CEDEX, Madrid	3 x 3	10	6	±100	±100	±50	?	?	?
32	Europe	Turkey	-	Bogazici University, Istanbul	0.7 x 0.7	0.1	3	±120	±120	±120	±1200	±1200	±1200
33	Europe	UK	-	University of Bristol (EERC), Bristol	3 x 3	17	6	±150	±150	±150	±1100	±1100	±1100
34	Asia	Pakistan	-	Earthquake Engineering Center, University of Engineering & Technology, Peshawar	6.0 x 6.0	60	6	±300	±300	±300	±1100	±1100	±1100
35	North America	Mexico	Mexico D. F.	Universidad Nacional Autónoma de México (UNAM), México	4 x 4	20	5	±150	±150	±75	±1100	±1100	±450
36	North America	USA	Colorado	ANCO Engineers, Inc Boulder, Colorado	3 x 3	10	3	±200	±200	±200	±2000	±2000	±2000
37	North America	USA	Alabama	Wyle Laboratories	2.7 x 2.7	4.5	3	±250	±250	±250	±1120	±1120	±1120
38	North America	USA	California	University of California at Berkeley, PEER-UCB lab	6.1 x 6.1	85	6	±127	±127	±51	±762	±762	±254
39	North America	USA	California	University of California at Berkeley, Structures Laboratory on main campus	3.3 x 2.6	10	1	±800	n/a	n/a	±2540	n/a	n/a
40	North America	USA	California	University of California at San Diego	12.2 x 7.6	2000	1	±750	n/a	n/a	±1800	n/a	n/a
41	North America	USA	Pennsylvania	Clark Testing, Jefferson Hills	3.7 x 3.7	17.2	3	±152	±152	±152	±1270	±1270	±1270
42	North America	USA	New York	University at Buffalo (State University of New York)	3.6 x 3.6	50	6	±150	±150	±75	±1250	±1250	±500
43	North America	USA	Nevada	University of Nevada at Reno (6 axis table)	2.75 x 2.75	50	6	±75	±300	±100	?	?	?
44	North America	USA	Nevada	Dynamic Certification Laboratories	2.0 diam.	4.5	6	±140	±120	±150	±1000	±1000	±1200
45	North America	USA	Virginia	AREVA, Inc Lynchburg, Virginia	3 x 3	10	6	±142	±142	±142	±1778	±1778	±1778
46	North America	USA	Maryland	Morgan State University	3 x 3	10	6	±254	±508	±152.4	±1000	±1000	-
47	South East Asia	Vietnam	Ha Noi		3 x 3	10	6	±142	±142	±142	±1778	±1778	±1778

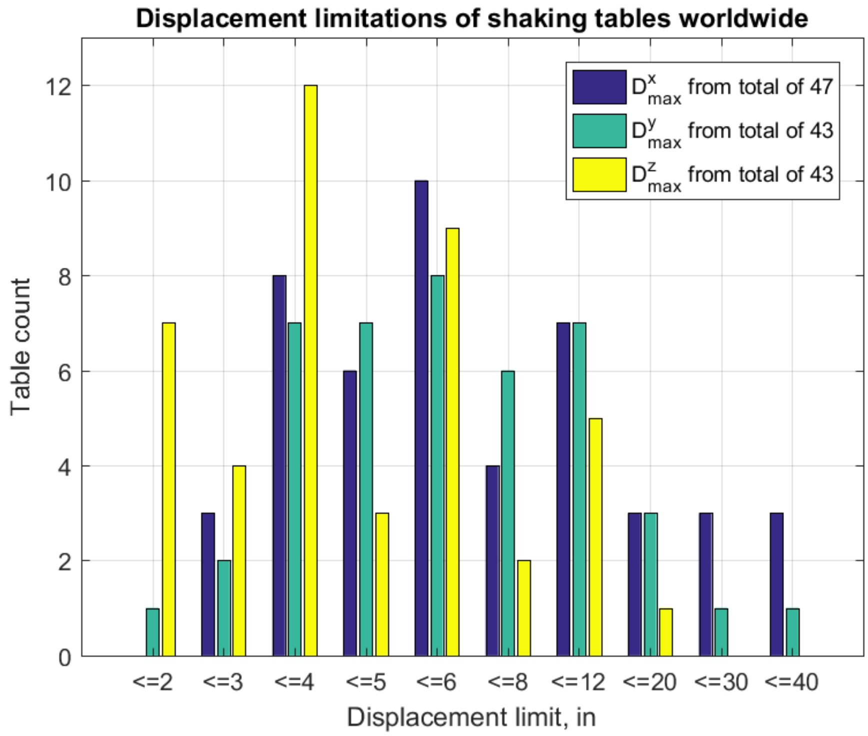

Figure 2.67 Summary of the displacement limitations of shaking tables worldwide.

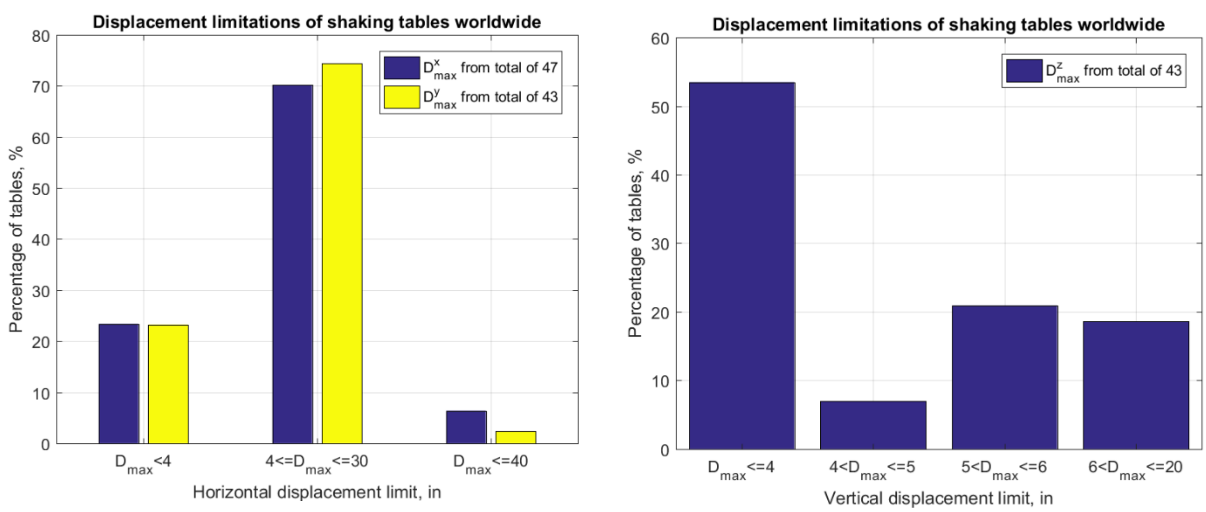

(a) (b)

Figure 2.68 Percentage of the major shaking tables within certain limitation groups: (a) limitations in the horizontal direction; and (b) limitation in the vertical direction.

Table 2.16 List of IEEE693-spectrum-compatible time histories filtered to meet limitations of majority of shaking tables.

	Displacement limit of shaking table						
TestQke	≤ 30in (750 mm)	≤ 8in (200 mm)	≤ 6in (150 mm)	≤ 5in (125 mm)	≤ 4in (100 mm)	≤ 3in (75 mm)	≤ 2in (50 mm)
TestQke4IEEE5-4X.AT2	TestQke4IEEE5-4X-0p150hz-28p650in.xlsx	TestQke4IEEE5-4X-0p585hz-7p806in.xlsx	TestQke4IEEE5-4X-0p665hz-5p694in.xlsx	TestQke4IEEE5-4X-0p785hz-4p887in.xlsx	TestQke4IEEE5-4X-0p980hz-3p870in.xlsx		
TestQke4IEEE5-4Y.AT2	TestQke4IEEE5-4Y-0p155hz-29p040in.xlsx	TestQke4IEEE5-4Y-0p572hz-7p704in.xlsx	TestQke4IEEE5-4Y-0p800hz-5p751in.xlsx	TestQke4IEEE5-4Y-0p855hz-4p808in.xlsx	TestQke4IEEE5-4Y-0p965hz-3p878in.xlsx		
TestQke4IEEE5-4Z.AT2			TestQke4IEEE5-4Z-0p665hz-5p733in.xlsx	TestQke4IEEE5-4Z-0p785hz-4p860in.xlsx	TestQke4IEEE5-4Z-0p885hz-3p897in.xlsx	TestQke4IEEE5-4Z-0p950hz-2p963in.xlsx	TestQke4IEEE5-4Z-1p235hz-1p982in.xlsx
TestQke4IEEE5-5X.AT2	TestQke4IEEE5-5X-0p175hz-29p628in.xlsx	TestQke4IEEE5-5X-0p560hz-7p764in.xlsx	TestQke4IEEE5-5X-0p665hz-5p826in.xlsx	TestQke4IEEE5-5X-0p805hz-4p866in.xlsx	TestQke4IEEE5-5X-0p880hz-3p811in.xlsx		
TestQke4IEEE5-5Y.AT2	TestQke4IEEE5-5Y-0p130hz-29p645in.xlsx	TestQke4IEEE5-5Y-0p550hz-7p753in.xlsx	TestQke4IEEE5-5Y-0p770hz-5p752in.xlsx	TestQke4IEEE5-5Y-0p795hz-4p829in.xlsx	TestQke4IEEE5-5Y-0p900hz-3p920in.xlsx		
TestQke4IEEE5-5Z.AT2			TestQke4IEEE5-5Z-0p685hz-5p846in.xlsx	TestQke4IEEE5-5Z-0p750hz-4p880in.xlsx	TestQke4IEEE5-5Z-0p650hz-3p899in.xlsx	TestQke4IEEE5-5Z-0p760hz-2p800in.xlsx	TestQke4IEEE5-5Z-0p980hz-1p852in.xlsx
TestQke4IEEE5-6X.AT2	TestQke4IEEE5-6X-0p175hz-29p623in.xlsx	TestQke4IEEE5-6X-0p540hz-7p619in.xlsx	TestQke4IEEE5-6X-0p635hz-5p416in.xlsx	TestQke4IEEE5-6X-0p695hz-4p496in.xlsx	TestQke4IEEE5-6X-0p860hz-3p765in.xlsx		
TestQke4IEEE5-6Y.AT2	TestQke4IEEE5-6Y-0p130hz-29p587in.xlsx	TestQke4IEEE5-6Y-0p410hz-7p894in.xlsx	TestQke4IEEE5-6Y-0p755hz-5p530in.xlsx	TestQke4IEEE5-6Y-0p790hz-4p873in.xlsx	TestQke4IEEE5-6Y-0p850hz-3p842in.xlsx		
TestQke4IEEE5-6Z.AT2			TestQke4IEEE5-6Z-0p570hz-5p743in.xlsx	TestQke4IEEE5-6Z-0p630hz-4p753in.xlsx	TestQke4IEEE5-6Z-0p775hz-3p705in.xlsx	TestQke4IEEE5-6Z-0p985hz-2p816in.xlsx	TestQke4IEEE5-6Z-0p980hz-1p963in.xlsx

3 Conclusions and Recommendations

3.1 CONCLUSIONS

Based on the results of this study, the following major conclusions were made.

1. The horizontal spectra of almost all crustal records are enveloped by the IEEE693 spectrum anchored at 1.0*g*. For the RotD50 spectral accelerations, only 5.9% of all records exceed the IEEE693 spectrum. In the case of the RotD50 spectral accelerations obtained at R_{JB} exceeding 10 km, this percentage is even lower and amounts to about 1.5% of all crustal records obtained beyond 10 km.
2. In the case of the subduction type records, the number of records which spectra exceed the IEEE693 spectrum is much higher, so the RotD50 spectral accelerations of about 16.9% of subduction records exceed the IEEE693 spectrum. This result is well correlated with the findings of the parallel study [Mazzoni et al. 2017] that clearly demonstrated that the IEEE693 spectrum has a much larger margin in case of the crustal records when compared to subduction records.
3. Analysis conducted on the ratio of vertical spectral accelerations to that of the RotD50 for horizontal components revealed the following: the mean value of this ratio for all crustal records is below 80% (assumed in IEEE Std 693-2005 and P693/D16) in the low-frequency range up to about 7 Hz for all crustal records and 8 Hz with $R_{JB} > 10$ km and RotD50 ($f_{\max}$) > 0.2*g*. It increases after that and has a peak at 125% for all crustal records and 112% for crustal records with $R_{JB} > 10$ km and RotD50 ($f_{\max}$) > 0.2*g*. In contrast, the mean value of this ratio for subduction records can exceed 80% in both low- and high-frequency ranges. It is below the 80% threshold from 0.3 Hz to 12.8 Hz and after 20.9 Hz. It peaks in the low-frequency range at around 120%.
4. The use of the many parameters and IMs was crucial in the identification of the seed motions to be used in the spectral matching procedure performed in time domain. The best fit factor and cumulative distance at the best fit were instrumental in determining the records with the closest proximity to the IEEE693 spectra. Since this approach is generic and spectrum independent, it can be used for any other target response spectrum.
5. In this study, the seed motions were matched to the target IEEE693 spectrum within a tight tolerance and five 3-component IEEE693-spectrum-compatible time histories from historic records were developed. This set was composed of four seed motions

were selected from the set of crustal records and one seed motion was selected from the set of subduction records. The spectral accelerations of the time histories fit into 16% and 15% strips, enveloping the IEEE693 spectrum at 1/24th and 1/12th octave resolutions, respectively. The same tolerance was achieved for three 3-component synthetic IEEE693-spectrum-compatible strong motions developed in the study. The suite of seven time histories (four from crustal records and three synthetic motions) is proposed for use in the IEEE693 seismic qualification testing and analysis. The historically-based subduction record also satisfies the requirements of P693/D16 and may be used for qualification purposes if desired by the user.

3.2 RECOMMENDATIONS

All spectrum-compatible time histories developed in this project satisfy the requirements of IEEE P693/D16. These motions are recommended for use in seismic qualification activities. Users should note that TestQke4IEEE5-5 was developed from a seed motion recorded from a subduction earthquake. Although it satisfies the requirements of IEEE P693/D16 and may be used for qualification activities, its main purpose is to aid research in the behavior and performance of equipment in subduction earthquakes, which are specifically not addressed in IEEE P693/D16. Further research is planned in this area.

REFERENCES

Abrahamson N.A. (1992). Non-stationary spectral matching, *Seismol. Res. Lett*., 63(1): 30.

AEC (2015). http://earthquake.alaska.edu/magnitude-71-iniskin-earthquake. Alaska Earthquake Center, University of Alaska, Fairbanks, AK.

Al Atik L., Abrahamson N.A. (2010). An improved method for nonstationary spectral matching, *Earthq. Spectra*, 26(3): 601–617.

Ancheta T.D., Bozorgnia Y., Darragh R., Silva W.J., Chiou B., Stewart J.P., Boore D.M., Graves R.W., Abrahamson N.A., Campbell K.W., Idriss I.M., Youngs R.R., Atkinson G.A. (2012). PEER NGA-West2 database: A database of ground motions recorded in shallow crustal earthquakes in active tectonic regions, *Proceedings, 15th World Conference on Earthquake Engineering*, Paper No. 5599, Lisbon, Portugal.

Ancheta T.D., Darragh R., Stewart J.P., Seyhan E., Silva W.J., Chiou B.S.J., Wooddell K.E., Graves R.W, Kottke A.R., Boore D.M., Kashida T., Donahue J.L. (2013). PEER NGA-West2 database, *PEER Report No. 2013/03*, Pacific Earthquake Engineering Research Center, University of California, Berkeley, CA.

Arias A. (1969). A measure of earthquake intensity, in *Seismic Design for Nuclear Power Plants*, R. Hansen, ed., Cambridge: Massachusetts Institute of Technology, Boston, MA.

ASCE (2017). Minimum design loads for buildings and other structures, *Technical Report ASCE/SEI 7-17*, American Society of Civil Engineers, Reston, VA (in press).

Atkinson G.M. (1993). Earthquake source spectra in eastern North America, *Bull. Seismol. Soc. Am*. 83: 1778–1798.

Bolt B.A. (1969). Duration of strong motion, *Proceedings, 4th World Conference Earthquake Engineering*, pp. 1304–1314, Santiago, Chile.

Boore D.M. (2012). Relations between GM_AR, GMRotI50, and RotD50. Presentation at USGS National Seismic Hazard Map (NSHMp) Workshop on Ground Motion Prediction Equations (GMPEs) for the 2014 Update, December 12-13, 2012, I-House, Berkeley, CA (at https://earthquake.usgs.gov/static/lfs/nshm/workshops/GMPE2012/THUR_PM06_Discussion_BOORE%20rotd50_v1.0(dmb)sm.pdf).

Boore D.M., Atkinson G.M. (1989). Spectral scaling of the 1985 to 1988 Nahanni, Northwest Territories, earthquakes, *Bull. Seismol. Soc. Am*., 79: 1736–1761.

Boore D.M., Atkinson G.M. (2007). Boore-Atkinson NGA ground motion relations for the geometric mean horizontal component of peak and spectral ground motion parameters, *PEER Report No. 2007/01*, Pacific Earthquake Engineering Research Center, University of California, Berkeley, CA.

Boore D.M., Atkinson G.M. (2008). Ground-motion prediction equations for the average horizontal component of PGA, PGV, and 5%-damped PSA at spectral Periods between 0.01 s and 10.0 s, *Earthq. Spectra,* 24: 99–138.

Boore D.M., Watson-Lamprey J., Abrahamson N.A. (2006). GMRotD and GMRotI: Orientation-independent measures of ground motion, *Bull. Seismol. Soc. Am*., 96: 1502–1511.

Campbell K.W., Bozorgnia Y. (2013). NGA-West2 Campbell-Bozorgnia ground motion model for the horizontal components of PGA, PGV, and 5%-damped elastic pseudo-acceleration response spectra for periods ranging from 0.01 to 10 sec, *PEER Report No. 2013/06*, Pacific Earthquake Engineering Research Center, University of California, Berkeley, CA.

Chandramohan R. Baker J.W., Deierlein G.G. (2016). Impact of hazard-consistent ground motion duration in structural collapse risk assessment, *Earthq. Eng. Struct. Dyn*., 45: 1357–1379.

CESMD (2016). *http://strongmotioncenter.org/*, Center for Engineering Strong Motion Data.

Dobry R., Idriss I.M., Ng E. (1978). Duration characteristics of horizontal components of strong motion earthquake records. *Bull. Seismol. Soc. Am*., 68(5): 1487–1520.

Gasparini D.A., Vanmarcke E.H. (1976). Simulated earthquake motions compatible with prescribed response spectra. *Department of Civil Engineering, Research Report R76-4*, Massachusetts Institute of Technology, Cambridge, MA.

Hancock J., Watson-Lamprey J., Abrahamson N. A., Bommer J. J., Markatis A., McCoy E., Mendis R. (2006). An improved method of matching response spectra of recorded earthquake ground motion using wavelets, *J. Earthq. Eng*., 10 (Special Issue 1): 67–89.

IEC (1999). *IEC60068-2-57 Environmental Testing*, Part 2-57: Tests - Test Ff: Vibration - Time-history and sine beat method, International Electrotechnical Commission, second ed., Geneva, Switzerland.

IEEE (2005). *IEEE Recommended Practice for Seismic Design of Substations*, IEEE Std 693-2005, Piscataway, NJ.

IEEE693 WG (2017). IEEE P693/D16 (IEEE693 WG, 2017) *Draft Recommended Practice for Seismic Design of Substations,* Piscataway, NJ.

EPRI (2017). *Development of IEEE 693 Spectrum-Compatible Time Histories for Seismic Qualifications*, the Electric Power Research Institute, Palo Alto, CA: 2017. 3002011880.

Mazzoni S., Bozorgnia Y., Abrahamson N.A. (2017). Evaluation of the shape of IEEE-693 response spectra for subduction and crustal earthquakes. *Proceedings, 16th World Conference on Earthquake,* Santiago Chile.

Lee W.H K., Shin T.C., Kuo K.W., Chen K.C., Wu C.F. (2001). Data files from "CWB free-field strong-motion data from the 21 September Chi-Chi, Taiwan, earthquake, *Bull. Seismol. Soc. Am*., 91(5): 1370–1376.

Naeim F., Anderson J.C. (1996). Design classification of horizontal and vertical earthquake ground motion (1933-1994). A Report to the U.S. Geological Survey (USGS). *JAMA Report No. 7738.68-96*, J.A. Martin and Associates, Inc., Los Angeles, CA.

NIST (2011). Selecting and scaling earthquake ground motions for performing response-history analyses, *Report NIST GCR 11-917-15*, National Institute of Standards and Technology, Gaithersburg, MD.

Page R.A., Boore D.M., Loyner W.M., Caulter H.W. (1972). Ground motion values for use in the seismic design of the Trans-Alaska Pipeline System, U.S. Geological Survey, *Circular 672*, Menlo Park, CA.

PEER (2013). *http://peer.berkeley.edu/assets/NGA_West2_flatfiles.zip,* Pacific Earthquake Engineering Research Center, University of California, Berkeley, CA.

PEER (2016). *https://ngawest2.berkeley.edu/,* Pacific Earthquake Engineering Research Center, University of California, Berkeley, CA.

PG&E (1988). *Final report of the Diablo Canyon Long Term Seismic Program*, Pacific Gas and Electric Co., Pacific Earthquake Engineering Research Center, University of California, Berkeley, CA., *http://ngawest2.berkeley.edu*.

Power M., Chiou B.-S.J., Abrahamson N.A., Bozorgnia Y., Shantz T., Roblee C. (2008). An overview of the NGA project, *Earthq. Spectra*, 24: 3–21.

Takhirov S., Fenves G.L., Fujisaki E., Clyde D. (2004). Ground motions for earthquake simulator qualification of electrical equipment, *PEER Report No. 2004/07*, Pacific Earthquake Engineering Research Center, University of California at Berkeley, CA.

Takhirov S., Fujisaki E., Kempner L., Riley M. (2017a). Development of time histories for IEEE693 testing/analysis and their validation by numerical simulations and full-scale testing of seismically isolated equipment. *Proceedings, 16th World Conference on Earthquake,* Santiago Chile.

Takhirov S., Fujisaki E., Kempner L., Riley M., Low B. (2017b). Nonlinear systems subjected to multiple seismic excitations matched to the same spectrum: numerical predictions versus shaking table tests, *Proceedings, COMPDYN2017, 6th International Conference on Computational Methods in Structural Dynamics and Earthquake Engineering*, Rhodes, Greece.

Takhirov S., Fujisaki E., Kempner L., Riley M., Low B. (2017c). Time histories for IEEE693 testing and analysis: A summary of unfiltered and filtered versions. *Structures Laboratory Report 2017/01*, Department of Civil and Environmental Engineering, University of California, Berkeley, CA.

UW (2016). *https://hazards.uw.edu/geology/m9/research/,* University of Washington, Seattle, WA.

Vanmarcke E.H. (1976). *Structural Response to Earthquakes. Chapter 8 in Seismic Risk and Engineering Decisions,* C. Lomitz and E. Rosenblueth, eds., Elsevier Publishing Co., Amsterdam.

Wikipedia (2017). . https://en.wikipedia.org/wiki/Earthquake_shaking_table.

Appendix A: Parameters of Strong-Motion Records and Response Indices

Appendix A presents definitions and discussions of parameters and indices used to characterize the strong-motion records. The parameters and the indices are used to describe the severity of the earthquake records and are divided into two groups. The first group consists of parameters obtained directly from the recorded strong motion data, the second of parameters and indices obtained by passing the recorded data through a single-degree-of-freedom (SDOF) system and by manipulating the system response. Therefore, the former group includes ground motion parameters, whereas the latter group includes spectra and other response indices delivered from a SDOF system analysis.

A.1 PARAMETERS OF STRONG-MOTION RECORD

This section discusses parameters delivered directly from an acceleration time history by means of simple manipulations. The parameters include peak values for acceleration and velocity, durations, CE, and cycle count.

A.1.1 Peak Values of Ground Motion

Peak ground acceleration. One of the most commonly used parameters to describe the strong-motion record is peak ground acceleration (PGA). The PGA is calculated as a maximum of absolute value of the acceleration. The value of PGA can be presented as a number with dimensions of the acceleration in any particular measuring system or as a fraction of *g*, where *g* is an acceleration due to gravity, that is 386.4 in./sec^2 (9.81 m/sec^2).

Peak ground velocity. Peak ground velocity (PGV) is another important parameter commonly used to characterize a strong-motion record. A strong-motion record usually represents an acceleration time history recorded at a particular location; therefore, the determination of the velocity time history involves some data manipulation. The acceleration time history has to be numerically integrated over time, and the absolute maximum of the delivered velocity time history yields the PGV. Depending on the selected measuring system, the PGV can be presented in in./sec (m/sec).

A.1.2 Cumulative Energy or Arias Intensity and Related Parameters

Cumulative energy. For engineering purposes, the cumulative energy (CE) of a strong-motion record is defined as the area under the squared acceleration record, and represents a measure of intensity of the record:

$$CE = \int_0^t a(\tau)^2 d\tau$$

where $a(\tau)$ is a time history of the acceleration, and t is a length (measured in seconds) of the strong-motion record.

The CE is a very important parameter commonly used to calculate other parameters of a strong-motion record, e.g., Arias intensity, root mean square (RMS) acceleration, and duration parameters. For instance, the CE is proportional to a measure of intensity of a strong motion, Arias intensity [Arias 1969], I_A.

$$I_A = \pi\, CE/g$$

Depending on the selected measuring system, the CE can be presented in in.^{2}/sec^3 (m^2/sec^3) or simply in g^2 sec.

Root mean square acceleration. The computed CE can be used in calculating the parameter of a strong-motion record known as the RMS acceleration a_{RMS}, commonly used to characterize amplitude of the accelerogram.

$$a_{\mathrm{RMS}} = \sqrt{CE/t}$$

In contrast to the PGA, the RMS acceleration takes into account the complete ground motion time history and is a factored mean amplitude for the entire accelerogram. The RMS acceleration is usually presented in fractions of g.

Duration based on CE. A method to calculate a duration of a strong-motion record based on using the cumulative energy or Arias intensity was proposed by Dobry et al. [1978]. The method defines the duration as the time interval required to accumulate between 5% and 95% of the accelerogram's maximum CE.

Strong-part duration based on CE. Another parameter for measuring the duration of a strong motion part of an accelerogram, or "strong-part duration," is introduced as follows. This duration is defined as the time interval required to accumulate between 25%–75% of the maximum cumulative energy. For CE normalized to the maximum value, these threshold values correspond to 0.25 and 0.75, respectively, and are represented by the horizontal dashed lines in Figure A.1. The ratio of the strong-part duration to the duration of the strong-motion history expressed by percent can serve as an important parameter to measure the intensity of the record. The ratio is extensively used in the study.

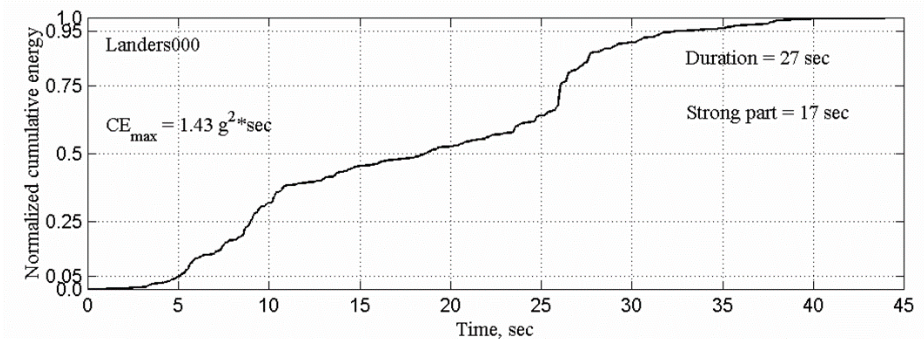

Figure A.1 Example of cumulative energy computation (example of Landers in the 0° direction is shown).

The term "duration of strong part" is also used in the IEC-1999 international standard [IEC 1999], although it is defined quite differently: the duration is taken as the length of the strong-motion record in seconds, and the definition of the strong-part duration coincides with the IEEE definition of the duration presented below.

A.1.3 Bracketed Duration

In the IEEE 693 standard the bracketed duration is defined as the time interval between the first and the last occurrences of accelerations equal to or larger than 25% of the maximum value of the acceleration. Bracketed durations based on this IEEE definition, and based on the CE, were extensively used in the study.

The other existing definition of the bracketed duration is a time interval between the first and last occurrences of accelerations equal to, or larger than, 0.05*g* [Bolt 1969; Page et al. 1972]. The comprehensive study conducted on a large database of strong-motion records by Naeim and Anderson [1996] showed that the bracketed duration based on the last definition is not effective for classification of strong-motion records. The duration calculated with a 0.05*g* threshold can produce a result that overestimates the engineering significance of the bracketed duration. The bracketed duration was calculated [Naeim and Anderson 1996) with various thresholds, namely 0.05*g*, 0.10*g*, and 0.30*g*; the analysis showed that low-level ground vibrations could produce a long duration based on a 0.05*g* threshold, whereas an actual duration of strong motion vibrations is much shorter.

A.1.4 Cycle Counting Procedure (ASTM)

In order to classify the strong motion in terms of fatigue analysis, a cycle counting procedure is used. The procedure is based on the commonly used ASTM procedure, called the "simplified rain flow cycle counting procedure." A detailed description of the procedure and some notes on fracture mechanics are presented in Takhirov et al. [2004]. As a result, the cycle counting procedure yields a histogram of cycle counts for the magnitude range of the cycles. The procedure counts the cycles of the accelerogram in order to deliver a number of cycles in the excitation's acceleration imposed on equipment during testing.

A.1.5 Power Spectral Density

Another important parameter of the strong-motion record is a power spectral density (PSD). This parameter is commonly used to obtain information on the frequency distribution of the energy contained in the accelerogram. The power spectral density presents how the modulus of the fast Fourier transforms of the strong motion depend on frequency, or period. For acceleration records, the PSD can be presented in g^2/Hz.

A.2 RESPONSE INDICES BASED ON ELASTIC SDOF SYSTEM ANALYSIS

A.2.1 Spectral Displacement, Velocity, and Acceleration

As previously mentioned, the second group of parameters and indices are based on analysis of a SDOF system impacted by a particular strong motion signal. The spectral relative displacement, usually denoted as S_d, is the most important index and is usually presented as an elastic response spectrum. The spectrum is the plot of the maximum response displacement of the SDOF system to a specified earthquake strong motion plotted as a function of the system's natural frequency or period for a particular critical damping of the system. The index presents the maximum value of the displacement relative to the displacement of the ground; therefore it has the term "relative" in its definition. For simplicity of further discussion, this term is omitted for all spectral indices.

Spectral pseudo-velocity. Electrical equipment has a relatively low damping value, usually below 10% of critical damping. In this case, it can be assumed (with some acceptable accuracy) that the maximum response velocity of the SDOF system is equal to spectral relative pseudo-velocity defined as the product of the natural frequency of the system, ω, and the spectral relative displacement:

$$S_V = \omega S_D$$

For simplicity, the spectral relative pseudo-velocity is referred to below as "spectral velocity."

Spectral pseudo-acceleration. Based on the same assumption of low damping, the spectral relative pseudo-acceleration, S_A, is defined as a product of the spectral relative velocity and the natural frequency of the system:

$$S_A = \omega S_V \text{ or } S_A = \omega^2 S_D$$

This index is the most commonly used spectral quantity to characterize the possible impact of the particular strong motion signal to the structure. For simplicity the spectral relative pseudo-acceleration is referred to below as "spectral acceleration."

A.2.2 Number of Cycles in SDOF Response

In order to rate an intensity of the strong-motion time history and its effect on a SDOF system, a new parameter was introduced. The parameter represents the number of high cycles in the acceleration response of the SDOF system plotted against the natural frequency of the system and calculated for a fixed damping value. Only cycles with a relatively high magnitude are included in the high-cycle count: the study uses a threshold of 70% of the maximum magnitude. The study uses a 2% damping value and calculates the number of high cycles only for frequencies of a strong part of the required response spectrum. The strong part of a required response spectrum (RRS) is a part of the spectrum for which the response acceleration is higher than for the –3 dB bandpass of the RRS [IEC 1999]. In other words it is a part of the spectrum where the spectral accelerations are higher than the plateau value divided by the square root of two. In the case of the IEEE spectrum, the strong part of the spectrum covers frequencies from 0.78–11.78 Hz.

A similar parameter, called the "number of high peaks of the response with 70% maximum amplitude threshold," is used in the international standard [IEC 1999]. The standard specifies that the elastic response of a SDOF to the application of a test time history shall result in 3–20 high peaks for a 5% damped system [IEC 1999: Section 6.4]. The high peak is defined as a positive or a negative maximum deviation (with 70% threshold) from the zero line between two consecutive zero crossing points.

Appendix B: Validation of Spectral Computational Procedures

Since the report relies heavily on the computation of spectral accelerations, a comparison study between procedures used in this report and the spectral accelerations tabulated in the Flatfile of the PEER NGA West-2 was conducted. The study was conducted on several strong motions with two different sampling rates: 100 Hz (Δt = 0.01 sec) and 200 Hz (Δt = 0.005 sec). As presented in Table B.1, two sets of strong motions were randomly selected from the set of records studied herein. The comparative study was conducted on the horizontal components of the strong motions with the names of the records listed in Table B.1.

The results of this study are presented in Figure B.1 and Figure B.2. The comparative analysis of these spectra clearly demonstrated the fact that the spectral procedure used in this study produces spectral accelerations that are essentially the same as the ones from PEER NGA West-2 Flatfile [PEER 2013]. The spectra were computed at a 5% critical damping ratio.

Table B.1 Spectral computation was compared for the horizontal components of the following strong-motion records

Record Sequence Number	Horizontal component 1	Horizontal component 2	Sampling rate, Hz
31	PARKF_C08050.AT2	PARKF_C08320.AT2	100
113	OROVILLE_D-DWR090.AT2	OROVILLE_D-DWR180.AT2	200

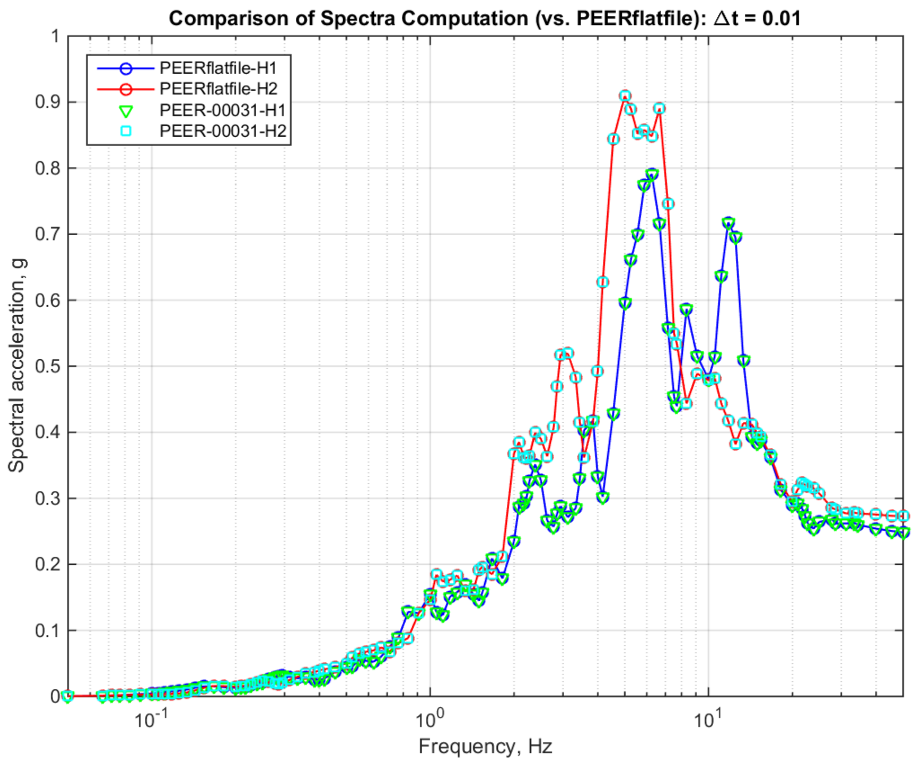

Figure B.1 Horizontal spectra for PEER sequence number 31.

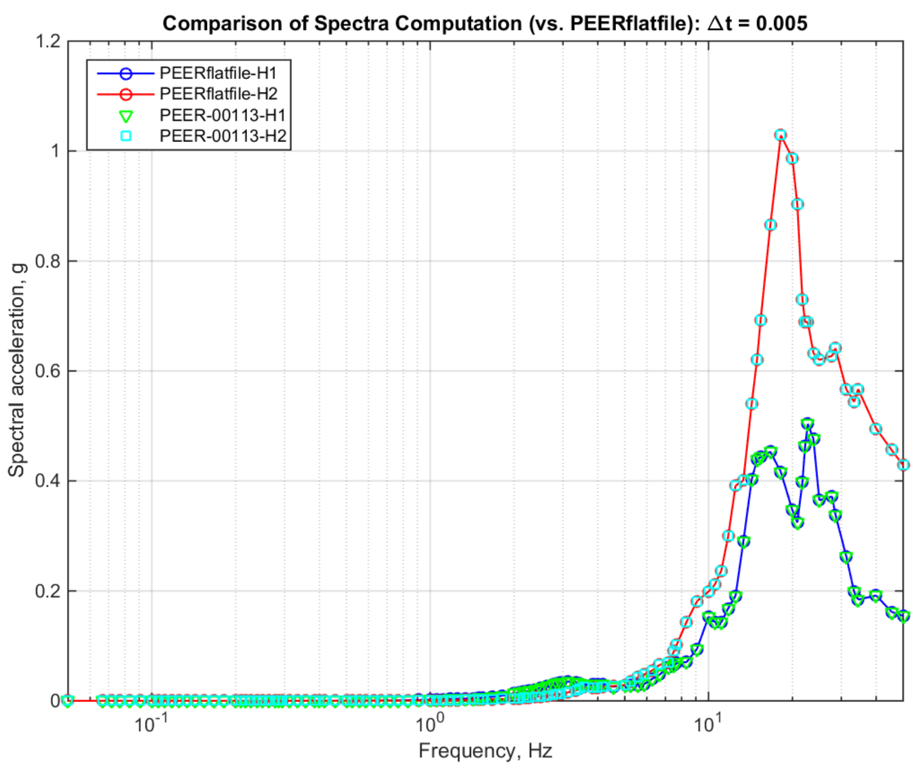

Figure B.2 Horizontal spectra for PEER sequence number 113.

PEER REPORTS

PEER reports are available as a free PDF download from https://peer.berkeley.edu/peer-reports. Printed hard copies of PEER reports can be ordered directly from our printer by following the instructions also available at https://peer.berkeley.edu/peer-reports. For other related questions about the PEER Report Series, contact the Pacific Earthquake Engineering Research Center, 325 Davis Hall; Mail Code 1792, Berkeley, CA 94720. Tel.: (510) 642-3437; and Email: peer_center@berkeley.edu.

PEER 2017/09 *“”R” Package for Computation of Earthquake Ground-Motion Response Spectra.* Pengfei Wang, Jonathan P. Stewart, Yousef Bozorgnia, David M. Boore, and Tadahiro Kishida. December 2017.

PEER 2017/08 *Influence of Kinematic SSI on Foundation Input Motions for Bridges on Deep Foundations*. Benjamin J. Turner, Scott J. Brandenberg, and Jonathan P. Stewart. November 2017.

PEER 2017/07 *A Nonlinear Kinetic Model for Multi-Stage Friction Pendulum Systems*. Paul L. Drazin and Sanjay Govindjee, September 2017.

PEER 2017/06 *Guidelines for Performance-Based Seismic Design of Tall Buildings, Version 2.02*. TBI Working Group led by co-chairs Ron Hamburger and Jack Moehle: Jack Baker, Jonathan Bray, C.B. Crouse, Greg Deierlein, John Hooper, Marshall Lew, Joe Maffei, Stephen Mahin, James Malley, Farzad Naeim, Jonathan Stewart, and John Wallace. May 2017.

PEER 2017/05 *Recommendations for Ergodic Nonlinear Site Amplification in Central and Eastern North America*. Youssef M.A. Hashash, Joseph A. Harmon, Okan Ilhan, Grace A. Parker, and Jonathan P. Stewart. March 2017.

PEER 2017/04 *Expert Panel Recommendations for Ergodic Site Amplification in Central and Eastern North America*. Jonathan P. Stewart, Grace A Parker, Joseph P. Harmon, Gail M. Atkinson, David M. Boore, Robert B. Darragh, Walter J. Silva, and Youssef M.A. Hashash. March 2017.

PEER 2017/03 *NGA-East Ground-Motion Models for the U.S. Geological Survey National Seismic Hazard Maps*. Christine A. Goulet, Yousef Bozorgnia, Nicolas Kuehn, Linda Al Atik, Robert R. Youngs, Robert W. Graves, and Gail M. Atkinson. March 2017.

PEER 2017/02 *U.S.–New Zealand–Japan Workshop: Liquefaction-Induced Ground Movements Effects, University of California, Berkeley, California, 2–4 November 2016.* Jonathan D. Bray, Ross W. Boulanger, Misko Cubrinovski, Kohji Tokimatsu, Steven L. Kramer, Thomas O’Rourke, Ellen Rathje, Russell A. Green, Peter K. Robinson, and Christine Z. Beyzaei. March 2017.

PEER 2017/01 *2016 PEER Annual Report*. Khalid M. Mosalam, Amarnath Kasalanati, and Grace Kang. March 2017.

PEER 2016/10 *Performance-Based Robust Nonlinear Seismic Analysis with Application to Reinforced Concrete Bridge Systems*. Xiao Ling and Khalid M. Mosalam. December 2016.

PEER 2016/08 *Resilience of Critical Structures, Infrastructure, and Communities***.** Gian Paolo Cimellaro, Ali Zamani-Noori, Omar Kamouh, Vesna Terzic, and Stephen A. Mahin. December 2016.

PEER 2016/07 *Hybrid Simulation Theory for a Classical Nonlinear Dynamical System*. Paul L. Drazin and Sanjay Govindjee. September 2016.

PEER 2016/06 *California Earthquake Early Warning System Benefit Study*. Laurie A. Johnson, Sharyl Rabinovici, Grace S. Kang, and Stephen A. Mahin. July 2016.

PEER 2016/05 *Ground-Motion Prediction Equations for Arias Intensity Consistent with the NGA-West2 Ground-Motion Models.* Charlotte Abrahamson, Hao-Jun Michael Shi, and Brian Yang. July 2016.

PEER 2016/04 *The M_W 6.0 South Napa Earthquake of August 24, 2014: A Wake-Up Call for Renewed Investment in Seismic Resilience Across California.* Prepared for the California Seismic Safety Commission, Laurie A. Johnson and Stephen A. Mahin. May 2016.

PEER 2016/03 *Simulation Confidence in Tsunami-Driven Overland Flow.* Patrick Lynett. May 2016.

PEER 2016/02 *Semi-Automated Procedure for Windowing time Series and Computing Fourier Amplitude Spectra for the NGA-West2 Database.* Tadahiro Kishida, Olga-Joan Ktenidou, Robert B. Darragh, and Walter J. Silva. May 2016.

PEER 2016/01 *A Methodology for the Estimation of Kappa (κ) from Large Datasets: Example Application to Rock Sites in the NGA-East Database and Implications on Design Motions.* Olga-Joan Ktenidou, Norman A. Abrahamson, Robert B. Darragh, and Walter J. Silva. April 2016.

PEER 2015/13 *Self-Centering Precast Concrete Dual-Steel-Shell Columns for Accelerated Bridge Construction: Seismic Performance, Analysis, and Design*. Gabriele Guerrini, José I. Restrepo, Athanassios Vervelidis, and Milena Massari. December 2015.

PEER 2015/12 *Shear-Flexure Interaction Modeling for Reinforced Concrete Structural Walls and Columns under Reversed Cyclic Loading*. Kristijan Kolozvari, Kutay Orakcal, and John Wallace. December 2015.

PEER 2015/11 *Selection and Scaling of Ground Motions for Nonlinear Response History Analysis of Buildings in Performance-Based Earthquake Engineering*. N. Simon Kwong and Anil K. Chopra. December 2015.

PEER 2015/10 *Structural Behavior of Column-Bent Cap Beam-Box Girder Systems in Reinforced Concrete Bridges Subjected to Gravity and Seismic Loads. Part II: Hybrid Simulation and Post-Test Analysis*. Mohamed A. Moustafa and Khalid M. Mosalam. November 2015.

PEER 2015/09 *Structural Behavior of Column-Bent Cap Beam-Box Girder Systems in Reinforced Concrete Bridges Subjected to Gravity and Seismic Loads. Part I: Pre-Test Analysis and Quasi-Static Experiments*. Mohamed A. Moustafa and Khalid M. Mosalam. September 2015.

PEER 2015/08 *NGA-East: Adjustments to Median Ground-Motion Models for Center and Eastern North America*. August 2015.

PEER 2015/07 *NGA-East: Ground-Motion Standard-Deviation Models for Central and Eastern North America*. Linda Al Atik. June 2015.

PEER 2015/06 *Adjusting Ground-Motion Intensity Measures to a Reference Site for which V_{S30} = 3000 m/sec*. David M. Boore. May 2015.

PEER 2015/05 *Hybrid Simulation of Seismic Isolation Systems Applied to an APR-1400 Nuclear Power Plant.* Andreas H. Schellenberg, Alireza Sarebanha, Matthew J. Schoettler, Gilberto Mosqueda, Gianmario Benzoni, and Stephen A. Mahin. April 2015.

PEER 2015/04 *NGA-East: Median Ground-Motion Models for the Central and Eastern North America Region*. April 2015.

PEER 2015/03 *Single Series Solution for the Rectangular Fiber-Reinforced Elastomeric Isolator Compression Modulus*. James M. Kelly and Niel C. Van Engelen. March 2015.

PEER 2015/02 *A Full-Scale, Single-Column Bridge Bent Tested by Shake-Table Excitation.* Matthew J. Schoettler, José I. Restrepo, Gabriele Guerrini, David E. Duck, and Francesco Carrea. March 2015.

PEER 2015/01 *Concrete Column Blind Prediction Contest 2010: Outcomes and Observations.* Vesna Terzic, Matthew J. Schoettler, José I. Restrepo, and Stephen A Mahin. March 2015.

PEER 2014/20 *Stochastic Modeling and Simulation of Near-Fault Ground Motions for Performance-Based Earthquake Engineering*. Mayssa Dabaghi and Armen Der Kiureghian. December 2014.

PEER 2014/19 *Seismic Response of a Hybrid Fiber-Reinforced Concrete Bridge Column Detailed for Accelerated Bridge Construction*. Wilson Nguyen, William Trono, Marios Panagiotou, and Claudia P. Ostertag. December 2014.

PEER 2014/18 *Three-Dimensional Beam-Truss Model for Reinforced Concrete Walls and Slabs Subjected to Cyclic Static or Dynamic Loading*. Yuan Lu, Marios Panagiotou, and Ioannis Koutromanos. December 2014.

PEER 2014/17 *PEER NGA-East Database.* Christine A. Goulet, Tadahiro Kishida, Timothy D. Ancheta, Chris H. Cramer, Robert B. Darragh, Walter J. Silva, Youssef M.A. Hashash, Joseph Harmon, Jonathan P. Stewart, Katie E. Wooddell, and Robert R. Youngs. October 2014.

PEER 2014/16 *Guidelines for Performing Hazard-Consistent One-Dimensional Ground Response Analysis for Ground Motion Prediction*. Jonathan P. Stewart, Kioumars Afshari, and Youssef M.A. Hashash. October 2014.

PEER 2014/15 *NGA-East Regionalization Report: Comparison of Four Crustal Regions within Central and Eastern North America using Waveform Modeling and 5%-Damped Pseudo-Spectral Acceleration Response*. Jennifer Dreiling, Marius P. Isken, Walter D. Mooney, Martin C. Chapman, and Richard W. Godbee. October 2014.

PEER 2014/14 *Scaling Relations between Seismic Moment and Rupture Area of Earthquakes in Stable Continental Regions*. Paul Somerville. August 2014.

PEER 2014/13 *PEER Preliminary Notes and Observations on the August 24, 2014, South Napa Earthquake*. Grace S. Kang and Stephen A. Mahin, Editors. September 2014.

PEER 2014/12 *Reference-Rock Site Conditions for Central and Eastern North America: Part II – Attenuation (Kappa) Definition*. Kenneth W. Campbell, Youssef M.A. Hashash, Byungmin Kim, Albert R. Kottke, Ellen M. Rathje, Walter J. Silva, and Jonathan P. Stewart. August 2014.

PEER 2014/11 *Reference-Rock Site Conditions for Central and Eastern North America: Part I - Velocity Definition*. Youssef M.A. Hashash, Albert R. Kottke, Jonathan P. Stewart, Kenneth W. Campbell, Byungmin Kim, Ellen M. Rathje, Walter J. Silva, Sissy Nikolaou, and Cheryl Moss. August 2014.

PEER 2014/10 *Evaluation of Collapse and Non-Collapse of Parallel Bridges Affected by Liquefaction and Lateral Spreading*. Benjamin Turner, Scott J. Brandenberg, and Jonathan P. Stewart. August 2014.

PEER 2014/09 *PEER Arizona Strong-Motion Database and GMPEs Evaluation*. Tadahiro Kishida, Robert E. Kayen, Olga-Joan Ktenidou, Walter J. Silva, Robert B. Darragh, and Jennie Watson-Lamprey. June 2014.

PEER 2014/08 *Unbonded Pretensioned Bridge Columns with Rocking Detail*. Jeffrey A. Schaefer, Bryan Kennedy, Marc O. Eberhard, and John F. Stanton. June 2014.

PEER 2014/07 *Northridge 20 Symposium Summary Report: Impacts, Outcomes, and Next Steps*. May 2014.

PEER 2014/06 *Report of the Tenth Planning Meeting of NEES/E-Defense Collaborative Research on Earthquake Engineering*. December 2013.

PEER 2014/05 *Seismic Velocity Site Characterization of Thirty-One Chilean Seismometer Stations by Spectral Analysis of Surface Wave Dispersion*. Robert Kayen, Brad D. Carkin, Skye Corbet, Camilo Pinilla, Allan Ng, Edward Gorbis, and Christine Truong. April 2014.

PEER 2014/04 Effect of Vertical Acceleration on Shear Strength of Reinforced Concrete Columns. Hyerin Lee and Khalid M. Mosalam. April 2014.

PEER 2014/03 *Retest of Thirty-Year-Old Neoprene Isolation Bearings.* James M. Kelly and Niel C. Van Engelen. March 2014.

PEER 2014/02 *Theoretical Development of Hybrid Simulation Applied to Plate Structures.* Ahmed A. Bakhaty, Khalid M. Mosalam, and Sanjay Govindjee. January 2014.

PEER 2014/01 *Performance-Based Seismic Assessment of Skewed Bridges.* Peyman Kaviani, Farzin Zareian, and Ertugrul Taciroglu. January 2014.

PEER 2013/26 *Urban Earthquake Engineerin*g. Proceedings of the U.S.-Iran Seismic Workshop. December 2013.

PEER 2013/25 *Earthquake Engineering for Resilient Communities: 2013 PEER Internship Program Research Report Collection.* Heidi Tremayne (Editor), Stephen A. Mahin (Editor), Jorge Archbold Monterossa, Matt Brosman, Shelly Dean, Katherine deLaveaga, Curtis Fong, Donovan Holder, Rakeeb Khan, Elizabeth Jachens, David Lam, Daniela Martinez Lopez, Mara Minner, Geffen Oren, Julia Pavicic, Melissa Quinonez, Lorena Rodriguez, Sean Salazar, Kelli Slaven, Vivian Steyert, Jenny Taing, and Salvador Tena. December 2013.

PEER 2013/24 *NGA-West2 Ground Motion Prediction Equations for Vertical Ground Motions*. September 2013.

PEER 2013/23 *Coordinated Planning and Preparedness for Fire Following Major Earthquakes*. Charles Scawthorn. November 2013.

PEER 2013/22 *GEM-PEER Task 3 Project: Selection of a Global Set of Ground Motion Prediction Equations.* Jonathan P. Stewart, John Douglas, Mohammad B. Javanbarg, Carola Di Alessandro, Yousef Bozorgnia, Norman A. Abrahamson, David M. Boore, Kenneth W. Campbell, Elise Delavaud, Mustafa Erdik, and Peter J. Stafford. December 2013.

PEER 2013/21 *Seismic Design and Performance of Bridges with Columns on Rocking Foundations*. Grigorios Antonellis and Marios Panagiotou. September 2013.

PEER 2013/20 *Experimental and Analytical Studies on the Seismic Behavior of Conventional and Hybrid Braced Frames*. Jiun-Wei Lai and Stephen A. Mahin. September 2013.

PEER 2013/19 *Toward Resilient Communities: A Performance-Based Engineering Framework for Design and Evaluation of the Built Environment.* Michael William Mieler, Bozidar Stojadinovic, Robert J. Budnitz, Stephen A. Mahin, and Mary C. Comerio. September 2013.

PEER 2013/18 *Identification of Site Parameters that Improve Predictions of Site Amplification*. Ellen M. Rathje and Sara Navidi. July 2013.

PEER 2013/17 *Response Spectrum Analysis of Concrete Gravity Dams Including Dam-Water-Foundation Interaction*. Arnkjell Løkke and Anil K. Chopra. July 2013.

PEER 2013/16 *Effect of Hoop Reinforcement Spacing on the Cyclic Response of Large Reinforced Concrete Special Moment Frame Beams.* Marios Panagiotou, Tea Visnjic, Grigorios Antonellis, Panagiotis Galanis, and Jack P. Moehle. June 2013.

PEER 2013/15 *A Probabilistic Framework to Include the Effects of Near-Fault Directivity in Seismic Hazard Assessment*. Shrey Kumar Shahi, Jack W. Baker. October 2013.

PEER 2013/14 *Hanging-Wall Scaling using Finite-Fault Simulations.* Jennifer L. Donahue and Norman A. Abrahamson. September 2013.

PEER 2013/13 *Semi-Empirical Nonlinear Site Amplification and its Application in NEHRP Site Factors*. Jonathan P. Stewart and Emel Seyhan. November 2013.

PEER 2013/12 *Nonlinear Horizontal Site Response for the NGA-West2 Project.* Ronnie Kamai, Norman A. Abramson, Walter J. Silva. May 2013.

PEER 2013/11 *Epistemic Uncertainty for NGA-West2 Models.* Linda Al Atik and Robert R. Youngs. May 2013.

PEER 2013/10 *NGA-West 2 Models for Ground-Motion Directionality.* Shrey K. Shahi and Jack W. Baker. May 2013.

PEER 2013/09 *Final Report of the NGA-West2 Directivity Working Group.* Paul Spudich, Jeffrey R. Bayless, Jack W. Baker, Brian S.J. Chiou, Badie Rowshandel, Shrey Shahi, and Paul Somerville. May 2013.

PEER 2013/08 *NGA-West2 Model for Estimating Average Horizontal Values of Pseudo-Absolute Spectral Accelerations Generated by Crustal Earthquakes*. I. M. Idriss. May 2013.

PEER 2013/07 *Update of the Chiou and Youngs NGA Ground Motion Model for Average Horizontal Component of Peak Ground Motion and Response Spectra*. Brian Chiou and Robert Youngs. May 2013.

PEER 2013/06 *NGA-West2 Campbell-Bozorgnia Ground Motion Model for the Horizontal Components of PGA, PGV, and 5%-Damped Elastic Pseudo-Acceleration Response Spectra for Periods Ranging from 0.01 to 10 sec.* Kenneth W. Campbell and Yousef Bozorgnia. May 2013.

PEER 2013/05 *NGA-West 2 Equations for Predicting Response Spectral Accelerations for Shallow Crustal Earthquakes*. David M. Boore, Jonathan P. Stewart, Emel Seyhan, and Gail M. Atkinson. May 2013.

PEER 2013/04 *Update of the AS08 Ground-Motion Prediction Equations Based on the NGA-West2 Data Set*. Norman Abrahamson, Walter Silva, and Ronnie Kamai. May 2013.

PEER 2013/03 *PEER NGA-West2 Database.* Timothy D. Ancheta, Robert B. Darragh, Jonathan P. Stewart, Emel Seyhan, Walter J. Silva, Brian S.J. Chiou, Katie E. Wooddell, Robert W. Graves, Albert R. Kottke, David M. Boore, Tadahiro Kishida, and Jennifer L. Donahue. May 2013.

PEER 2013/02 *Hybrid Simulation of the Seismic Response of Squat Reinforced Concrete Shear Walls*. Catherine A. Whyte and Bozidar Stojadinovic. May 2013.

PEER 2013/01 *Housing Recovery in Chile: A Qualitative Mid-program Review*. Mary C. Comerio. February 2013.

PEER 2012/08 *Guidelines for Estimation of Shear Wave Velocity.* Bernard R. Wair, Jason T. DeJong, and Thomas Shantz. December 2012.

PEER 2012/07 *Earthquake Engineering for Resilient Communities: 2012 PEER Internship Program Research Report Collection.* Heidi Tremayne (Editor), Stephen A. Mahin (Editor), Collin Anderson, Dustin Cook, Michael Erceg, Carlos Esparza, Jose Jimenez, Dorian Krausz, Andrew Lo, Stephanie Lopez, Nicole McCurdy, Paul Shipman, Alexander Strum, Eduardo Vega. December 2012.

PEER 2012/06 *Fragilities for Precarious Rocks at Yucca Mountain.* Matthew D. Purvance, Rasool Anooshehpoor, and James N. Brune. December 2012.

PEER 2012/05 *Development of Simplified Analysis Procedure for Piles in Laterally Spreading Layered Soils.* Christopher R. McGann, Pedro Arduino, and Peter Mackenzie–Helnwein. December 2012.

PEER 2012/04 *Unbonded Pre-Tensioned Columns for Bridges in Seismic Regions.* Phillip M. Davis, Todd M. Janes, Marc O. Eberhard, and John F. Stanton. December 2012.

PEER 2012/03 *Experimental and Analytical Studies on Reinforced Concrete Buildings with Seismically Vulnerable Beam-Column Joints*. Sangjoon Park and Khalid M. Mosalam. October 2012.

PEER 2012/02 *Seismic Performance of Reinforced Concrete Bridges Allowed to Uplift during Multi-Directional Excitation*. Andres Oscar Espinoza and Stephen A. Mahin. July 2012.

PEER 2012/01 *Spectral Damping Scaling Factors for Shallow Crustal Earthquakes in Active Tectonic Regions.* Sanaz Rezaeian, Yousef Bozorgnia, I. M. Idriss, Kenneth Campbell, Norman Abrahamson, and Walter Silva. July 2012.

PEER 2011/10 *Earthquake Engineering for Resilient Communities: 2011 PEER Internship Program Research Report Collection*. Heidi Faison and Stephen A. Mahin, Editors. December 2011.

PEER 2011/09 *Calibration of Semi-Stochastic Procedure for Simulating High-Frequency Ground Motions*. Jonathan P. Stewart, Emel Seyhan, and Robert W. Graves. December 2011.

PEER 2011/08 *Water Supply in regard to Fire Following Earthquake*. Charles Scawthorn. November 2011.

PEER 2011/07 *Seismic Risk Management in Urban Areas*. Proceedings of a U.S.-Iran-Turkey Seismic Workshop. September 2011.

PEER 2011/06 *The Use of Base Isolation Systems to Achieve Complex Seismic Performance Objectives*. Troy A. Morgan and Stephen A. Mahin. July 2011.

PEER 2011/05 *Case Studies of the Seismic Performance of Tall Buildings Designed by Alternative Means.* Task 12 Report for the Tall Buildings Initiative. Jack Moehle, Yousef Bozorgnia, Nirmal Jayaram, Pierson Jones, Mohsen Rahnama, Nilesh Shome, Zeynep Tuna, John Wallace, Tony Yang, and Farzin Zareian. July 2011.

PEER 2011/04 *Recommended Design Practice for Pile Foundations in Laterally Spreading Ground.* Scott A. Ashford, Ross W. Boulanger, and Scott J. Brandenberg. June 2011.

PEER 2011/03 *New Ground Motion Selection Procedures and Selected Motions for the PEER Transportation Research Program*. Jack W. Baker, Ting Lin, Shrey K. Shahi, and Nirmal Jayaram. March 2011.

PEER 2011/02 *A Bayesian Network Methodology for Infrastructure Seismic Risk Assessment and Decision Support*. Michelle T. Bensi, Armen Der Kiureghian, and Daniel Straub. March 2011.

PEER 2011/01 *Demand Fragility Surfaces for Bridges in Liquefied and Laterally Spreading Ground.* Scott J. Brandenberg, Jian Zhang, Pirooz Kashighandi, Yili Huo, and Minxing Zhao. March 2011.

PEER 2010/05 *Guidelines for Performance-Based Seismic Design of Tall Buildings.* Developed by the Tall Buildings Initiative. November 2010.

PEER 2010/04 *Application Guide for the Design of Flexible and Rigid Bus Connections between Substation Equipment Subjected to Earthquakes.* Jean-Bernard Dastous and Armen Der Kiureghian. September 2010.

PEER 2010/03 *Shear Wave Velocity as a Statistical Function of Standard Penetration Test Resistance and Vertical Effective Stress at Caltrans Bridge Sites.* Scott J. Brandenberg, Naresh Bellana, and Thomas Shantz. June 2010.

PEER 2010/02 *Stochastic Modeling and Simulation of Ground Motions for Performance-Based Earthquake Engineering.* Sanaz Rezaeian and Armen Der Kiureghian. June 2010.

PEER 2010/01 *Structural Response and Cost Characterization of Bridge Construction Using Seismic Performance Enhancement Strategies.* Ady Aviram, Božidar Stojadinović, Gustavo J. Parra-Montesinos, and Kevin R. Mackie. March 2010.

PEER 2009/03 *The Integration of Experimental and Simulation Data in the Study of Reinforced Concrete Bridge Systems Including Soil-Foundation-Structure Interaction.* Matthew Dryden and Gregory L. Fenves. November 2009.

PEER 2009/02 *Improving Earthquake Mitigation through Innovations and Applications in Seismic Science, Engineering, Communication, and Response*. Proceedings of a U.S.-Iran Seismic Workshop. October 2009.

PEER 2009/01 *Evaluation of Ground Motion Selection and Modification Methods: Predicting Median Interstory Drift Response of Buildings*. Curt B. Haselton, Editor. June 2009.

PEER 2008/10 *Technical Manual for Strata.* Albert R. Kottke and Ellen M. Rathje. February 2009.

PEER 2008/09 *NGA Model for Average Horizontal Component of Peak Ground Motion and Response Spectra.* Brian S.-J. Chiou and Robert R. Youngs. November 2008.

PEER 2008/08 *Toward Earthquake-Resistant Design of Concentrically Braced Steel Structures*. Patxi Uriz and Stephen A. Mahin. November 2008.

PEER 2008/07 *Using OpenSees for Performance-Based Evaluation of Bridges on Liquefiable Soils*. Stephen L. Kramer, Pedro Arduino, and HyungSuk Shin. November 2008.

PEER 2008/06 *Shaking Table Tests and Numerical Investigation of Self-Centering Reinforced Concrete Bridge Columns*. Hyung IL Jeong, Junichi Sakai, and Stephen A. Mahin. September 2008.

PEER 2008/05 *Performance-Based Earthquake Engineering Design Evaluation Procedure for Bridge Foundations Undergoing Liquefaction-Induced Lateral Ground Displacement*. Christian A. Ledezma and Jonathan D. Bray. August 2008.

PEER 2008/04 *Benchmarking of Nonlinear Geotechnical Ground Response Analysis Procedures.* Jonathan P. Stewart, Annie On-Lei Kwok, Youssef M. A. Hashash, Neven Matasovic, Robert Pyke, Zhiliang Wang, and Zhaohui Yang. August 2008.

PEER 2008/03 *Guidelines for Nonlinear Analysis of Bridge Structures in California.* Ady Aviram, Kevin R. Mackie, and Božidar Stojadinović. August 2008.

PEER 2008/02 *Treatment of Uncertainties in Seismic-Risk Analysis of Transportation Systems*. Evangelos Stergiou and Anne S. Kiremidjian. July 2008.

PEER 2008/01 *Seismic Performance Objectives for Tall Buildings.* William T. Holmes, Charles Kircher, William Petak, and Nabih Youssef. August 2008.

PEER 2007/12 *An Assessment to Benchmark the Seismic Performance of a Code-Conforming Reinforced Concrete Moment-Frame Building.* Curt Haselton, Christine A. Goulet, Judith Mitrani-Reiser, James L. Beck, Gregory G. Deierlein, Keith A. Porter, Jonathan P. Stewart, and Ertugrul Taciroglu. August 2008.

PEER 2007/11 *Bar Buckling in Reinforced Concrete Bridge Columns.* Wayne A. Brown, Dawn E. Lehman, and John F. Stanton. February 2008.

PEER 2007/10 *Computational Modeling of Progressive Collapse in Reinforced Concrete Frame Structures*. Mohamed M. Talaat and Khalid M. Mosalam. May 2008.

PEER 2007/09 *Integrated Probabilistic Performance-Based Evaluation of Benchmark Reinforced Concrete Bridges*. Kevin R. Mackie, John-Michael Wong, and Božidar Stojadinović. January 2008.

PEER 2007/08 *Assessing Seismic Collapse Safety of Modern Reinforced Concrete Moment-Frame Buildings*. Curt B. Haselton and Gregory G. Deierlein. February 2008.

PEER 2007/07 *Performance Modeling Strategies for Modern Reinforced Concrete Bridge Columns*. Michael P. Berry and Marc O. Eberhard. April 2008.

PEER 2007/06 *Development of Improved Procedures for Seismic Design of Buried and Partially Buried Structures*. Linda Al Atik and Nicholas Sitar. June 2007.

PEER 2007/05 *Uncertainty and Correlation in Seismic Risk Assessment of Transportation Systems*. Renee G. Lee and Anne S. Kiremidjian. July 2007.

PEER 2007/04 *Numerical Models for Analysis and Performance-Based Design of Shallow Foundations Subjected to Seismic Loading.* Sivapalan Gajan, Tara C. Hutchinson, Bruce L. Kutter, Prishati Raychowdhury, José A. Ugalde, and Jonathan P. Stewart. May 2008.

PEER 2007/03 *Beam-Column Element Model Calibrated for Predicting Flexural Response Leading to Global Collapse of RC Frame Buildings*. Curt B. Haselton, Abbie B. Liel, Sarah Taylor Lange, and Gregory G. Deierlein. May 2008.

PEER 2007/02 *Campbell-Bozorgnia NGA Ground Motion Relations for the Geometric Mean Horizontal Component of Peak and Spectral Ground Motion Parameters*. Kenneth W. Campbell and Yousef Bozorgnia. May 2007.

PEER 2007/01 *Boore-Atkinson NGA Ground Motion Relations for the Geometric Mean Horizontal Component of Peak and Spectral Ground Motion Parameters*. David M. Boore and Gail M. Atkinson. May 2007.

PEER 2006/12 Societal Implications of Performance-Based Earthquake Engineering. Peter J. May. May 2007.

PEER 2006/11 *Probabilistic Seismic Demand Analysis Using Advanced Ground Motion Intensity Measures, Attenuation Relationships, and Near-Fault Effects*. Polsak Tothong and C. Allin Cornell. March 2007.

PEER 2006/10 *Application of the PEER PBEE Methodology to the I-880 Viaduct*. Sashi Kunnath. February 2007.

PEER 2006/09 *Quantifying Economic Losses from Travel Forgone Following a Large Metropolitan Earthquake*. James Moore, Sungbin Cho, Yue Yue Fan, and Stuart Werner. November 2006.

PEER 2006/08 *Vector-Valued Ground Motion Intensity Measures for Probabilistic Seismic Demand Analysis*. Jack W. Baker and C. Allin Cornell. October 2006.

PEER 2006/07 *Analytical Modeling of Reinforced Concrete Walls for Predicting Flexural and Coupled–Shear-Flexural Responses*. Kutay Orakcal, Leonardo M. Massone, and John W. Wallace. October 2006.

PEER 2006/06 *Nonlinear Analysis of a Soil-Drilled Pier System under Static and Dynamic Axial Loading*. Gang Wang and Nicholas Sitar. November 2006.

PEER 2006/05 *Advanced Seismic Assessment Guidelines.* Paolo Bazzurro, C. Allin Cornell, Charles Menun, Maziar Motahari, and Nicolas Luco. September 2006.

PEER 2006/04 *Probabilistic Seismic Evaluation of Reinforced Concrete Structural Components and Systems*. Tae Hyung Lee and Khalid M. Mosalam. August 2006.

PEER 2006/03 *Performance of Lifelines Subjected to Lateral Spreading.* Scott A. Ashford and Teerawut Juirnarongrit. July 2006.

PEER 2006/02 *Pacific Earthquake Engineering Research Center Highway Demonstration Project.* Anne Kiremidjian, James Moore, Yue Yue Fan, Nesrin Basoz, Ozgur Yazali, and Meredith Williams. April 2006.

PEER 2006/01 *Bracing Berkeley. A Guide to Seismic Safety on the UC Berkeley Campus.* Mary C. Comerio, Stephen Tobriner, and Ariane Fehrenkamp. January 2006.

PEER 2005/17 *Earthquake Simulation Tests on Reducing Residual Displacements of Reinforced Concrete Bridges.* Junichi Sakai, Stephen A Mahin, and Andres Espinoza. December 2005.

PEER 2005/16 *Seismic Response and Reliability of Electrical Substation Equipment and Systems.* Junho Song, Armen Der Kiureghian, and Jerome L. Sackman. April 2006.

PEER 2005/15 *CPT-Based Probabilistic Assessment of Seismic Soil Liquefaction Initiation.* R. E. S. Moss, R. B. Seed, R. E. Kayen, J. P. Stewart, and A. Der Kiureghian. April 2006.

PEER 2005/14 *Workshop on Modeling of Nonlinear Cyclic Load-Deformation Behavior of Shallow Foundations.* Bruce L. Kutter, Geoffrey Martin, Tara Hutchinson, Chad Harden, Sivapalan Gajan, and Justin Phalen. March 2006.

PEER 2005/13 *Stochastic Characterization and Decision Bases under Time-Dependent Aftershock Risk in Performance-Based Earthquake Engineering*. Gee Liek Yeo and C. Allin Cornell. July 2005.

PEER 2005/12 *PEER Testbed Study on a Laboratory Building: Exercising Seismic Performance Assessment.* Mary C. Comerio, Editor. November 2005.

PEER 2005/11 *Van Nuys Hotel Building Testbed Report: Exercising Seismic Performance Assessment.* Helmut Krawinkler, Editor. October 2005.

PEER 2005/10 *First NEES/E-Defense Workshop on Collapse Simulation of Reinforced Concrete Building Structures.* September 2005.

PEER 2005/09 *Test Applications of Advanced Seismic Assessment Guidelines.* Joe Maffei, Karl Telleen, Danya Mohr, William Holmes, and Yuki Nakayama. August 2006.

PEER 2005/08 *Damage Accumulation in Lightly Confined Reinforced Concrete Bridge Columns.* R. Tyler Ranf, Jared M. Nelson, Zach Price, Marc O. Eberhard, and John F. Stanton. April 2006.

PEER 2005/07 *Experimental and Analytical Studies on the Seismic Response of Freestanding and Anchored Laboratory Equipment.* Dimitrios Konstantinidis and Nicos Makris. January 2005.

PEER 2005/06 *Global Collapse of Frame Structures under Seismic Excitations*. Luis F. Ibarra and Helmut Krawinkler. September 2005.

PEER 2005//05 *Performance Characterization of Bench- and Shelf-Mounted Equipment.* Samit Ray Chaudhuri and Tara C. Hutchinson. May 2006.

PEER 2005/04 *Numerical Modeling of the Nonlinear Cyclic Response of Shallow Foundations.* Chad Harden, Tara Hutchinson, Geoffrey R. Martin, and Bruce L. Kutter. August 2005.

PEER 2005/03 *A Taxonomy of Building Components for Performance-Based Earthquake Engineering.* Keith A. Porter. September 2005.

PEER 2005/02 *Fragility Basis for California Highway Overpass Bridge Seismic Decision Making*. Kevin R. Mackie and Božidar Stojadinović. June 2005.

PEER 2005/01 *Empirical Characterization of Site Conditions on Strong Ground Motion.* Jonathan P. Stewart, Yoojoong Choi, and Robert W. Graves. June 2005.

PEER 2004/09 *Electrical Substation Equipment Interaction: Experimental Rigid Conductor Studies.* Christopher Stearns and André Filiatrault. February 2005.

PEER 2004/08 *Seismic Qualification and Fragility Testing of Line Break 550-kV Disconnect Switches.* Shakhzod M. Takhirov, Gregory L. Fenves, and Eric Fujisaki. January 2005.

PEER 2004/07 *Ground Motions for Earthquake Simulator Qualification of Electrical Substation Equipment.* Shakhzod M. Takhirov, Gregory L. Fenves, Eric Fujisaki, and Don Clyde. January 2005.

PEER 2004/06 *Performance-Based Regulation and Regulatory Regimes.* Peter J. May and Chris Koski. September 2004.

PEER 2004/05 *Performance-Based Seismic Design Concepts and Implementation: Proceedings of an International Workshop.* Peter Fajfar and Helmut Krawinkler, Editors. September 2004.

PEER 2004/04 *Seismic Performance of an Instrumented Tilt-up Wall Building.* James C. Anderson and Vitelmo V. Bertero. July 2004.

PEER 2004/03 *Evaluation and Application of Concrete Tilt-up Assessment Methodologies.* Timothy Graf and James O. Malley. October 2004.

PEER 2004/02 *Analytical Investigations of New Methods for Reducing Residual Displacements of Reinforced Concrete Bridge Columns.* Junichi Sakai and Stephen A. Mahin. August 2004.

PEER 2004/01 *Seismic Performance of Masonry Buildings and Design Implications.* Kerri Anne Taeko Tokoro, James C. Anderson, and Vitelmo V. Bertero. February 2004.

PEER 2003/18 *Performance Models for Flexural Damage in Reinforced Concrete Columns.* Michael Berry and Marc Eberhard. August 2003.

PEER 2003/17 *Predicting Earthquake Damage in Older Reinforced Concrete Beam-Column Joints.* Catherine Pagni and Laura Lowes. October 2004.

PEER 2003/16 *Seismic Demands for Performance-Based Design of Bridges.* Kevin Mackie and Božidar Stojadinović. August 2003.

PEER 2003/15 *Seismic Demands for Nondeteriorating Frame Structures and Their Dependence on Ground Motions.* Ricardo Antonio Medina and Helmut Krawinkler. May 2004.

PEER 2003/14 *Finite Element Reliability and Sensitivity Methods for Performance-Based Earthquake Engineering*. Terje Haukaas and Armen Der Kiureghian. April 2004.

PEER 2003/13 *Effects of Connection Hysteretic Degradation on the Seismic Behavior of Steel Moment-Resisting Frames.* Janise E. Rodgers and Stephen A. Mahin. March 2004.

PEER 2003/12 *Implementation Manual for the Seismic Protection of Laboratory Contents: Format and Case Studies*. William T. Holmes and Mary C. Comerio. October 2003.

PEER 2003/11 *Fifth U.S.-Japan Workshop on Performance-Based Earthquake Engineering Methodology for Reinforced Concrete Building Structures*. February 2004.

PEER 2003/10 *A Beam-Column Joint Model for Simulating the Earthquake Response of Reinforced Concrete Frames.* Laura N. Lowes, Nilanjan Mitra, and Arash Altoontash. February 2004.

PEER 2003/09 *Sequencing Repairs after an Earthquake: An Economic Approach.* Marco Casari and Simon J. Wilkie. April 2004.

PEER 2003/08 *A Technical Framework for Probability-Based Demand and Capacity Factor Design (DCFD) Seismic Formats*. Fatemeh Jalayer and C. Allin Cornell. November 2003.

PEER 2003/07 *Uncertainty Specification and Propagation for Loss Estimation Using FOSM Methods.* Jack W. Baker and C. Allin Cornell. September 2003.

PEER 2003/06 *Performance of Circular Reinforced Concrete Bridge Columns under Bidirectional Earthquake Loading*. Mahmoud M. Hachem, Stephen A. Mahin, and Jack P. Moehle. February 2003.

PEER 2003/05 *Response Assessment for Building-Specific Loss Estimation.* Eduardo Miranda and Shahram Taghavi. September 2003.

PEER 2003/04 *Experimental Assessment of Columns with Short Lap Splices Subjected to Cyclic Loads*. Murat Melek, John W. Wallace, and Joel Conte. April 2003.

PEER 2003/03 *Probabilistic Response Assessment for Building-Specific Loss Estimation*. Eduardo Miranda and Hesameddin Aslani. September 2003.

PEER 2003/02 *Software Framework for Collaborative Development of Nonlinear Dynamic Analysis Program*. Jun Peng and Kincho H. Law. September 2003.

PEER 2003/01 *Shake Table Tests and Analytical Studies on the Gravity Load Collapse of Reinforced Concrete Frames.* Kenneth John Elwood and Jack P. Moehle. November 2003.

PEER 2002/24 *Performance of Beam to Column Bridge Joints Subjected to a Large Velocity Pulse.* Natalie Gibson, André Filiatrault, and Scott A. Ashford. April 2002.

PEER 2002/23 *Effects of Large Velocity Pulses on Reinforced Concrete Bridge Columns.* Greg L. Orozco and Scott A. Ashford. April 2002.

PEER 2002/22 *Characterization of Large Velocity Pulses for Laboratory Testing.* Kenneth E. Cox and Scott A. Ashford. April 2002.

PEER 2002/21 *Fourth U.S.-Japan Workshop on Performance-Based Earthquake Engineering Methodology for Reinforced Concrete Building Structures*. December 2002.

PEER 2002/20 *Barriers to Adoption and Implementation of PBEE Innovations.* Peter J. May. August 2002.

PEER 2002/19 *Economic-Engineered Integrated Models for Earthquakes: Socioeconomic Impacts.* Peter Gordon, James E. Moore II, and Harry W. Richardson. July 2002.

PEER 2002/18 *Assessment of Reinforced Concrete Building Exterior Joints with Substandard Details.* Chris P. Pantelides, Jon Hansen, Justin Nadauld, and Lawrence D. Reaveley. May 2002.

PEER 2002/17 *Structural Characterization and Seismic Response Analysis of a Highway Overcrossing Equipped with Elastomeric Bearings and Fluid Dampers: A Case Study*. Nicos Makris and Jian Zhang. November 2002.

PEER 2002/16 *Estimation of Uncertainty in Geotechnical Properties for Performance-Based Earthquake Engineering*. Allen L. Jones, Steven L. Kramer, and Pedro Arduino. December 2002.

PEER 2002/15 *Seismic Behavior of Bridge Columns Subjected to Various Loading Patterns*. Asadollah Esmaeily-Gh. and Yan Xiao. December 2002.

PEER 2002/14 *Inelastic Seismic Response of Extended Pile Shaft Supported Bridge Structures.* T.C. Hutchinson, R.W. Boulanger, Y.H. Chai, and I.M. Idriss. December 2002.

PEER 2002/13 *Probabilistic Models and Fragility Estimates for Bridge Components and Systems.* Paolo Gardoni, Armen Der Kiureghian, and Khalid M. Mosalam. June 2002.

PEER 2002/12 *Effects of Fault Dip and Slip Rake on Near-Source Ground Motions: Why Chi-Chi Was a Relatively Mild M7.6 Earthquake*. Brad T. Aagaard, John F. Hall, and Thomas H. Heaton. December 2002.

PEER 2002/11 *Analytical and Experimental Study of Fiber-Reinforced Strip Isolators*. James M. Kelly and Shakhzod M. Takhirov. September 2002.

PEER 2002/10 *Centrifuge Modeling of Settlement and Lateral Spreading with Comparisons to Numerical Analyses***.** Sivapalan Gajan and Bruce L. Kutter. January 2003.

PEER 2002/09 *Documentation and Analysis of Field Case Histories of Seismic Compression during the 1994 Northridge, California, Earthquake*. Jonathan P. Stewart, Patrick M. Smith, Daniel H. Whang, and Jonathan D. Bray. October 2002.

PEER 2002/08 *Component Testing, Stability Analysis and Characterization of Buckling-Restrained Unbonded Braces^{TM}*. Cameron Black, Nicos Makris, and Ian Aiken. September 2002.

PEER 2002/07 *Seismic Performance of Pile-Wharf Connections.* Charles W. Roeder, Robert Graff, Jennifer Soderstrom, and Jun Han Yoo. December 2001.

PEER 2002/06 *The Use of Benefit-Cost Analysis for Evaluation of Performance-Based Earthquake Engineering Decisions*. Richard O. Zerbe and Anthony Falit-Baiamonte. September 2001.

PEER 2002/05 *Guidelines, Specifications, and Seismic Performance Characterization of Nonstructural Building Components and Equipment*. André Filiatrault, Constantin Christopoulos, and Christopher Stearns. September 2001.

PEER 2002/04 *Consortium of Organizations for Strong-Motion Observation Systems and the Pacific Earthquake Engineering Research Center Lifelines Program: Invited Workshop on Archiving and Web Dissemination of Geotechnical Data, 4–5 October 2001*. September 2002.

PEER 2002/03 *Investigation of Sensitivity of Building Loss Estimates to Major Uncertain Variables for the Van Nuys Testbed*. Keith A. Porter, James L. Beck, and Rustem V. Shaikhutdinov. August 2002.

PEER 2002/02 *The Third U.S.-Japan Workshop on Performance-Based Earthquake Engineering Methodology for Reinforced Concrete Building Structures*. July 2002.

PEER 2002/01 *Nonstructural Loss Estimation: The UC Berkeley Case Study.* Mary C. Comerio and John C. Stallmeyer. December 2001.

PEER 2001/16 *Statistics of SDF-System Estimate of Roof Displacement for Pushover Analysis of Buildings.* Anil K. Chopra, Rakesh K. Goel, and Chatpan Chintanapakdee. December 2001.

PEER 2001/15 *Damage to Bridges during the 2001 Nisqually Earthquake.* R. Tyler Ranf, Marc O. Eberhard, and Michael P. Berry. November 2001.

PEER 2001/14 *Rocking Response of Equipment Anchored to a Base Foundation.* Nicos Makris and Cameron J. Black. September 2001.

PEER 2001/13 *Modeling Soil Liquefaction Hazards for Performance-Based Earthquake Engineering*. Steven L. Kramer and Ahmed-W. Elgamal. February 2001.

PEER 2001/12 *Development of Geotechnical Capabilities in OpenSees*. Boris Jeremić. September 2001.

PEER 2001/11 *Analytical and Experimental Study of Fiber-Reinforced Elastomeric Isolators*. James M. Kelly and Shakhzod M. Takhirov. September 2001.

PEER 2001/10 *Amplification Factors for Spectral Acceleration in Active Regions.* Jonathan P. Stewart, Andrew H. Liu, Yoojoong Choi, and Mehmet B. Baturay. December 2001.

PEER 2001/09 *Ground Motion Evaluation Procedures for Performance-Based Design.* Jonathan P. Stewart, Shyh-Jeng Chiou, Jonathan D. Bray, Robert W. Graves, Paul G. Somerville, and Norman A. Abrahamson. September 2001.

PEER 2001/08 *Experimental and Computational Evaluation of Reinforced Concrete Bridge Beam-Column Connections for Seismic Performance.* Clay J. Naito, Jack P. Moehle, and Khalid M. Mosalam. November 2001.

PEER 2001/07 *The Rocking Spectrum and the Shortcomings of Design Guidelines.* Nicos Makris and Dimitrios Konstantinidis. August 2001.

PEER 2001/06 *Development of an Electrical Substation Equipment Performance Database for Evaluation of Equipment Fragilities*. Thalia Agnanos. April 1999.

PEER 2001/05 *Stiffness Analysis of Fiber-Reinforced Elastomeric Isolators.* Hsiang-Chuan Tsai and James M. Kelly. May 2001.

PEER 2001/04 *Organizational and Societal Considerations for Performance-Based Earthquake Engineering*. Peter J. May. April 2001.

PEER 2001/03 *A Modal Pushover Analysis Procedure to Estimate Seismic Demands for Buildings: Theory and Preliminary Evaluation*. Anil K. Chopra and Rakesh K. Goel. January 2001.

PEER 2001/02 *Seismic Response Analysis of Highway Overcrossings Including Soil-Structure Interaction*. Jian Zhang and Nicos Makris. March 2001.

PEER 2001/01 *Experimental Study of Large Seismic Steel Beam-to-Column Connections.* Egor P. Popov and Shakhzod M. Takhirov. November 2000.

PEER 2000/10 *The Second U.S.-Japan Workshop on Performance-Based Earthquake Engineering Methodology for Reinforced Concrete Building Structures*. March 2000.

PEER 2000/09 *Structural Engineering Reconnaissance of the August 17, 1999 Earthquake: Kocaeli (Izmit), Turkey.* Halil Sezen, Kenneth J. Elwood, Andrew S. Whittaker, Khalid Mosalam, John J. Wallace, and John F. Stanton. December 2000.

PEER 2000/08 *Behavior of Reinforced Concrete Bridge Columns Having Varying Aspect Ratios and Varying Lengths of Confinement*. Anthony J. Calderone, Dawn E. Lehman, and Jack P. Moehle. January 2001.

PEER 2000/07 *Cover-Plate and Flange-Plate Reinforced Steel Moment-Resisting Connections.* Taejin Kim, Andrew S. Whittaker, Amir S. Gilani, Vitelmo V. Bertero, and Shakhzod M. Takhirov. September 2000.

PEER 2000/06 *Seismic Evaluation and Analysis of 230-kV Disconnect Switches.* Amir S. J. Gilani, Andrew S. Whittaker, Gregory L. Fenves, Chun-Hao Chen, Henry Ho, and Eric Fujisaki. July 2000.

PEER 2000/05 *Performance-Based Evaluation of Exterior Reinforced Concrete Building Joints for Seismic Excitation*. Chandra Clyde, Chris P. Pantelides, and Lawrence D. Reaveley. July 2000.

PEER 2000/04 *An Evaluation of Seismic Energy Demand: An Attenuation Approach*. Chung-Che Chou and Chia-Ming Uang. July 1999.

PEER 2000/03 *Framing Earthquake Retrofitting Decisions: The Case of Hillside Homes in Los Angeles.* Detlof von Winterfeldt, Nels Roselund, and Alicia Kitsuse. March 2000.

PEER 2000/02 *U.S.-Japan Workshop on the Effects of Near-Field Earthquake Shaking*. Andrew Whittaker, Editor. July 2000.

PEER 2000/01 *Further Studies on Seismic Interaction in Interconnected Electrical Substation Equipment.* Armen Der Kiureghian, Kee-Jeung Hong, and Jerome L. Sackman. November 1999.

PEER 1999/14 *Seismic Evaluation and Retrofit of 230-kV Porcelain Transformer Bushings*. Amir S. Gilani, Andrew S. Whittaker, Gregory L. Fenves, and Eric Fujisaki. December 1999.

PEER 1999/13 *Building Vulnerability Studies: Modeling and Evaluation of Tilt-up and Steel Reinforced Concrete Buildings*. John W. Wallace, Jonathan P. Stewart, and Andrew S. Whittaker, Editors. December 1999.

PEER 1999/12 *Rehabilitation of Nonductile RC Frame Building Using Encasement Plates and Energy-Dissipating Devices*. Mehrdad Sasani, Vitelmo V. Bertero, James C. Anderson. December 1999.

PEER 1999/11 *Performance Evaluation Database for Concrete Bridge Components and Systems under Simulated Seismic Loads*. Yael D. Hose and Frieder Seible. November 1999.

PEER 1999/10 *U.S.-Japan Workshop on Performance-Based Earthquake Engineering Methodology for Reinforced Concrete Building Structures*. December 1999.

PEER 1999/09 *Performance Improvement of Long Period Building Structures Subjected to Severe Pulse-Type Ground Motions*. James C. Anderson, Vitelmo V. Bertero, and Raul Bertero. October 1999.

PEER 1999/08 *Envelopes for Seismic Response Vectors.* Charles Menun and Armen Der Kiureghian. July 1999.

PEER 1999/07 *Documentation of Strengths and Weaknesses of Current Computer Analysis Methods for Seismic Performance of Reinforced Concrete Members*. William F. Cofer. November 1999.

PEER 1999/06 *Rocking Response and Overturning of Anchored Equipment under Seismic Excitations*. Nicos Makris and Jian Zhang. November 1999.

PEER 1999/05 *Seismic Evaluation of 550 kV Porcelain Transformer Bushings.* Amir S. Gilani, Andrew S. Whittaker, Gregory L. Fenves, and Eric Fujisaki. October 1999.

PEER 1999/04 *Adoption and Enforcement of Earthquake Risk-Reduction Measures.* Peter J. May, Raymond J. Burby, T. Jens Feeley, and Robert Wood. August 1999.

PEER 1999/03 *Task 3 Characterization of Site Response General Site Categories*. Adrian Rodriguez-Marek, Jonathan D. Bray and Norman Abrahamson. February 1999.

PEER 1999/02 *Capacity-Demand-Diagram Methods for Estimating Seismic Deformation of Inelastic Structures: SDF Systems*. Anil K. Chopra and Rakesh Goel. April 1999.

PEER 1999/01 *Interaction in Interconnected Electrical Substation Equipment Subjected to Earthquake Ground Motions*. Armen Der Kiureghian, Jerome L. Sackman, and Kee-Jeung Hong. February 1999.

PEER 1998/08 *Behavior and Failure Analysis of a Multiple-Frame Highway Bridge in the 1994 Northridge Earthquake*. Gregory L. Fenves and Michael Ellery. December 1998.

PEER 1998/07 *Empirical Evaluation of Inertial Soil-Structure Interaction Effects.* Jonathan P. Stewart, Raymond B. Seed, and Gregory L. Fenves. November 1998.

PEER 1998/06 *Effect of Damping Mechanisms on the Response of Seismic Isolated Structures*. Nicos Makris and Shih-Po Chang. November 1998.

PEER 1998/05 *Rocking Response and Overturning of Equipment under Horizontal Pulse-Type Motions*. Nicos Makris and Yiannis Roussos. October 1998.

PEER 1998/04 *Pacific Earthquake Engineering Research Invitational Workshop Proceedings, May 14–15, 1998: Defining the Links between Planning, Policy Analysis, Economics and Earthquake Engineering*. Mary Comerio and Peter Gordon. September 1998.

PEER 1998/03 *Repair/Upgrade Procedures for Welded Beam to Column Connections*. James C. Anderson and Xiaojing Duan. May 1998.

PEER 1998/02 *Seismic Evaluation of 196 kV Porcelain Transformer Bushings.* Amir S. Gilani, Juan W. Chavez, Gregory L. Fenves, and Andrew S. Whittaker. May 1998.

PEER 1998/01 *Seismic Performance of Well-Confined Concrete Bridge Columns.* Dawn E. Lehman and Jack P. Moehle. December 2000.

PEER REPORTS: ONE HUNDRED SERIES

PEER 2012/103 *Performance-Based Seismic Demand Assessment of Concentrically Braced Steel Frame Buildings.* Chui-Hsin Chen and Stephen A. Mahin. December 2012.

PEER 2012/102 *Procedure to Restart an Interrupted Hybrid Simulation: Addendum to PEER Report 2010/103.* Vesna Terzic and Bozidar Stojadinovic. October 2012.

PEER 2012/101 *Mechanics of Fiber Reinforced Bearings.* James M. Kelly and Andrea Calabrese. February 2012.

PEER 2011/107 *Nonlinear Site Response and Seismic Compression at Vertical Array Strongly Shaken by 2007 Niigata-ken Chuetsu-oki Earthquake.* Eric Yee, Jonathan P. Stewart, and Kohji Tokimatsu. December 2011.

PEER 2011/106 *Self Compacting Hybrid Fiber Reinforced Concrete Composites for Bridge Columns.* Pardeep Kumar, Gabriel Jen, William Trono, Marios Panagiotou, and Claudia Ostertag. September 2011.

PEER 2011/105 *Stochastic Dynamic Analysis of Bridges Subjected to Spacially Varying Ground Motions.* Katerina Konakli and Armen Der Kiureghian. August 2011.

PEER 2011/104 *Design and Instrumentation of the 2010 E-Defense Four-Story Reinforced Concrete and Post-Tensioned Concrete Buildings.* Takuya Nagae, Kenichi Tahara, Taizo Matsumori, Hitoshi Shiohara, Toshimi Kabeyasawa, Susumu Kono, Minehiro Nishiyama (Japanese Research Team) and John Wallace, Wassim Ghannoum, Jack Moehle, Richard Sause, Wesley Keller, Zeynep Tuna (U.S. Research Team). June 2011.

PEER 2011/103 *In-Situ Monitoring of the Force Output of Fluid Dampers: Experimental Investigation.* Dimitrios Konstantinidis, James M. Kelly, and Nicos Makris. April 2011.

PEER 2011/102 *Ground-Motion Prediction Equations 1964–2010.* John Douglas. April 2011.

PEER 2011/101 *Report of the Eighth Planning Meeting of NEES/E-Defense Collaborative Research on Earthquake Engineering.* Convened by the Hyogo Earthquake Engineering Research Center (NIED), NEES Consortium, Inc. February 2011.

PEER 2010/111 *Modeling and Acceptance Criteria for Seismic Design and Analysis of Tall Buildings.* Task 7 Report for the Tall Buildings Initiative - Published jointly by the Applied Technology Council. October 2010.

PEER 2010/110 *Seismic Performance Assessment and Probabilistic Repair Cost Analysis of Precast Concrete Cladding Systems for Multistory Buildlings.* Jeffrey P. Hunt and Božidar Stojadinovic. November 2010.

PEER 2010/109 *Report of the Seventh Joint Planning Meeting of NEES/E-Defense Collaboration on Earthquake Engineering. Held at the E-Defense, Miki, and Shin-Kobe, Japan, September 18–19, 2009.* August 2010.

PEER 2010/108 *Probabilistic Tsunami Hazard in California.* Hong Kie Thio, Paul Somerville, and Jascha Polet, preparers. October 2010.

PEER 2010/107 *Performance and Reliability of Exposed Column Base Plate Connections for Steel Moment-Resisting Frames.* Ady Aviram, Božidar Stojadinovic, and Armen Der Kiureghian. August 2010.

PEER 2010/106 *Verification of Probabilistic Seismic Hazard Analysis Computer Programs.* Patricia Thomas, Ivan Wong, and Norman Abrahamson. May 2010.

PEER 2010/105 *Structural Engineering Reconnaissance of the April 6, 2009, Abruzzo, Italy, Earthquake, and Lessons Learned.* M. Selim Günay and Khalid M. Mosalam. April 2010.

PEER 2010/104 *Simulating the Inelastic Seismic Behavior of Steel Braced Frames, Including the Effects of Low-Cycle Fatigue.* Yuli Huang and Stephen A. Mahin. April 2010.

PEER 2010/103 *Post-Earthquake Traffic Capacity of Modern Bridges in California.* Vesna Terzic and Božidar Stojadinović. March 2010.

PEER 2010/102 *Analysis of Cumulative Absolute Velocity (CAV) and JMA Instrumental Seismic Intensity (I_{JMA}) Using the PEER–NGA Strong Motion Database.* Kenneth W. Campbell and Yousef Bozorgnia. February 2010.

PEER 2010/101 *Rocking Response of Bridges on Shallow Foundations.* Jose A. Ugalde, Bruce L. Kutter, and Boris Jeremic. April 2010.

PEER 2009/109 *Simulation and Performance-Based Earthquake Engineering Assessment of Self-Centering Post-Tensioned Concrete Bridge Systems.* Won K. Lee and Sarah L. Billington. December 2009.

PEER 2009/108 *PEER Lifelines Geotechnical Virtual Data Center.* J. Carl Stepp, Daniel J. Ponti, Loren L. Turner, Jennifer N. Swift, Sean Devlin, Yang Zhu, Jean Benoit, and John Bobbitt. September 2009.

PEER 2009/107 *Experimental and Computational Evaluation of Current and Innovative In-Span Hinge Details in Reinforced Concrete Box-Girder Bridges: Part 2: Post-Test Analysis and Design Recommendations.* Matias A. Hube and Khalid M. Mosalam. December 2009.

PEER 2009/106 *Shear Strength Models of Exterior Beam-Column Joints without Transverse Reinforcement.* Sangjoon Park and Khalid M. Mosalam. November 2009.

PEER 2009/105 *Reduced Uncertainty of Ground Motion Prediction Equations through Bayesian Variance Analysis.* Robb Eric S. Moss. November 2009.

PEER 2009/104 *Advanced Implementation of Hybrid Simulation.* Andreas H. Schellenberg, Stephen A. Mahin, Gregory L. Fenves. November 2009.

PEER 2009/103 *Performance Evaluation of Innovative Steel Braced Frames.* T. Y. Yang, Jack P. Moehle, and Božidar Stojadinovic. August 2009.

PEER 2009/102 *Reinvestigation of Liquefaction and Nonliquefaction Case Histories from the 1976 Tangshan Earthquake.* Robb Eric Moss, Robert E. Kayen, Liyuan Tong, Songyu Liu, Guojun Cai, and Jiaer Wu. August 2009.

PEER 2009/101 *Report of the First Joint Planning Meeting for the Second Phase of NEES/E-Defense Collaborative Research on Earthquake Engineering.* Stephen A. Mahin et al. July 2009.

PEER 2008/104 *Experimental and Analytical Study of the Seismic Performance of Retaining Structures.* Linda Al Atik and Nicholas Sitar. January 2009.

PEER 2008/103 *Experimental and Computational Evaluation of Current and Innovative In-Span Hinge Details in Reinforced Concrete Box-Girder Bridges. Part 1: Experimental Findings and Pre-Test Analysis.* Matias A. Hube and Khalid M. Mosalam. January 2009.

PEER 2008/102 *Modeling of Unreinforced Masonry Infill Walls Considering In-Plane and Out-of-Plane Interaction.* Stephen Kadysiewski and Khalid M. Mosalam. January 2009.

PEER 2008/101 *Seismic Performance Objectives for Tall Buildings.* William T. Holmes, Charles Kircher, William Petak, and Nabih Youssef. August 2008.

PEER 2007/101 *Generalized Hybrid Simulation Framework for Structural Systems Subjected to Seismic Loading*. Tarek Elkhoraibi and Khalid M. Mosalam. July 2007.

PEER 2007/100 *Seismic Evaluation of Reinforced Concrete Buildings Including Effects of Masonry Infill Walls*. Alidad Hashemi and Khalid M. Mosalam. July 2007.

The Pacific Earthquake Engineering Research Center (PEER) is a multi-institutional research and education center with headquarters at the University of California, Berkeley. Investigators from over 20 universities, several consulting companies, and researchers at various state and federal government agencies contribute to research programs focused on performance-based earthquake engineering.

These research programs aim to identify and reduce the risks from major earthquakes to life safety and to the economy by including research in a wide variety of disciplines including structural and geotechnical engineering, geology/seismology, lifelines, transportation, architecture, economics, risk management, and public policy.

PEER is supported by federal, state, local, and regional agencies, together with industry partners.

PEER Core Institutions

University of California, Berkeley (Lead Institution)
California Institute of Technology
Oregon State University
Stanford University
University of California, Davis
University of California, Irvine
University of California, Los Angeles
University of California, San Diego
University of Nevada, Reno
University of Southern California
University of Washington

PEER reports can be ordered at https://peer.berkeley.edu/peer-reports or by contacting

Pacific Earthquake Engineering Research Center
University of California, Berkeley
325 Davis Hall, Mail Code 1792
Berkeley, CA 94720-1792
Tel: 510-642-3437
Email: peer_center@berkeley.edu

ISSN 1547-0587X